3-14-2016

Selective Enhancement of Macropinocytosis for the Treatment of Non-Small Cell Lung Cancer

Raul Iglesias

Selective Enhancement of Macropinocytosis for the Treatment of Non-Small Cell Lung Cancer

by

Raul Iglesias

A dissertation submitted in partial fulfillment
of the requirements for the degree of
Doctor of Philosophy
Department of Chemical and Biomedical Engineering
College of Engineering
University of South Florida

Major Professor: Piyush Koria, Ph.D.
Nathan Gallant, Ph.D.
Subhra Mohapatra, Ph.D.
Venkat Bhethanabotla, Ph.D.
Mark Jaroszeski, Ph.D.

Date of Approval:
March 9, 2016

Keywords: ELP, Lytic Peptide, Growth Factor, Receptor

DEDICATION

This work is dedicated to my daughter, Kelsey.

ACKNOWLEDGMENTS

I would like to thank my family for their constant support during all these years. Their patience and understanding have had an everlasting impact in my life. I hope they are as proud of me as I am of them.

I would also like to thank my major professor Dr. Piyush Koria. He gave me the opportunity to work in his laboratory even when I did not have any lab experience. He has been a great support and guidance all these years. This work is, in great part, the result of his constant and countless advice.

I would like to express my thankfulness to my committee members Dr. Nathan Gallant, Dr. Subhra Mohapatra, Dr. Venkat Bhethanabotla and Dr. Mark Jaroszeski for being part of my committee and being there when help was needed.

Lastly, I like to extend my gratitude to my lab colleagues. They have been great people to work with; I could not have asked for a better team. Their support over these years has been enormous.

TABLE OF CONTENTS

LIST OF TABLES

LIST OF FIGURES

ABSTRACT

Over the past few years, researchers have focused their attention on the development of targeted cancer therapies to minimize the side effects associated with non-targeted treatments such as chemotherapy. Specifically, these approaches have focused on blocking growth factor receptors (GFR) that are overexpressed in cancer cells. In this thesis, we also focus on targeting overexpressed GFR; however, instead of blocking the GFR, our novel approach aims at using them to selectively enhance the endocytotic process of macropinocytosis to deliver peptides that either disrupts the mitochondria or inhibits glycolysis.

Herein, we show the selective enhancement of macropinocytosis by the fusion protein comprised of the keratinocyte growth factor (KGF) fused to elastin like polypeptide (ELP), KGF-ELP. Furthermore, we report the synthesis of the fusion protein consisting of mitochondriotoxic peptide $(KLAKLAK)_2$ with ELP, $(KLAKLAK)_2$-ELP. We show that $(KLAKLAK)_2$-ELP forms nanoparticles (NPs) that are internalized via macropinocytosis and their internalization is facilitated by the interaction between the ELP domain and heparan sulfate proteoglycan (HSPG) on the cell surface. This internalization results in mitochondrial swelling, depolarization and subsequent cell death. Moreover, we show that heterogeneous NPs comprising of the two fusions KGF-ELP and $(KLAKLAK)_2$-ELP selectively kill lung cancer cells expressing the keratinocyte growth factor receptor (KGFR).

We also report the synthesis of the fusion consisting of peptides derived from a phosphorylated domain of the glycolytic enzyme phophoglycerate mutase (PGM) and ELP,

PGM-ELP. We demonstrate that this fusion inhibits the step in glycolysis that converts 3-phosphoglycerate (3PG) to 2-phosphoglycerate (2PG); the results show that cell death occurred preferentially in lung cancer cells compared to normal cells. Additionally, the heterogeneous NPs comprising of KGF-ELP and PGM-ELP selectively enhanced killing in lung cells with high levels KGFR. Finally, the synthesis of a fusion proteins consisting of four PGM domains fused to ELP, (PGM)4-ELP, exhibits higher cytotoxic effect and efficiency when compared to the single PGM domain fusion, PGM-ELP.

Overall, we conclude that targeting overexpressed growth factor receptors to stimulate macropinocytosis can be a tremendously selective therapy for the treatment of lung cancer. This can result in attenuating side effects and improvement of the patient's prognosis.

CHAPTER 1: INTRODUCTION

1.1 The Lungs

The lungs are a pair of spongy organs located in the thoracic cavity where they are protected by the rib cage. They are divided into lobes. The right lung consists of three lobes: superior, middle and inferior. The superior and middle lobes are separated by a gap called the horizontal fissure; the oblique fissure separates the middle and inferior lobes. The left lung is smaller and comprised of only two lobes, superior and inferior, separated by an oblique fissure, Figure 1.1.

The main function of the lungs is the oxygenation of blood and removal of carbon dioxide (CO_2). To achieve this gas exchange air travels deep into the lungs through structures named air passages. First, air is inhaled through the nose or mouth, and then it continues to the trachea, which splits into two branches, the bronchi. The air continues its path into smaller branches of the bronchi called bronchioles, which end in air sacs called alveoli. The alveolus is the site where gas exchange actually occurs. Capillaries cover the alveoli and bring blood that has been depleted of oxygen (O_2) and is rich is CO_2 in contact with the alveoli which have high concentration of O_2 and low concentration of CO_2. Because of the different in concentration, O_2 diffuses into the blood stream while CO_2 travels into the alveoli, Figure 1.2.

The oxygenation of blood is a very critical process; O_2 in the blood is delivered to all different tissues in the body, cells in these tissues use it to produce energy in the form of ATP. Life could not be sustained without O_2. Just as important is the removal of CO_2. This gas is a

byproduct of respiration and its accumulation in the body can cause the blood to become acidic Increase in the acidity of the blood can damage the function of vital organs such as the brain.

1.2 Lung Cancer

Lung cancer is the abnormal, uncontrolled growth of cells in the lungs, usually originating from the epithelial cells in the air passages. This uncontrolled growth can result in the formation of a mass of cells called a lung tumor. Tumors may remain at the site where they originated in which case they are considered to be benign; contrastingly, tumors may also spread to other parts of the body in which case they are identified as malignant. The spreading of cancer cells over the body is termed metastasis and makes the treatment of any cancer very challenging.

The American Cancer Society recognizes three main types of lung cancers: Non-Small Cell Lung Cancer (NSCLC), Small Cell Lung Cancer (SCLC), and Lung Carcinoid Tumors. The frequency of each of these types of lung cancer varies considerably with NSCLC being the most common with 85% prevalence, while SCLC and Lung Carcinoid Tumors only represent 15% and 5%, respectively [1]. Lung cancer is associated with factors that include smoking, exposure to second hand smoking, exposure to chemicals such asbestos, and even air pollution [2].

There are more than one hundred types of cancer; among which, lung cancer is the leading cause of death in the United States [3]. The American Cancer Society estimated 221,200 new cases and 158,040 deaths due to lung cancer in the year 2015. Lung cancer is responsible for 28% of cancer related deaths in the United States; this is more than the mortality rate of the next four most common cancer types (colon, breast, prostate, pancreas) combined [4], Figure 1.3. In addition, the 5-year observed survival rate is low; it varies from 49% to 1%. The variation depends on the stage at which the cancer was detected.

1.3 Stages of NSCLC

As discussed above, lung cancer is the uncontrolled growth of cells in the lungs. Continued growth can result in the invasion of nearby tissues and organs. Furthermore, cancer can expand to distant organs and tissues through the lymphatic system or the blood stream. The characterization of this progression in size and spreading is called staging. Staging is important because it allows the identification of proper treatment as well as the prognosis of the patient. Staging can also determine if a patient is suitable to be part of a clinical trial. The following stages are used for NSCLC: occult stage, stage 0, stage I (A and B), stage II (A and B), stage III (A and B), and stage IV [5].

Briefly, the occult stage is the earliest stage at which NSCLC can be detected. In this stage, cancer has not metastasized but remains in situ. Cancer cells can be found in the sputum. In stage 0, abnormal cells can be found in the lining of the lungs. These cells are localized; therefore, this stage is also called carcinoma in situ. In stage I, a tumor has formed. This stage is further subdivided depending on the size and invasion. In stage IA, the tumor is less than 3 cm while in stage IB the tumor is between 3 and 5 cm. and may have spread to the bronchus or may have invaded the inner membrane that covers the lung.[5]. Stage II is characterized by the spreading of the tumor to the lymph node located on the same side of the tumor. Furthermore, stage IIA is characterized by a size that is less than 5 cm while stage IIB size is between 5 and 7 cm. In stage III, cancer can be of any size and spread to the lymph nodes of the same side of the tumor. In addition in stage IIIA, other structures may have also been invaded such as the chest wall, diaphragm, and the membrane around the heart. Similarly, in stage IIIB, cancer is present in the lymph nodes and can be of any size. In addition to the structures that are invaded during stage IIIA, in this stage the cancer may have also spread to the esophagus, the trachea, and the

heart. In stage IV, cancer may have all the characteristics of the previous stages; in addition, tumors will be present in both lungs. Moreover, the cancer has spread to various organs such as the brain and the liver.

1.4 Common Lung Cancer Treatments for NSCLC

The treatment of choice for lung cancer as well as any other cancer depends on several aspects: stage of cancer, patient's health, side effects, and presence of other lung complications such as bronchitis. The most common options for the treatment of lung cancer include surgery, radiation therapy, chemotherapy, targeted therapy or a combination of the aforementioned.

1.4.1 Surgery

Lung surgery is very complex and is mainly limited to the removal of tumors that have not metastasized. In addition, the patient's health and lung functionality need to be addressed before surgery can be conducted; therefore, surgery is not always an option. However, surgery remains the best alternative to cure NSCLC. Studies have shown that surgery complemented with chemotherapy and/or radiation therapy has further improved the outcome in early stages of NSCLC [6]. Furthermore, after the removal of a lung mass by surgery, there is a 1% to 2% risk of recurrence [7]. The types of lung surgery for the removal of a lung tumor include segmentectomy, lobectomy, and pneumonectomy; the choice depends on whether part of a lobe, a lobe or the entire lung needs removal, respectively.

1.4.2 Radiation Therapy

This type of therapy involves the use of ionizing radiation such as x-rays or gamma rays. Radiotherapy can be used as a primary treatment or an adjuvant treatment. The main goal radiation therapy is to shrink tumors and/or kill cancer cells. Similar to surgery, the use of radiation therapy is limited to localized tumors. In addition, there are limits to the amount of

radiation lungs and other organs can be exposed to without causing irreversible damage. This therapy however offers an alternative for stage I NSCLC patients for whom surgery is not an option. Studies have suggested that this type of therapy may have cure rates equivalent to surgery in stage I patients [8].

1.4.3 Chemotherapy

Chemotherapy consists of the use of anti-cancer drugs; the function of these drugs is mainly targeting fast dividing cells. Contrary to surgery and radiation therapy that are commonly used when the cancer is localized, chemotherapy can act throughout the body, which allows for the treatment of cancer that has already metastasized. However, this inherent characteristic of chemotherapeutic drugs can also affect non-cancerous cells that divide quickly such as red blood cells and epithelial cells lining the intestines. Therefore, even though chemotherapy is commonly used to treat lung cancer, it involves the indiscriminate killing of normal, healthy cells resulting in side effects. Furthermore, the development of resistance to chemotherapeutics often occurs, making this therapy, in many cases, ineffective over a period of time. Several chemotherapeutic drugs have been developed, they include DNA damaging drugs such as cisplatin or doxorubicin, and mitotic inhibitors such as paclitaxel [9]. However, due to significant side effects such as nephrotoxicity that may result from its nonspecific systemic organ distribution and inadequate intratumor concentrations, researchers are developing therapeutic agents that selectively affect tumor cells, targeted therapy.

1.4.4 Targeted Therapy

The goal of targeted therapy is to minimize side effects associated with the unselective killing of cells due to chemotherapeutics. Targeted therapy exploits differences between normal and cancerous cells. One of the most popular targets for lung cancer is the epidermal growth

factor receptor (EGFR) that is overexpressed in 50 % to 90 % of lung cancers [10, 11]. Consequently, monoclonal antibodies against the EGFR (cetuximab) and tyrosine kinase inhibitors (TKI) that inhibit the tyrosine kinase activity of EGFR (erlotinib or gefitinib) have been developed and have shown mixed results in the treatment of lung cancer in several clinical trials [9]. Although, TKIs show good response rates in lung cancer patients, acquired resistance to TKI treatment always develops after a median of 10 months from the initiation of treatment [12]. This acquired resistance can be attributed to several factors such as secondary mutation of the EGFR gene, amplification of the MET gene or overexpression of HGF [12]. The issue of acquired resistance is present not only in TKI treatment but in all other chemotherapy treatments as well, since tumor cells bypass the pathways that these drugs target; rendering the drugs ineffective. Therefore, patient prognosis still remains poor with 5-year survival rate of less than 5% and a median survival of approximately 1 year.

1.5 Novel Strategy for Targeting NSCLC Cells

Current targeted therapies aim at blocking growth factor receptors to prevent cells from proliferating and growing. The problem faced by this strategy is that cancer cells are highly mutagenic and a minimal change in the target renders the therapy ineffective. In this thesis, we look into a novel strategy that takes advantage of overexpressed growth factor receptor and use them to selectively enhance the endocytotic mechanism of macropinocytosis (chapter 3). This stimulation occurs through the activation of the keratinocyte growth factor receptor (KGFR), which has been reported to be overexpressed in lung cancer [13, 14]. Furthermore, this activation is used to deliver a mitochondriotoxic peptide (Chapter 3) or a glycolytic inhibiting peptide (Chapter 4) to KGFR overexpressing cells.

1.6 Summary

Lung cancer is the leading cause of death among all the different cancer types, being non-small cell lung cancer (NSCLC) the most common with an 85% incidence. There are different options for the treatment of this type of cancer including surgery, radiotherapy, chemotherapy, targeted therapy, and a combination of the aforementioned. The treatment of choice depends on various aspects such as stage of the cancer and health of the patient. Although much progress has been achieved in the treatment of lung cancer, the 5-year survival rate remains as low as 5% with a median survival of approximately 1 year. Furthermore, the issue of acquired resistance and the recurrence of the cancer seem to be a common theme regardless of the treatment of choice. Altogether, there is a clear need for further research and development of novel therapies for the treatment of lung cancer.

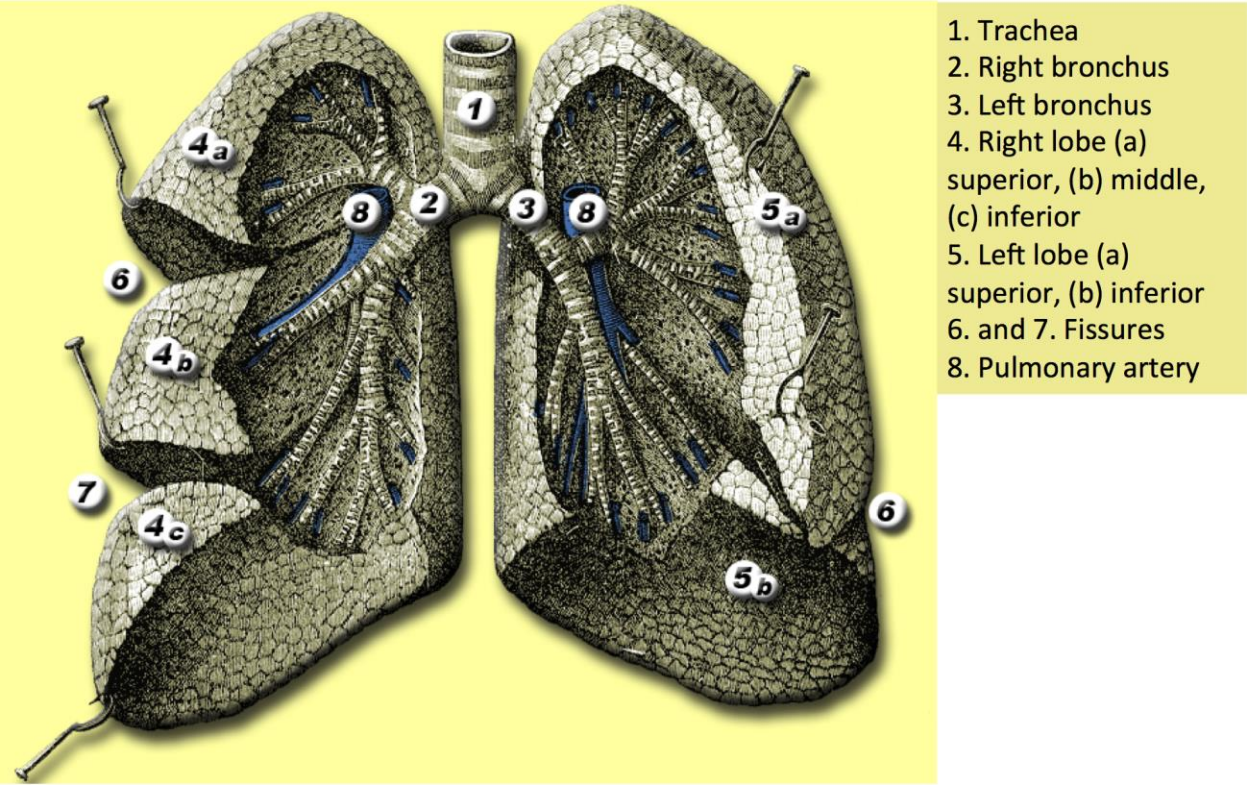

Figure 1.1 Anatomy of the lung and related structures [15].

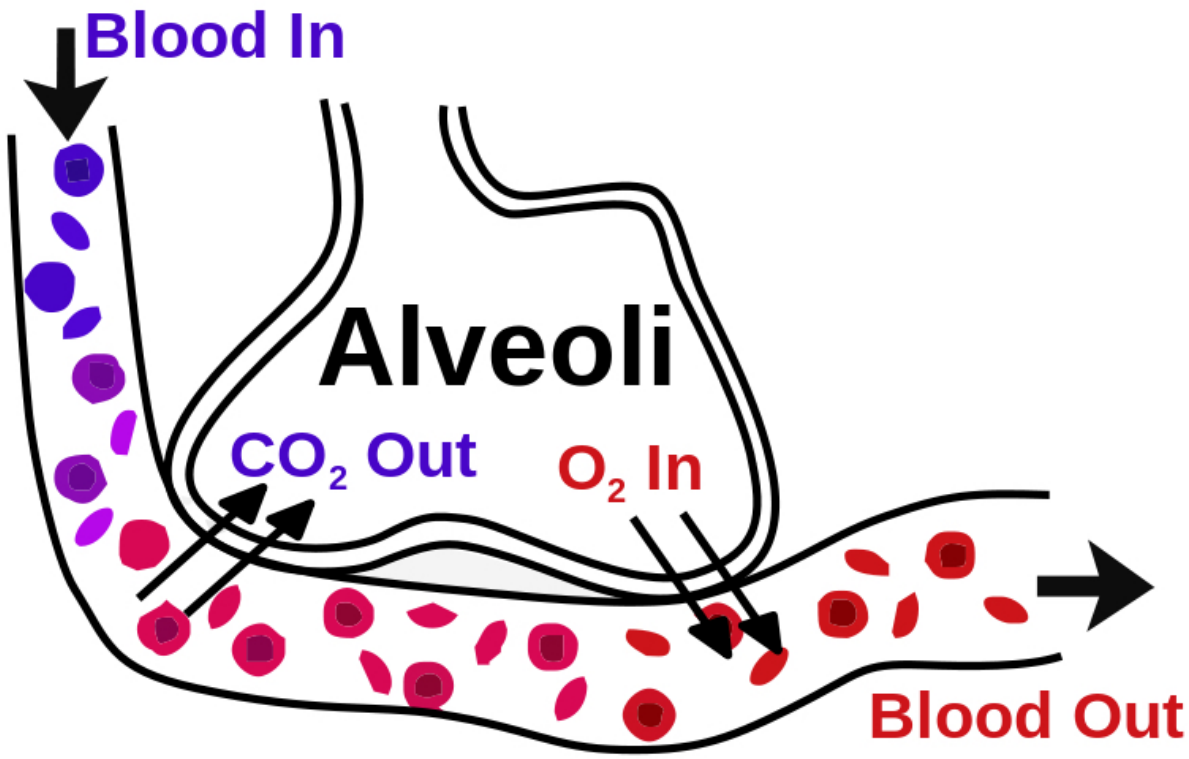

Figure 1.2 Gas exchange in the alveoli [16].

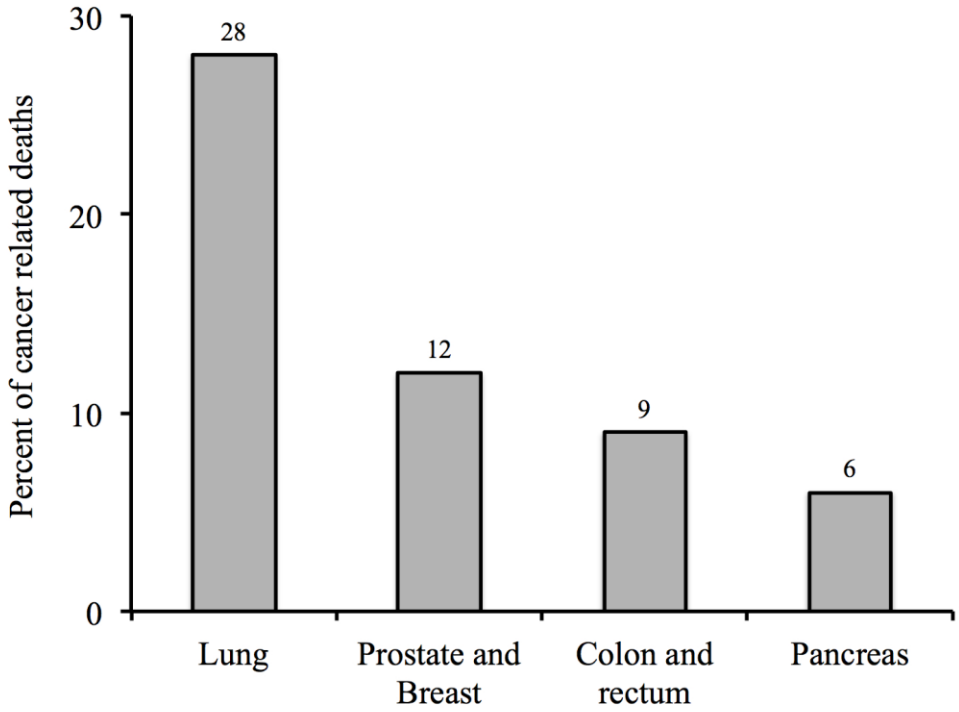

Figure 1.3 Mortality rates of different cancer types [1].

1.7 References

[1] N. A. Howlader N, Krapcho M, Garshell J, Miller D, Altekruse SF, Kosary CL, Yu M, Ruhl J, Tatalovich Z,Mariotto A, Lewis DR, Chen HS, Feuer EJ, Cronin KA (eds). (1975-2012). *SEER Cancer Statistics Review*. Available: http://seer.cancer.gov/csr-/1975_2012/

[2] P. A. Wingo, L. A. Ries, G. A. Giovino, D. S. Miller, H. M. Rosenberg, D. R. Shopland, *et al.*, "Annual report to the nation on the status of cancer, 1973-1996, with a special section on lung cancer and tobacco smoking," *J Natl Cancer Inst*, vol. 91, pp. 675-90, Apr 21 1999.

[3] L. A. Torre, R. L. Siegel, and A. Jemal, "Lung Cancer Statistics," *Adv Exp Med Biol*, vol. 893, pp. 1-19, 2016.

[4] R. Siegel, J. Ma, Z. Zou, and A. Jemal, "Cancer statistics, 2014," *CA Cancer J Clin*, vol. 64, pp. 9-29, Jan-Feb 2014.

[5] N. C. Institute. (2015, 15 January). *Stages of Non-Small Cell Lung Cancer*. Available: http://www.cancer.gov/types/lung/patient/non-small-cell-lung-treatment-pdqsec-tion/_134

[6] J. D. Predina, J. Keating, N. Patel, S. Nims, and S. Singhal, "Clinical implications of positive margins following non-small cell lung cancer surgery," *J Surg Oncol*, Dec 30 2015.

[7] B. E. Johnson, "Second lung cancers in patients after treatment for an initial lung cancer," *Journal of the National Cancer Institute*, vol. 90, pp. 1335-1345, 1998.

[8] U. Ricardi, S. Badellino, and A. R. Filippi, "Stereotactic body radiotherapy for early stage lung cancer: History and updated role," *Lung Cancer*, vol. 90, pp. 388-96, Dec 2015.

[9] J. E. Larsen, T. Cascone, D. E. Gerber, J. V. Heymach, and J. D. Minna, "Targeted therapies for lung cancer: clinical experience and novel agents," *Cancer J*, vol. 17, pp. 512-27, Nov 2011.

[10] V. Rusch, J. Baselga, C. Cordon-Cardo, J. Orazem, M. Zaman, S. Hoda, *et al.*, "Differential expression of the epidermal growth factor receptor and its ligands in primary non-small cell lung cancers and adjacent benign lung," *Cancer Res*, vol. 53, pp. 2379-85, May 15 1993.

[11] T. Dutu, S. Michiels, P. Fouret, F. Penault-Llorca, P. Validire, S. Benhamou, *et al.*, "Differential expression of biomarkers in lung adenocarcinoma: a comparative study between smokers and never-smokers," *Ann Oncol*, vol. 16, pp. 1906-14, Dec 2005.

[12] T. Kosaka, E. Yamaki, A. Mogi, and H. Kuwano, "Mechanisms of resistance to EGFR TKIs and development of a new generation of drugs in non-small-cell lung cancer," *J Biomed Biotechnol*, vol. 2011, p. 165214, 2011.

[13] M. Yoshino, T. Ishiwata, M. Watanabe, T. Matsunobu, O. Komine, Y. Ono, *et al.*, "Expression and roles of keratinocyte growth factor and its receptor in esophageal cancer cells," *Int J Oncol*, vol. 31, pp. 721-8, Oct 2007.

[14] T. Yamayoshi, T. Nagayasu, K. Matsumoto, T. Abo, Y. Hishikawa, and T. Koji, "Expression of keratinocyte growth factor/fibroblast growth factor-7 and its receptor in human lung cancer: correlation with tumour proliferative activity and patient prognosis," *J Pathol*, vol. 204, pp. 110-8, Sep 2004.

[15] E. Kempeneers. (1918). *Lungs Anatomy*. Available: https://commons.wikimedia.org-/wiki/File:Lungs_anatomy.png

[16] Helix84. (2007). *Gaseous Exchange in the Lungs*. Available: https://commons.wikimedia.org/wiki/File:Alveoli.svg

CHAPTER 2: $(KLAKLAK)_2$-ELP CAUSES APOPTOSIS THROUGH MITOCHONDRIAL DEPOLARIZATION

2.1 Note to Reader

Part of this chapter was published in Medical Oncology: R. Iglesias and P. Koria, "Leveraging growth factor induced macropinocytosis for targeted treatment of lung cancer," Med Oncol, vol. 32, p. 259, Dec 2015. Permission is included in Appendix B.

2.2 Introduction

KLAKLAKKLAKLAK, $(KLAKLAK)_2$, is a peptide that disrupts the outer mitochondrial membrane once uptaken by cells. However, cells are impermeable to it; therefore, its cytotoxic effect in mammalian cells is hindered. In this chapter we show that the fusion comprising of **(**$KLAKLAK)_2$ and elastin like polypeptide (ELP), $(KLAKLAK)_2$-ELP, is internalized by cells. Surprisingly, the functionalization of the fusion was not required as others have suggested. Furthermore, the fusion retains the self-assemble property of ELPs and the bioactivity of **(**$KLAKLAK)_2$; therefore, the fusion causes mitochondrial depolarization. We also show that the ELP domain of the fusion interacts with heparan sulfate proteoglycan (HSPG) on the cell surface. Moreover, we establish that $(KLAKLAK)_2$-ELP is internalized by the transient, endocytotic mechanism of macropinocytosis.

2.3 Elastin Like Polypeptide (ELP)

Elastin like peptides (ELPs) are biodegradable, non-immunogenic protein-based polymers composed of tandemly repeated blocks of $(Val\text{-}Pro\text{-}Gly\text{-}X\text{-}Gly)_N$ where X can be any

residue but *Pro* [1-3]. This sequence motif is derived from the hydrophobic domain of tropoelastin, a soluble precursor form of elastin. An interesting property of ELPs is their ability to undergo a phase transition at physiological temperatures [4, 5]. When the temperature is below their inverse transition temperature, also known as the lower critical solution temperature (LCST), they assume a random coil structure and are soluble in aqueous solution. However, at temperatures higher than the LCST, ELPs undergo an entropy driven self-assembly rendering them insoluble. This property enables recombinant ELPs to be expressed in bacteria and rapidly purified to high homogeneity using inverse temperature cycling (ITC) [2, 6]. Since ELPs are genetically encodable, biologically active peptides or proteins can be genetically fused to ELPs. These fusions can be expressed and readily purified since they maintain the phase transitioning property of the fused ELP domain. Moreover, owing to the transition property of ELPs, the chimeric fusion proteins can self-assemble into nanoparticles [7, 8]. Finally, the biological activity of the fused moiety in the chimeric fusion is retained [9, 10].

2.4 Mitochondriotoxic Peptide $(KLAKLAK)_2$

$(KLAKLAK)_2$, is a synthetic 14-amino acid peptide whose structure was designed to mimic natural occurring antimicrobial peptides [11]. These peptides are usually characterized by their positive charge as well as their alpha helix structure [12]. Their selective antimicrobial action is attributed to the difference in overall membrane charge between bacterial and mammalian cells; bacterial membranes have an overall negative charge while mammalian cells are neutral. This translates to the higher transmembrane potential observed in bacterial cells. This same high transmembrane potential is also noted in the mitochondria, an organelle the main function of which is the production of energy through the electron transport chain (ETC). The ETC consist of a series of molecules whose main function is the creation of a proton gradient

which drives the production of ATP. Among those molecules that are part of the ETC is Cytochrome c (cyt c). Cyt c is a small molecule that when released to the cytoplasm causes cell death, apoptosis.

$(KLAKLAK)_2$ is an amphipathic molecule that has a high positive charge, it has been shown to interact with the mitochondria causing swelling and mitochondrial depolarization [13]. Its mode of action is speculated to be through the creation of pores on the outer mitochondrial membrane that disrupts the proton gradient resulting in swelling and eventual release of cyt c [14, 15]. For $(KLAKLAK)_2$ to be effective, it must be internalized; however, mammalian cells are impermeable to $(KLAKLAK)_2$. Previous works have demonstrated that when $(KLAKLAK)_2$ is part of a nanostructure, cells become more permeable to it [16, 17]. Therefore, we reasoned that creating the fusion $(KLAKLAK)_2$-ELP would result in its internalization by taking advantage of the ELP phase transition characteristic above its T_t.

2.5 Fusion $(KLAKLAK)_2$-ELP

2.5.1 Materials and Methods

2.5.1.1 Materials

Fetal bovine serum (FBS) and Dulbecco modified Eagle Medium (DMEM) were purchased from Life Technologies. The restriction enzymes and other enzymes used for cloning were purchased from New England Biolabs (Ipswich, MA). Dr. Haura from Moffit Cancer Center kindly donated A549 and HCC827 cells. The apoptotic peptide gene and ELP gene were purchased from GenScript (Piscataway, NJ). The miniprep and gel extraction kits were purchased from QIAGEN.

2.5.1.2 Synthesis of $(KLAKLAK)_2$-ELP

The PUC57 plasmids containing the genes **(**VPGVG)5 , (VPGVG)2VPGCG(VPGVG)2 and $(KLAKLAK)_2$ were purchased from Genscript (Piscataway, NJ). The V40C2 encoding gene was made using the recursive direction ligation method as described previously [18]. The $(KLAKLAK)_2$ gene was excised using PflMI and Bgll enzymes. These genes were then run on a 0.08% agarose gel and extracted using a QIAquick Gel Extraction Kit. PflMI linearized the pUC19 vector containing the ELP sequence and the excised $(KLAKLAK)_2$ gene was cloned in frame with the ELP gene. This resulted in the pUC19 vector containing the $(KLAKLAK)_2$-ELP fusion protein gene flanked by pfIMI and BgII sites. The sequences encoding for the fusion proteins were then removed from the pUC19 vector using pflMI and BgII enzymes and recovered by gel extraction as explained above. After extraction, these genes were cloned in a modified pET25b+ expression vector through SfiI site. This vector was modified to incorporate an SfiI cloning site for the cloning of the fusion protein.

The pET25b+ vector containing the fusion protein gene was transformed into BLRD competent cells through heat shock at 42^oC. A starting culture of 50 ml was inoculated overnight and added to a 1 L culture the next day. The 1 L culture was then grown overnight and subsequently purified by inverse transition cycling as described previously [19]. Figure 2.1 shows a representation of the genes for $(KLAKLAK)_2$ and ELP and the production of the fusion $(KLAKLAK)_2$-ELP. Also, the illustration of the thermoresponsive property of the synthesized fusion above and below its T_t is represented.

2.5.1.3 Cell Culture

Cells were cultured in a humidified incubator at 37^0C and 5% CO_2. Cells were seeded on 24 or 48-well plates until they were approximately 70% confluent. A549 and HCC827 (human

lung carcinoma) were grown in DMEM supplemented with 10% FBS and 1% AA (Complete Medium).

2.5.1.4 Dynamic Light Scattering of $(KLAKLAK)_2$-ELP

Lyophilized $(KLAKLAK)_2$-ELP was resuspended in PBS to a final concentration of 50 μM. The solution was filter using a 220 μm filter and transfer to a cuvette. The analysis was performed using Zetasizer Nano S at different temperatures (20°C and 37 °C).

2.5.1.5 Transmission Electron Microscopy of $(KLAKLAK)_2$-ELP

Lyophilized $(KLAKLAK)_2$-ELP was diluted in PBS to a final concentration of 50 μM. Enough solution was added to a carbon-coated grid to cover its surface. The grid was placed on an incubator at 37 °C for the $(KLAKLAK)_2$-ELP to form nanoparticles. Once adsorbed on the grid, the particles were stained with uranyl formate staining solution and analyzed at Electron Microscopy Core Lab in the Interdisciplinary Science Building at the University of South Florida.

2.5.1.6 Mitochondrial Swelling

Cells (HCC827) were treated for 24 Hrs. with 50 μM of $(KLAKLAK)_2$-ELP. After the treatment, cells were fixed with 2.5% glutaraldehyde in 100 mM phosphate buffer at pH 7. Following fixation, standard embedding protocol for resin section was followed. TEM imaging was performed at Electron Microscopy Core Lab in the Interdisciplinary Science Building at the University of South Florida.

2.5.1.7 Mitochondrial Depolarization Assay

Cells (10,000/well) were seeded on 48-well plates using fresh complete media. After 24 hours, cells were treated with the indicated treatment of $(KLAKLAK)_2$-ELP or $(KLAKLAK)_2$ peptide. A JC-1 assay kit (Life Technologies cat # M34152) was used for mitochondrial

depolarization analysis. After treatment, media was removed and cells were washed with ice-cold PBS. JC-1 was added to fresh media to a final concentration of 2uM and this was added to the cells for 1 hour after which media was removed and cells were washed with ice-cold PBS before fluorescent pictures were taken (10X magnification) using EVOS fluorescence microscope (Life technologies). For the positive control sample, Carbonylcyanide m-chlorophenylhydrazone (CCCP) to a final concentration of 50 uM was added simultaneously with JC-1.

Mitochondrial depolarization analysis was also performed using flow cytometry. Cells (50,000/well) were seeded on 24 well plates and let grow to about 70% confluency; after which, they received no treatment, CCCP treatment or $(KLAKLAK)_2$-ELP treatment.; one sample (assay control) was used for gating purposes. The CCCP treatment was added 30 minutes before analysis. After $(KLAKLAK)_2$-ELP treatment for 24 hours, cells were washed with PBS and trypsinized (0.25 % trypsin). Trypsin was removed by centrifugation (800 rpm) and cells were resuspended in 300 µl of PBS. To exclude non-viable cells, 4',6-diamidino-2-phenylindole (DAPI) was added to the samples before analysis. Cells were analyzed using flow cytometry and the intensity in the red (PI) and green (FITC) channels were reported.

2.5.1.8 Labeling of the Fusion Proteins

The cysteines present in the ELP sequence were labeled using maleimide chemistry for the particle internalization experiments. Fluorescein-5-maleimide (AnaSpec Inc cat # 81405) was mixed with the fusion proteins. The mixture was placed on an orbital shaker and incubated at room temperature for 2 hours. Unconjugated fluorescein was removed by a series of hot and cold cycles on a bench top centrifuge ran at a speed of 20000g for 10 minutes each time. The supernatant was discarded after the hot spin and an equal amount of cold sterile PBS was added.

This mixture was spun at 4 ^{0}C and the supernatant was collected while the pellet was discarded. This formed one complete cycle of inverse temperature cycling. To get rid of all the unconjugated fluorescein, at least 5 cycles were performed.

2.5.1.9 Fusion Protein Internalization Assay

Cells (50,000/well) were seeded in 24-well plates and cultured as described above. They were let grow until they were about 70% confluent and were treated with the indicated treatments. For analysis, cells were washed twice with ice-cold PBS and were trypsinized using 0.25% trypsin (100 µl). Cells were pelleted and re-suspended in 300 µl of PBS containing 50 □g/ml of trypan blue to quench signal arising from the cell surface and 4',6-diamidino-2-phenylindole (DAPI) to allow exclusion of nonviable cells. The cells were analyzed using flow cytometry and either the percent of fluorescent cells or the average intensity was quantified and reported.

Some wells were pre-treated for 30 minutes with either inhibitors of macropinocytosis (amiloride and wortmannin) or receptor-mediated endocytosis (chlorpromazine). After the pre-treatment, cells were treated with the indicated labeled fusion proteins and internalization was measured by flow cytometry as described above. The inhibitor concentrations were used as described previously [20]. The following concentrations were used: wortmannin (10 □M), hexamethylene amiloride (20 □M), and chlorpromazine (10 □M). For investigating the role of heparan sulfate proteoglycans (HSPG) or the elastin receptor, cells were pre-treated with either surfen (20 □M), heparinase III (20mIU/ml) or lactose (5 mM).

2.5.1.10 Live/Dead Assay

Cells were seeded and treated with the indicated treatments for 3 days. After their respective treatments, ethidium homodimer-1 (Life Technologies cat # E1169) was added to each well to a final concentration of 4uM. Cells were then incubated for 1 hour at 37°C. After the incubation time, cells were washed twice with PBS to remove floating cells. NucBlue (Life Technologies R37605) was then added for 20 minutes to stain nuclei, followed by two washes with PBS. Eight random pictures were taken per well using the EVOS fluorescence microscope (10X magnification). Pictures were taken in different channels (blue, green, red) and overlay. Live/dead cell discrimination was performed using image J. A macro was created using the functions split channel, threshold, and cell counter to count the total number of live cells (blue) in each picture. Dead cells that were not removed after the washes were stained red or magenta (blue and red); adjusting the threshold for the picture being analyzed easily isolated these cells. Therefore, the final count of cells per picture only included live cells.

2.5.1.11 Statistical Analysis

For statistical significance, the p value was calculated using ANOVA single factor. P values < 0.05 were considered significant. The reported errors indicate the ±SEM.

2.5.2 Results

2.5.2.1 $(KLAKLAK)_2$-ELP Preserves the Phase Transition Property of ELPs

ELPs are genetically encodable; therefore, they are relatively easy to functionalize using simple recombinant DNA technology techniques. In addition, ELPs' phase transition property makes them very appealing for the synthesis of nanoparticles that are thermoresponsive and allow for improve concentration of treatment to a site that has been exposed to a temperature that is equal to or higher than the ELP T_t [10, 21, 22] Many studies have shown that ELPs greatly

preserve this phase transition property when fused to other domains [23, 24]. Based on these studies, we tested if our fusion $(KLAKLAK)_2$-ELP preserve the self-assemble property of ELPs. Our results clearly showed that $(KLAKLAK)_2$-ELP is in its soluble form at a temperature of 20 ^oC while it aggregates to a size of about 350 nm at a temperature of 37 ^oC (Figure 2.2). Since these experiments were carried out as a cycle, with one cycle consisting of increasing and decreasing the temperature from 20 ^oC to 37 ^oC and back, we concluded that the ELP self-assemble property was retained. TEM further confirmed the size of the $(KLAKLAK)_2$-ELP aggregate to be about 350 nm (Fig 2.3).

2.5.2.2 $(KLAKLAK)_2$-ELP Causes Mitochondrial Swelling

Previous work has shown that $(KLAKLAK)_2$ causes mitochondrial swelling through the disruption of the outer mitochondrial membrane [13]. We wanted to confirm that our fusion $(KLAKLAK)_2$-ELP had the same toxic effect in cells. TEM analysis of our samples clearly indicated a difference between the mitochondria of the control compare the mitochondria of the $(KLAKLAK)_2$-ELP treated sample (Figures 2.4 and 2.5). Therefore, we concluded that the mode of action of our fusion is similar to the $(KLAKLAK)_2$ peptide.

2.5.2.3 $(KLAKLAK)_2$ Fused to ELPs Induces Cell Death Via Mitochondrial Depolarization

Previous studies have shown that $(KLAKLAK)_2$ has low mammalian cell toxicity but can induce mitochondrial depolarization and subsequent apoptosis when fused to a homing domain [11, 13]. Furthermore, others have demonstrated that when $(KLAKLAK)_2$ is part of a nanostructure that is functionalized with a cell penetrating peptide (CPP), it is internalized and causes cell death [16, 17]. Based on these findings, we fused $(KLAKLAK)_2$ to elastin like peptides (ELP), $(KLAKLAK)_2$-ELP, making it possible to form nanostructures as mentioned above. Surprisingly, after a 48-hour treatment, $(KLAKLAK)_2$-ELP caused 30%, 85%, and 93%

of cell death at 20μM, 50μM and 100μM, respectively, without the need of a functionalizing domain. Moreover, the same treatment with the $(KLAKLAK)_2$ peptide did not affect cell viability (Figure 2.6). To further test if cell death occurred due to mitochondrial depolarization as previously reported, we performed a JC-1 assay that distinguishes between healthy and depolarized mitochondria. This assay stains healthy mitochondria in red and depolarized mitochondria in green. After a 24 Hr. treatment with the $(KLAKLAK)_2$-ELP fusion, cells displayed the presence of depolarized mitochondria, (Figures 2.7 and 2.8). Combined, these results suggest that the $(KLAKLAK)_2$-ELP nanostructure caused cell death through mitochondrial depolarization even in the absence of a functionalized domain.

2.5.2.4 Internalization of $(KLAKLAK)_2$-ELP is Assisted by HSPG on the Cell Surface

Since the lack of a functionalizing domain in $(KLAKLAK)_2$-ELP still resulted in cell death, we reasoned that ELPs might be involved in the uptake of $(KLAKLAK)_2$-ELP. Previous works have found that ELPs interact with the elastin receptor [25]. Furthermore, tropoelastin from which ELPs are derived interacts with HSPG on the cell surface [26]. Thus, we hypothesized that the internalization of $(KLAKLAK)_2$-ELP could also be mediated by the interaction between the ELP portion of the fusion and one of these aforementioned molecules. To test this hypothesis, we carried out experiments in the presence of molecules that block the elastin receptor (lactose), cleave HSPG (heparinase III) or serve as a HSPG antagonist (surfen) [27]. First, cells were pretreated with lactose that binds to the elastin receptor preventing other molecules from binding to it. The presence of lactose did not affect the internalization of $(KLAKLAK)_2$-ELP (Figure 2.9) suggesting that the elastin receptor is not involved in the internalization. Second, we pretreated the cells with heparinase III that cleaves HSPG from the cell surface. Our results showed a 70% decrease in $(KLAKLAK)_2$-ELP internalization when

compared to control (Figure 2.9). Finally, to further confirm that HSPG was involved in $(KLAKLAK)_2$-ELP internalization, cells were pretreated with surfen, which is a small molecule antagonist to HSPG [27]. The result showed that about 90% of (KLAKLAK)2-ELP internalization was blocked (Figure 2.9). Thus, these results clearly indicate that the internalization of $(KLAKLAK)_2$-ELP depends on its interaction with HSPG.

2.5.2.5 $(KLAKLAK)_2$-ELP is Internalized by Macropinocytosis

To gain insight into the mechanism of uptake of $(KLAKLAK)_2$-ELP aggregates, we used known blockers for two major endocytotic pathways. Chlorpromazine was used to block clathrin mediated endocytosis, amiloride and wortmannin to block macropinocytosis. Internalization experiments were carried out in the presence of each of these blockers using concentrations previously determined [20]. The results showed that $(KLAKLAK)_2$-ELP uptake was not affected by chlorpromazine; however, amiloride and wortmannin decreased $(KLAKLAK)_2$-ELP internalization by 70% and 75% , respectively (Figure 2.10). Altogether, these results indicate that macropinocytosis is the major mechanism involved in $(KLAKLAK)_2$-ELP internalization.

2.6 Discussion and Summary

The mitochondriotoxic peptide $(KLAKLAK)_2$ is well known to disrupt the outer mitochondrial membrane causing swelling and mitochondrial depolarization; this translates to cell death. However, as demonstrated by others and us, cells are impermeable to $(KLAKLAK)_2$; therefore, it has not cytotoxic effect unless it is uptaken by cells. Other groups have reported various strategies to improve $(KLAKLAK)_2$ internalization by cells such as fusing it to cell penetrating peptides (CPP). Also, previous work suggested that $(KLAKLAK)_2$ internalization can be improved by making it part of a nanoparticle in addition to functionalizing it with a CPP. Based on the latter, we synthesized $(KLAKLAK)_2$-ELP, the ELP portion of the fusion provides

the nanoparticle backbone when expose to a temperature higher than its T_t. Interestingly, we found that functionalization of the $(KLAKLAK)_2$ was not needed to improve its uptake, but the nanoparticle formation was enough for its internalization and subsequent cell death. Furthermore, we show that $(KLAKLAK)_2$-ELP causes mitochondrial swelling and depolarization; this is consistent with previously reported data. Therefore, our results clearly indicate that the cytotoxic mechanism of $(KLAKLAK)_2$-ELP follows that of $(KLAKLAK)_2$ peptide.

We found that the predominant mechanism of uptake of $(KLAKLAK)_2$-ELP nanoparticles by cells was macropinocytosis. Tumor cells exhibit higher levels of macropinocytosis than the normally quiescent non-cancerous cells [28, 29]. Thus, macropinocytosis on its own may provide certain level of selectivity towards killing of cancer cells. Indeed, it was observed that $(KLAKLAK)_2$ nanoparticles demonstrated certain level of killing selectivity towards cancer cells [17]. Though, the mechanism of internalization was not reported in that study it is plausible that those nanoparticles were also being internalized by macropinocytosis thereby explaining the selectivity.

We also show that the internalization of ELP nanoparticles was dependent on their interaction with cell surface heparan sulfate proteoglycans (HSPG). This is in agreement with previous studies that have reported that tropoelastin from which ELPs are derived interacts with cell surface HSPG [26, 30]. The interaction of ELPs with HSPG may ensure proximity of the NPs to the cell surface where they will be uptaken by macropinocytosis. Interestingly, previous work has reported the importance of phase transition for the internalization of ELP based molecules [31]. Our data may explain this observation because during phase transition ELPs form β-strand structure, which has been reported as a common secondary structure for variety of

proteins that interact with cell membrane bound HSPG [32]. Thus, the phase transition allows ELPs to interact with HSPG facilitating its internalization.

In summary, we found that the fusion $(KLAKLAK)_2$-ELP is mitochondriotoxic without the need to be functionalized; the nanoparticle conformation provided by the ELP backbone was enough to cause the internalization and cytotoxicity of the fusion. Furthermore, cell death occurs via mitochondrial depolarization and swelling. We found that the mechanism of internalization of $(KLAKLAK)_2$-ELP is macropinocytosis; we believe the interaction between the ELP domain of the fusion and heparan sulfate on the cell membrane allows for the proximity required for macropinocytosis to act on the $(KLAKLAK)_2$-ELP nanoparticles

Table 2.1 $(KLAKLAK)_2$ and ELP amino acid sequences.

$(KLAKLAK)_2$	KLAKLAKKLAKLAK
ELP	V40C2
V	VPGVG
C	$(VPGVG)_2$-VPGCG-$(VPGVG)_2$

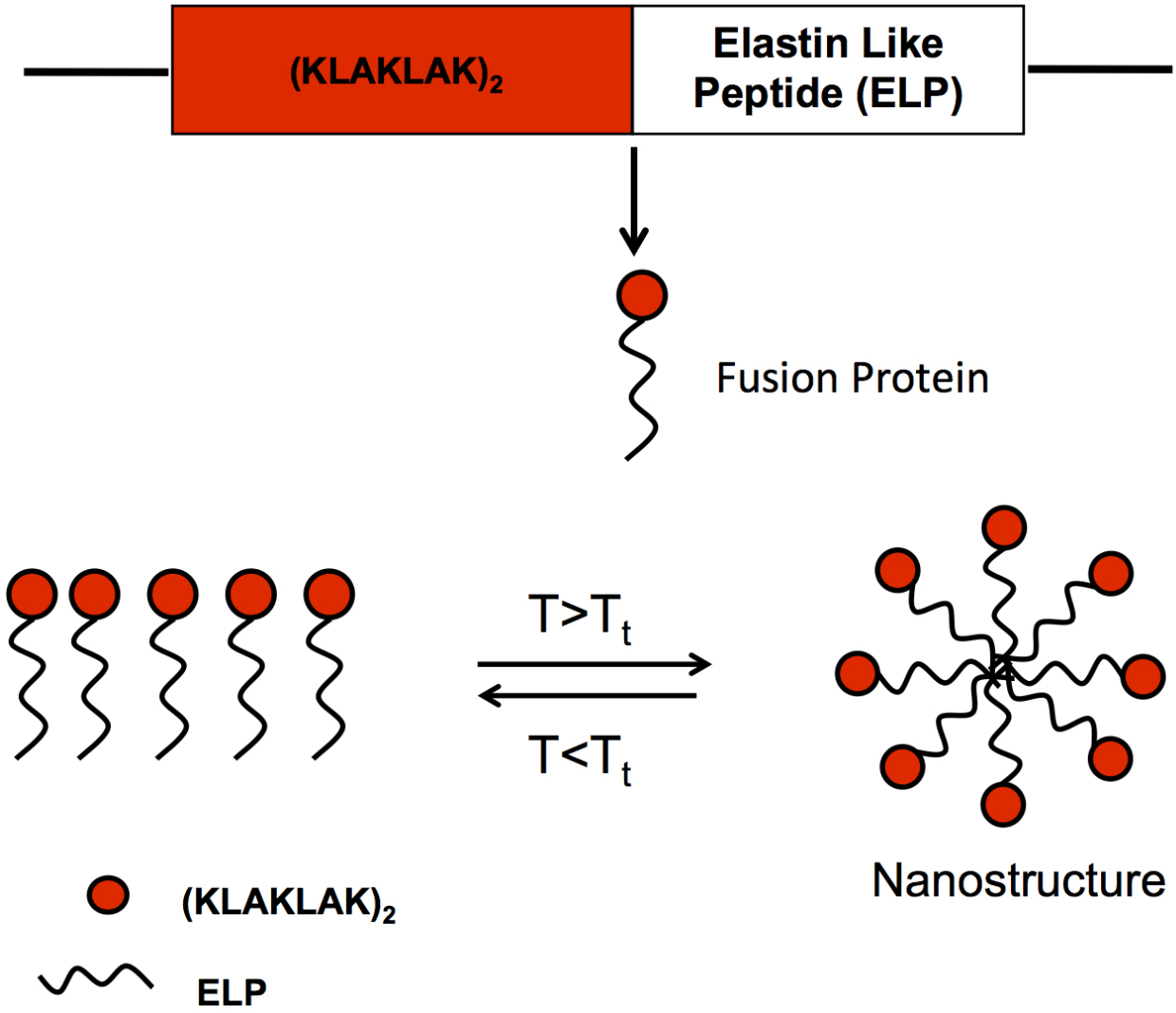

Figure 2.1 Representation of $(KLAKLAK)_2$-ELP synthesis and its thermoresponsive property. Top, representation of $(KLAKLAK)_2$ gene, the ELP, and their translation to the fusion $(KLAKLAK)_2$-ELP. Bottom, illustration of the phase transition property of the fusion above and below its transition temperature (T_t). The fusion is soluble below its T_t and aggregates above its T_t.

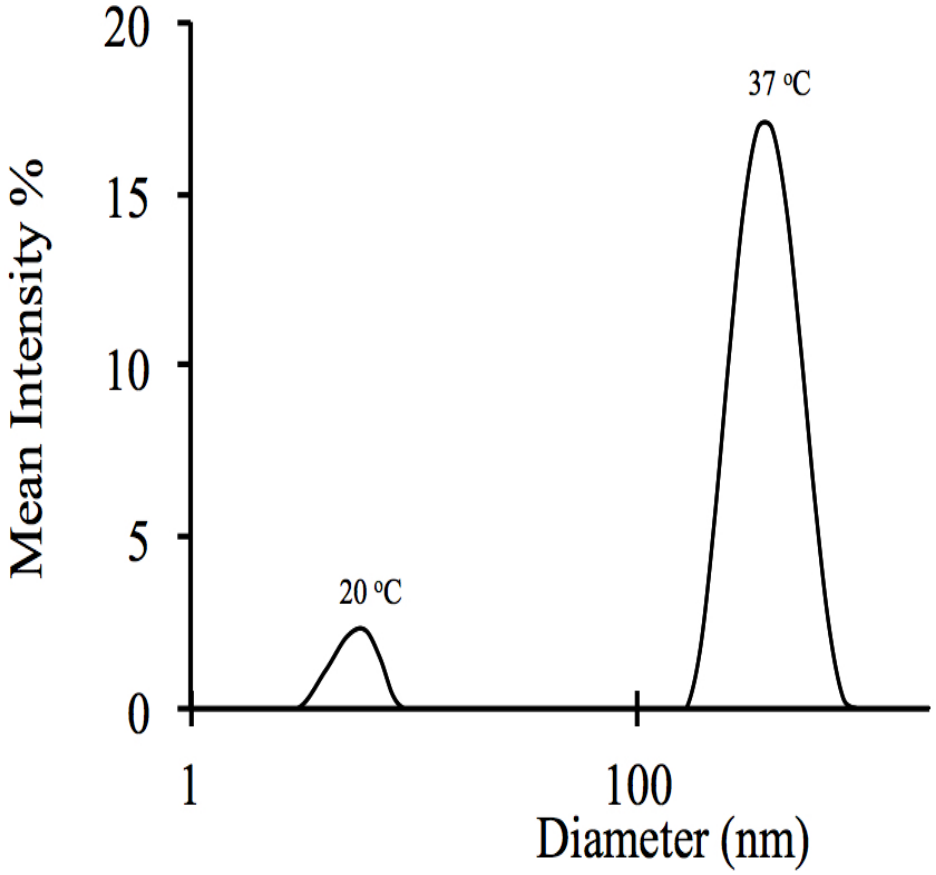

Figure 2.2 Characterization of $(KLAKLAK)_2$-ELP by dynamic light scattering. $(KLAKLAK)_2$-ELP retains the self-assemble property of ELPs. Lyophilized $(KLAKLAK)_2$-ELP resuspended in PBS to a final concentration of 50 μM was analyzed by DLS at 20 °C and 37 °C.. The graph shows clearly two peaks at about 5 nm and 350 nm representing the $(KLAKLAK)_2$-ELP as unimers and as aggregates, respectively.

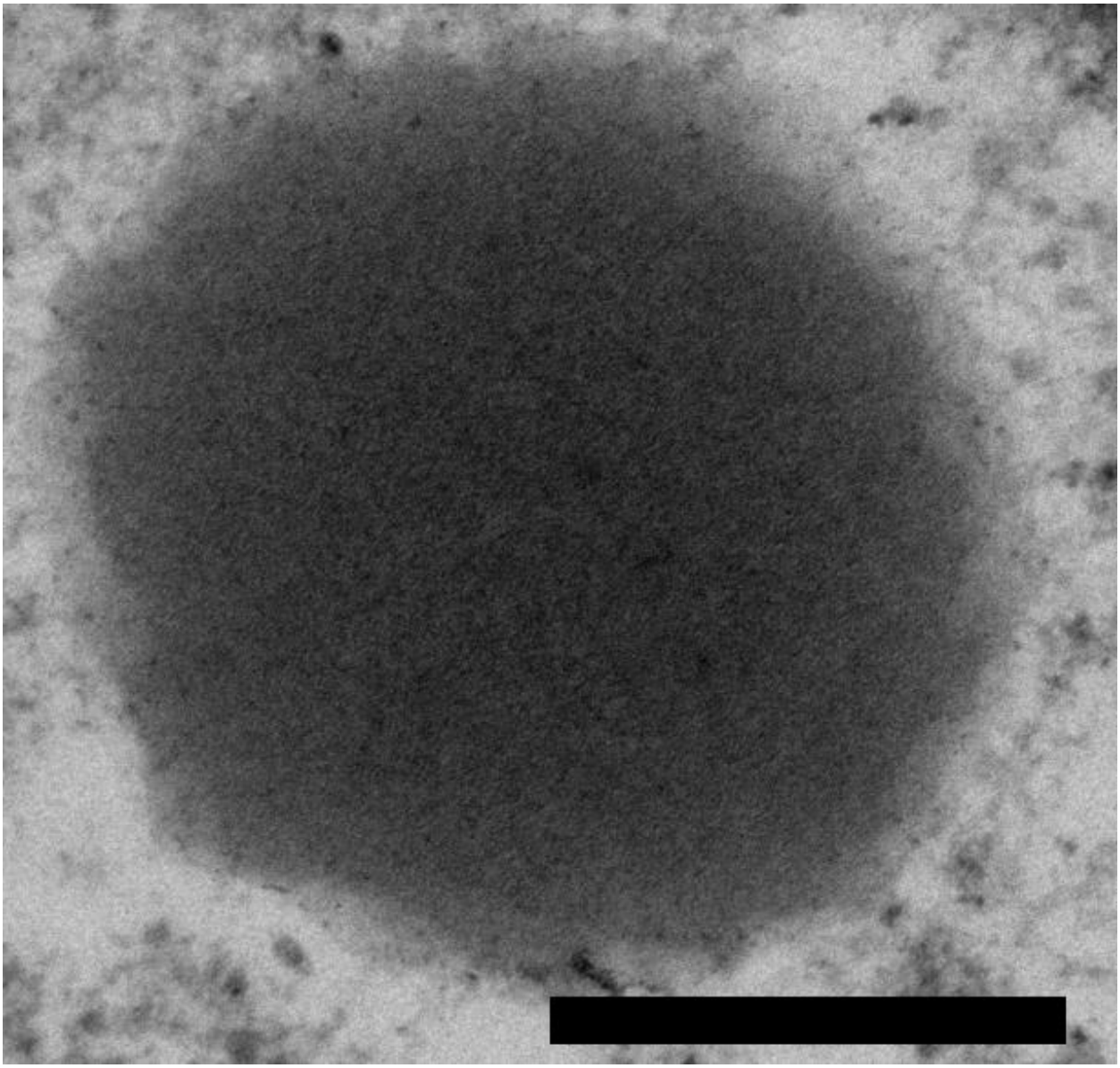

Figure 2.3 TEM of $(KLAKLAK)_2$-ELP. This fusion protein aggregates to a size of about 360 nm as confirmed by TEM. $(KLAKLAK)_2$-ELP was adsorbed on a carbon-coated grid, incubated at 37 ^oC and stained with uranyl formate. Bar = 200 nm.

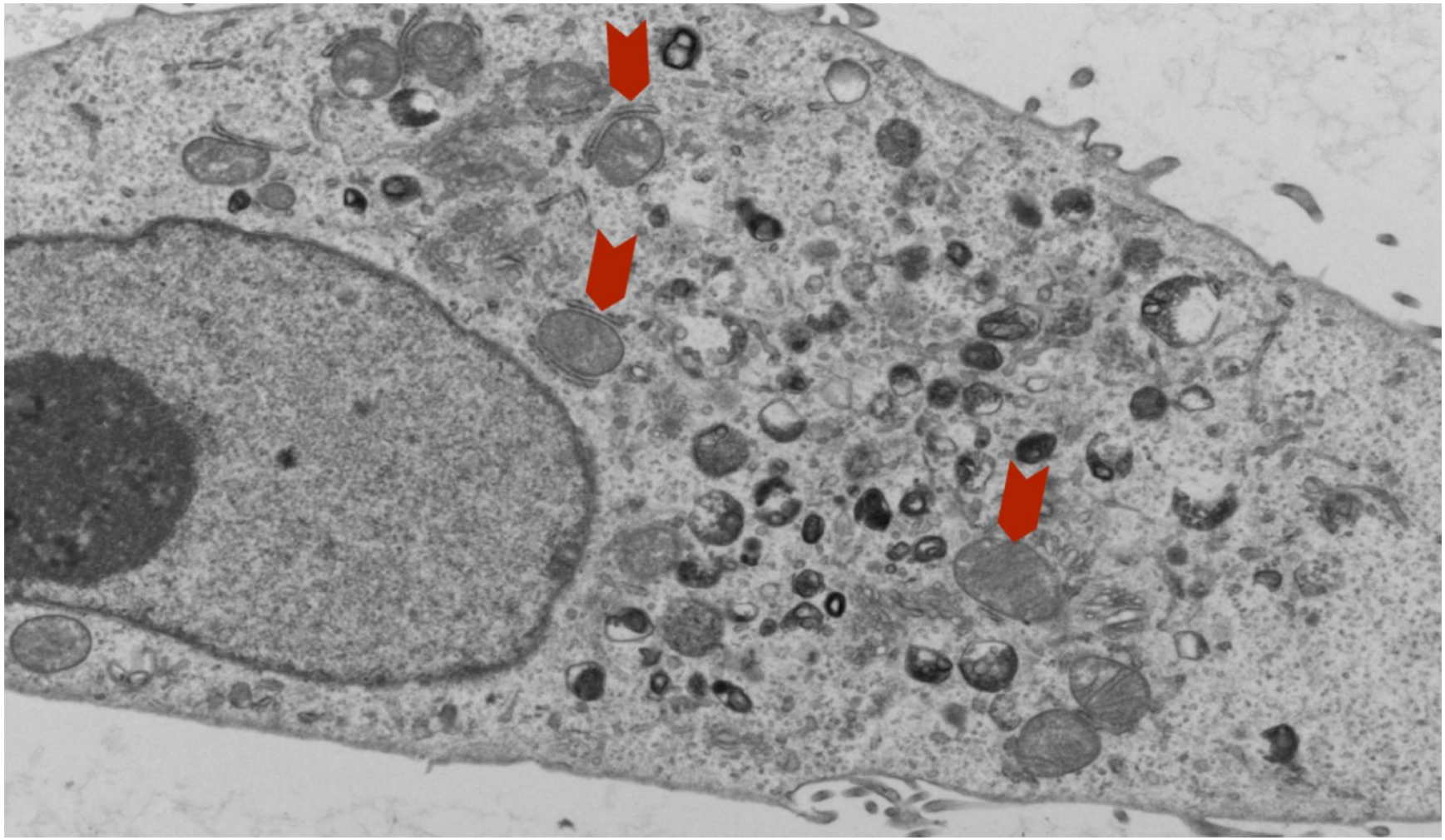

Figure 2.4 TEM of normal mitochondria. HCC827 were imaged by TEM. Red arrows show the location of the mitochondria.

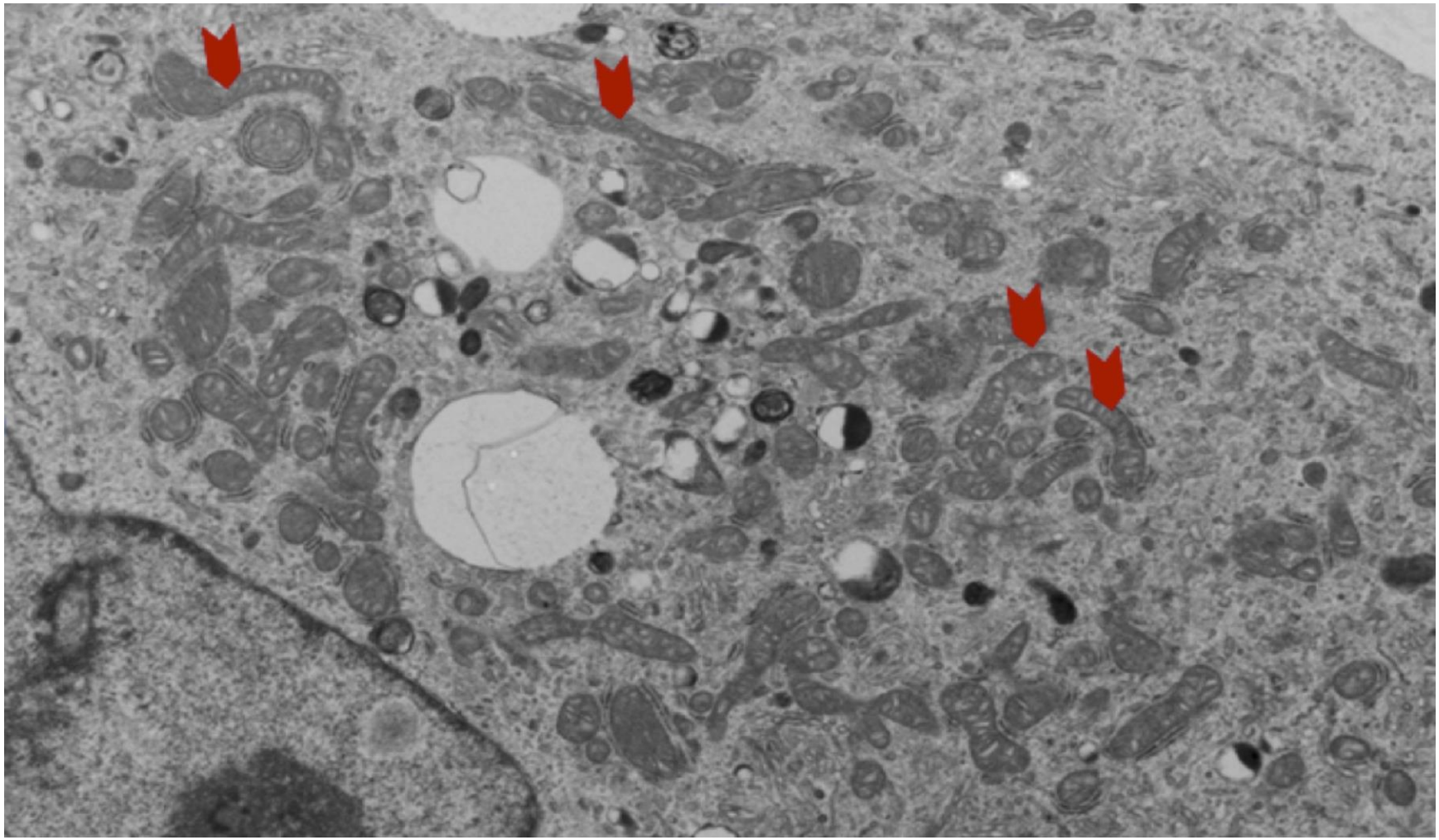

Figure 2.5 TEM of mitochondrial swelling. HCC27 cells were treated with 50 μM of $(KLAKLAK)_2$-ELP for 24 Hrs. Cells were then imaged by TEM. Red arrows indicate the location of the elongated mitochondria.

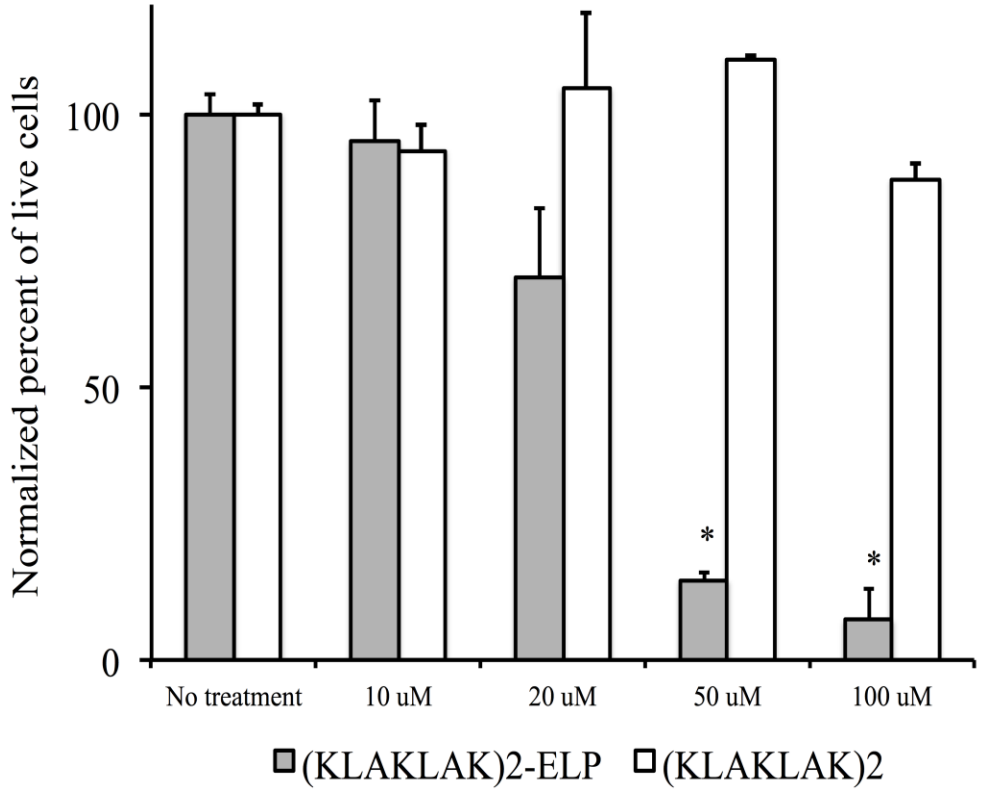

Figure 2.6 Cytotoxic effect of $(KLAKLAK)_2$-ELP and $(KLAKLAK)_2$ peptide. $(KLAKLAK)_2$-ELP induces cell death at high concentrations while the $(KLAKLAK)_2$ peptide does not. Lung adenocarcinoma cells, A549, were treated for 48 Hrs. with different concentrations of $(KLAKLAK)_2$-ELP or $(KLAKLAK)_2$ peptide. The percent of live cells was calculated using a live/dead assay; pictures were then taken using a fluorescent microscope and the counting was done using image J. All the treatments were normalized to the control (no treatment).

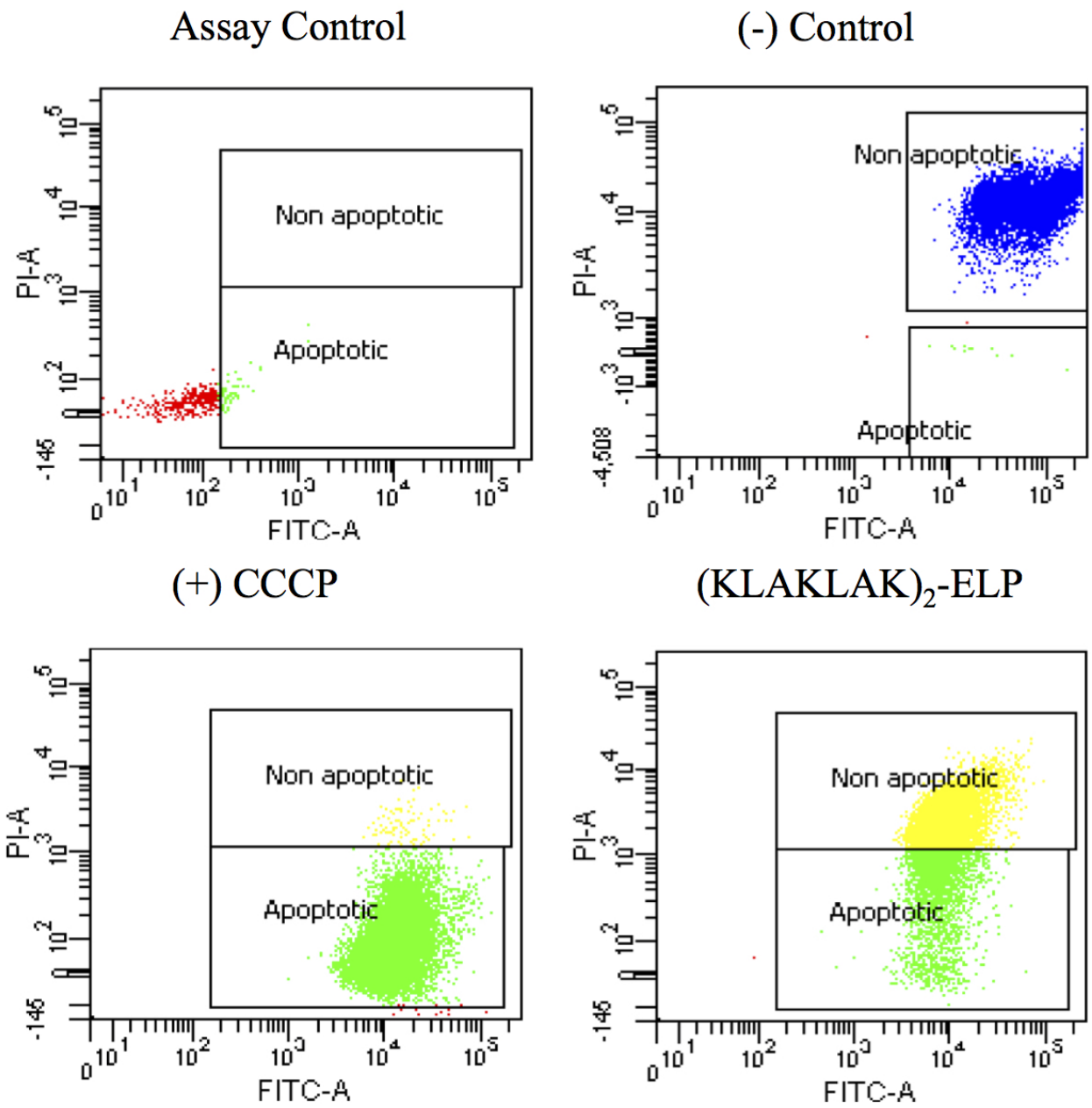

Figure 2.7 Mitochondrial depolarization analysis by flow cytometry. A549 cells were treated for 24 Hr. with 10μM of $(KLAKLAK)_2$-ELP or 30 min. with a known mitochondrial depolarizer, CCCP. A JC-1 assay, which distinguishes between healthy and depolarized mitochondria, was then performed. Analysis was carried out by flow cytometry. The assay control is for gating purposes; the negative control consisted of untreated cells. The apoptotic label shows the area where cells with depolarized mitochondria are found while the non-apoptotic label shows the area where cells with healthy mitochondria are found. The results clearly show the mitochondriotoxic effect of $(KLAKLAK)_2$-ELP. PI-A and FITC-A refer to red and green fluorescent channels, respectively.

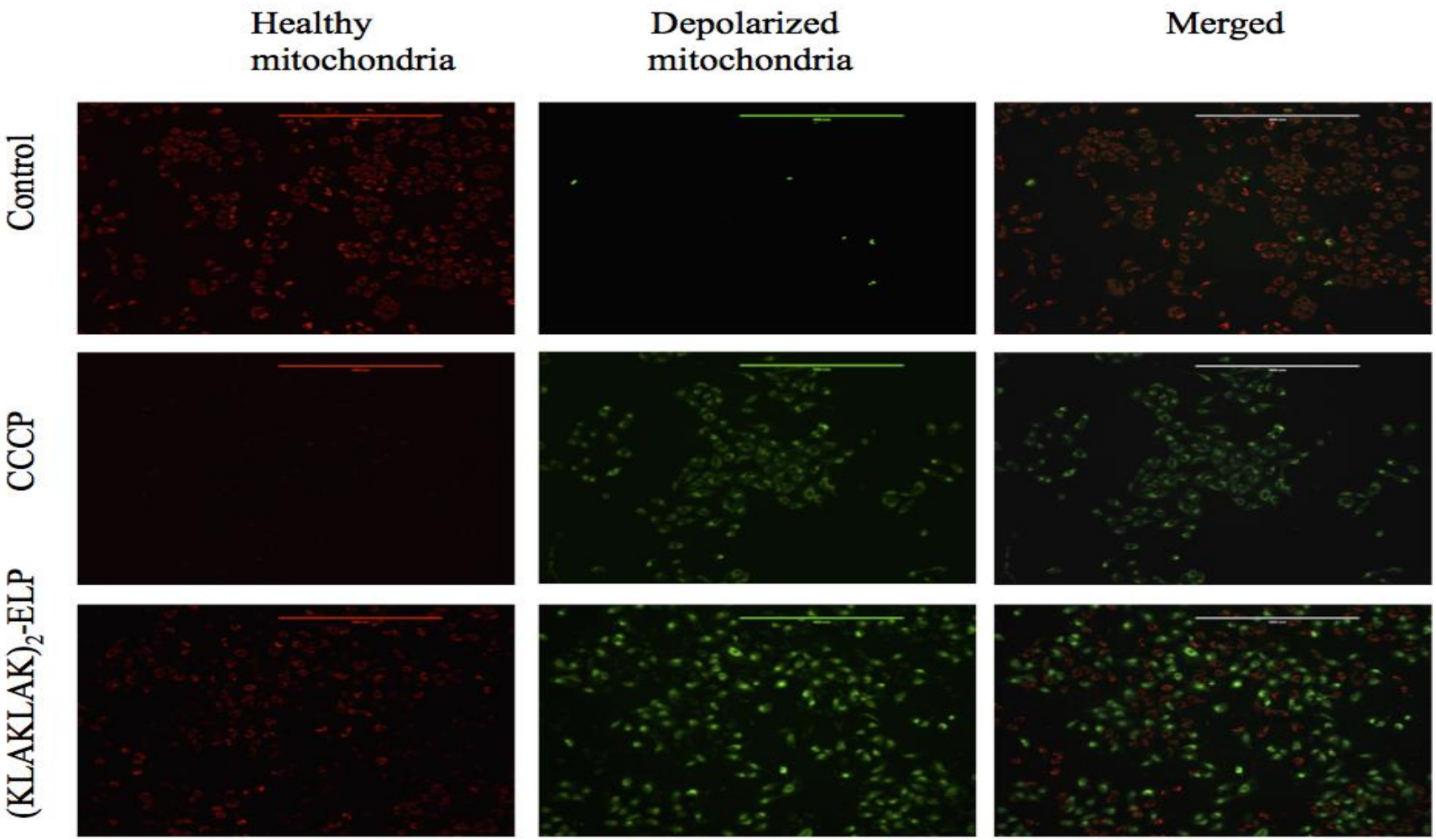

Figure 2.8 Mitochondrial depolarization analysis by fluorescent microscopy. Cells were treated with either 10 μM of $(KLAKLAK)_2$-ELP or CCCP diluted to a final concentration of 50 μM. The control consisted of untreated cells. Mitochondria are stained red (healthy) or green (depolarized). The results clearly show that the fusion $(KLAKLAK)_2$-ELP causes mitochondrial depolarization. Bar = 400μm.

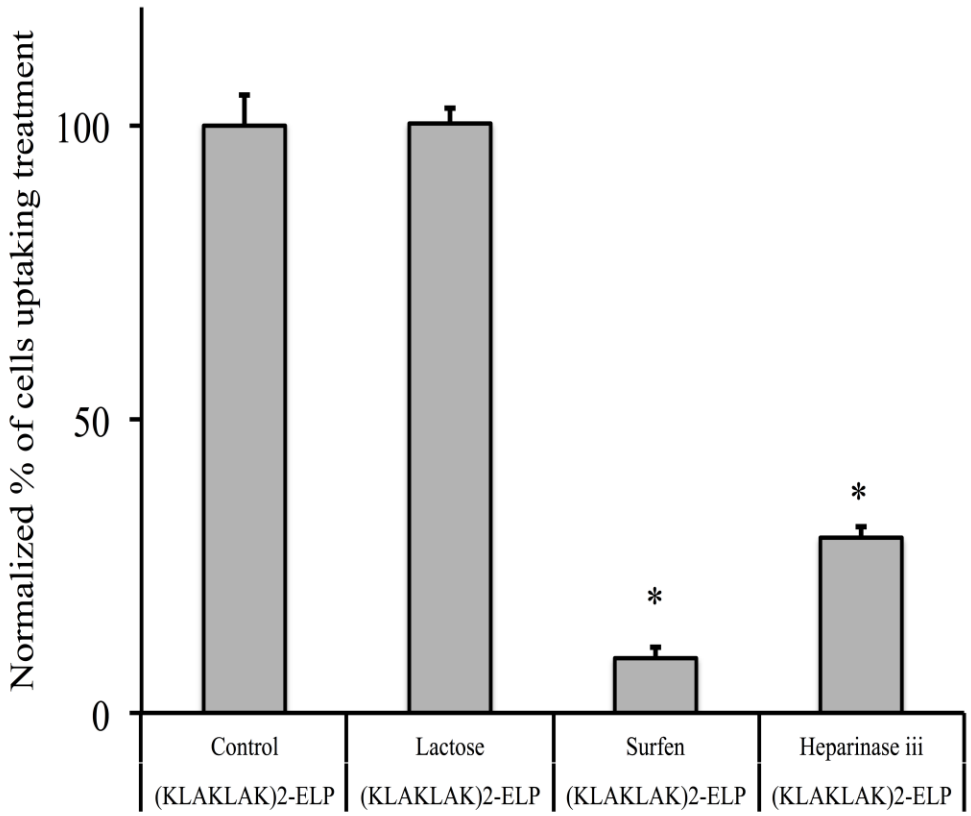

Figure 2.9 $(KLAKLAK)_2$-ELP internalization after blocking the elastin receptor complex and heparan sulfate proteoglycan. A549 cells were pretreated with lactose, Heparinase III, or surfen for 30 minutes, except for control. These cells were then treated with 10μM of labeled $(KLAKLAK)_2$-ELP for 24 Hrs. The percent of cells uptaking the treatment was quantified by flow cytometry. To make sure that only internalized $(KLAKLAK)_2$-ELP was quantified, trypan blue was added to the cell suspension before analysis to quench any labeled molecule bound to the cell surface. This experiment was repeated two times with triplicates. * indicates $p < 0.05$ when compared to control.

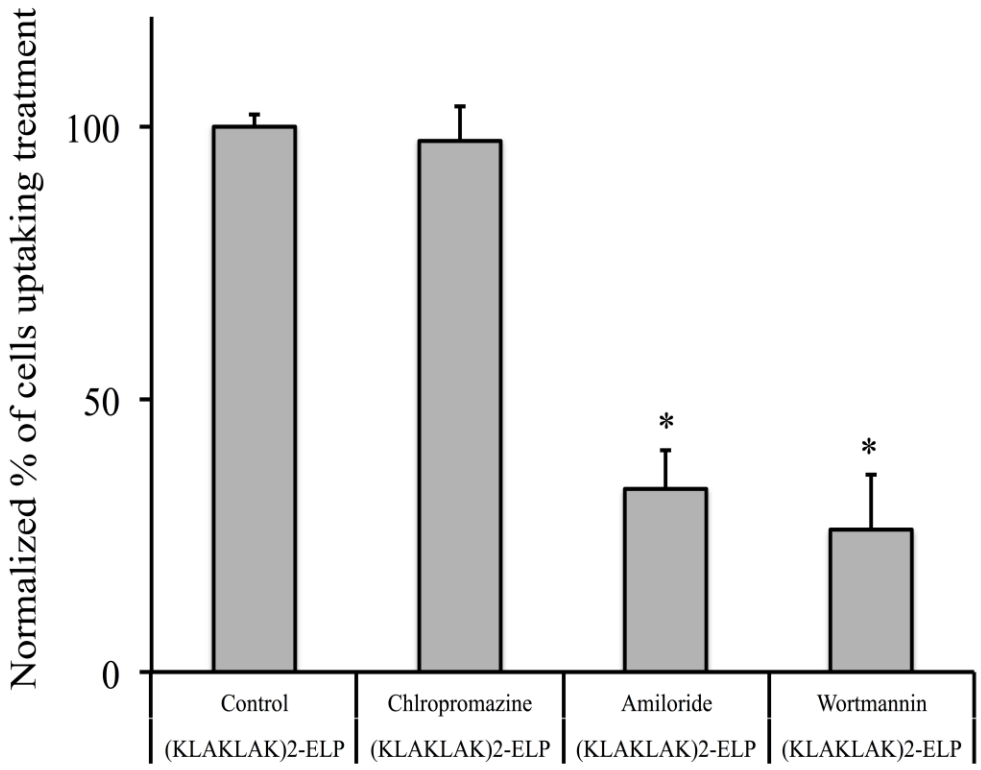

Figure 2.10 $(KLAKLAK)_2$-ELP internalization after blocking receptor mediated endocytosis and macropinocytosis. A549 cells were pretreated with chlorpromazine (receptor-mediated endocytosis blocker), wortmannin or amiloride (macropinocytosis blockers) for 1 Hr. The cells were then treated with 10μM of labeled $(KLAKLAK)_2$-ELP for 24 Hrs. in the presence of the blockers before analysis by flow cytometry. Trypan blue was added to the cell suspension before analysis to prevent including particles that may be bound to the cell surface. This experiment was repeated two times with triplicates. * indicates $p < 0.05$ when compared to control. Error bars represent ±SEM.

2.7 References

[1] M. Shah, P. Y. Hsueh, G. Sun, H. Y. Chang, S. M. Janib, and J. A. MacKay, "Biodegradation of elastin-like polypeptide nanoparticles," *Protein Sci,* vol. 21, pp. 743-50, Jun 2012.

[2] M. R. D. Ashutosh Chilkoti, Dan E. Meyer, "Design of thermally responsive, recombinant polypeptide carriers for targeted drug delivery," *Adv Drug Deliv Rev,* vol. 54, pp. 1093-1111, 2002.

[3] J. Despanie, J. P. Dhandhukia, S. F. Hamm-Alvarez, and J. A. MacKay, "Elastin-like polypeptides: Therapeutic applications for an emerging class of nanomedicines," *J Control Release,* Nov 11 2015.

[4] D. W. Urry, "Physical Chemistry of Biological Free Energy Transduction As Demonstrated by Elastic Protein-Based Polymers†," *J Phys Chem B,* vol. 101, pp. 11007-11028, 1997.

[5] T. Christensen, W. Hassouneh, K. Trabbic-Carlson, and A. Chilkoti, "Predicting transition temperatures of elastin-like polypeptide fusion proteins," *Biomacromolecules,* vol. 14, pp. 1514-9, May 13 2013.

[6] D. M. Floss, K. Schallau, S. Rose-John, U. Conrad, and J. Scheller, "Elastin-like polypeptides revolutionize recombinant protein expression and their biomedical application," *Trends Biotechnol,* vol. 28, pp. 37-45, Jan 2010.

[7] C. M. Bellingham, M. A. Lillie, J. M. Gosline, G. M. Wright, B. C. Starcher, A. J. Bailey, *et al.*, "Recombinant human elastin polypeptides self-assemble into biomaterials with elastin-like properties," *Biopolymers,* vol. 70, pp. 445-55, Dec 2003.

[8] F. W. Keeley, C. M. Bellingham, and K. A. Woodhouse, "Elastin as a self-organizing biomaterial: use of recombinantly expressed human elastin polypeptides as a model for investigations of structure and self-assembly of elastin," *Philos Trans R Soc Lond B Biol Sci,* vol. 357, pp. 185-9, Feb 28 2002.

[9] G. L. Bidwell, 3rd and D. Raucher, "Cell penetrating elastin-like polypeptides for therapeutic peptide delivery," *Adv Drug Deliv Rev,* vol. 62, pp. 1486-96, Dec 30 2010.

[10] W. Hassouneh, S. R. MacEwan, and A. Chilkoti, "Fusions of elastin-like polypeptides to pharmaceutical proteins," *Methods Enzymol,* vol. 502, pp. 215-37, 2012.

[11] M. Javadpour, M. Juban, W. Lo, and S. Bishop, "De Novo Antimicrobial peptides with Low Mammalian Cell Toxicity," *Journal of Medicinal Chemistry,* vol. 39, 1996.

[12] C. Leuschner and W. Hansel, "Membrane disrupting lytic peptides for cancer treatments," *Curr Pharm Des,* vol. 10, pp. 2299-310, 2004.

[13] M. Ellerby, A. Wadih, L. Ellerby, and R. Kain, "Anti-cancer activity of targeted pro-apoptotic peptides," *Nature America Inc.,* vol. 5, 1999.

[14] E. M. Barbu, F. Shirazi, D. M. McGrath, N. Albert, R. L. Sidman, R. Pasqualini, *et al.*, "An antimicrobial peptidomimetic induces Mucorales cell death through mitochondria-mediated apoptosis," *PLoS One,* vol. 8, p. e76981, 2013.

[15] S. Bouchet, R. Tang, F. Fava, O. Legrand, and B. Bauvois, "The CNGRC-GG-D(KLAKLAK)2 peptide induces a caspase-independent, Ca2+-dependent death in human leukemic myeloid cells by targeting surface aminopeptidase N/CD13," *Oncotarget,* Dec 9 2015.

[16] S. Moktan and D. Raucher, "Anticancer activity of proapoptotic peptides is highly improved by thermal targeting using elastin-like polypeptides," *Int J Pept Res Ther,* vol. 18, pp. 227-237, Sep 2012.

[17] S. M. Standley, D. J. Toft, H. Cheng, S. Soukasene, J. Chen, S. M. Raja, *et al.*, "Induction of cancer cell death by self-assembling nanostructures incorporating a cytotoxic peptide," *Cancer Res,* vol. 70, pp. 3020-6, Apr 15 2010.

[18] D. E. Meyer and A. Chilkoti, "Genetically encoded synthesis of protein-based polymers with precisely specified molecular weight and sequence by recursive directional ligation: examples from the elastin-like polypeptide system," *Biomacromolecules,* vol. 3, pp. 357-67, Mar-Apr 2002.

[19] P. Koria, H. Yagi, Y. Kitagawa, Z. Megeed, Y. Nahmias, R. Sheridan, *et al.*, "Self-assembling elastin-like peptides growth factor chimeric nanoparticles for the treatment of chronic wounds," *Proc Natl Acad Sci U S A,* vol. 108, pp. 1034-9, Jan 18 2011.

[20] X. X. Zhang, P. G. Allen, and M. Grinstaff, "Macropinocytosis is the major pathway responsible for DNA transfection in CHO cells by a charge-reversal amphiphile," *Mol Pharm,* vol. 8, pp. 758-66, Jun 6 2011.

[21] J. R. McDaniel, D. J. Callahan, and A. Chilkoti, "Drug delivery to solid tumors by elastin-like polypeptides," *Adv Drug Deliv Rev,* vol. 62, pp. 1456-67, Dec 30 2010.

[22] W. Liu, M. R. Dreher, D. Y. Furgeson, K. V. Peixoto, H. Yuan, M. R. Zalutsky, *et al.*, "Tumor accumulation, degradation and pharmacokinetics of elastin-like polypeptides in nude mice," *J Control Release,* vol. 116, pp. 170-8, Nov 28 2006.

[23] A. J. S. Matthew R. Dreher, Karl Fischer, Richard J. Smith, Anand Patel, Manfred Schmidt, and Ashutosh Chilkot, "Temperature Triggered Self-Assembly of Polypeptides into Multivalent Spherical Micelles," *J Am. Che. Soc.*, vol. 130, pp. 687-694, 2007.

[24] I. Massodi, G. L. Bidwell, 3rd, and D. Raucher, "Evaluation of cell penetrating peptides fused to elastin-like polypeptide for drug delivery," *J Control Release,* vol. 108, pp. 396-408, Nov 28 2005.

[25] L. Duca, C. Blanchevoye, B. Cantarelli, C. Ghoneim, S. Dedieu, F. Delacoux, *et al.*, "The elastin receptor complex transduces signals through the catalytic activity of its Neu-1 subunit," *J Biol Chem,* vol. 282, pp. 12484-91, Apr 27 2007.

[26] D. Gheduzzi, D. Guerra, B. Bochicchio, A. Pepe, A. M. Tamburro, D. Quaglino, *et al.*, "Heparan sulphate interacts with tropoelastin, with some tropoelastin peptides and is present in human dermis elastic fibers," *Matrix Biol,* vol. 24, pp. 15-25, Feb 2005.

[27] M. Schuksz, M. M. Fuster, J. R. Brown, B. E. Crawford, D. P. Ditto, R. Lawrence, *et al.*, "Surfen, a small molecule antagonist of heparan sulfate," *Proc Natl Acad Sci U S A,* vol. 105, pp. 13075-80, Sep 2 2008.

[28] C. Commisso, S. M. Davidson, R. G. Soydaner-Azeloglu, S. J. Parker, J. J. Kamphorst, S. Hackett, *et al.*, "Macropinocytosis of protein is an amino acid supply route in Ras-transformed cells," *Nature,* vol. 497, pp. 633-7, May 30 2013.

[29] G. Redelman-Sidi, G. Iyer, D. B. Solit, and M. S. Glickman, "Oncogenic activation of Pak1-dependent pathway of macropinocytosis determines BCG entry into bladder cancer cells," *Cancer Res,* vol. 73, pp. 1156-67, Feb 1 2013.

[30] T. J. Broekelmann, B. A. Kozel, H. Ishibashi, C. C. Werneck, F. W. Keeley, L. Zhang, *et al.*, "Tropoelastin interacts with cell-surface glycosaminoglycans via its COOH-terminal domain," *J Biol Chem,* vol. 280, pp. 40939-47, Dec 9 2005.

[31] D. Raucher and A. Chilkoti, "Enhanced uptake of a thermally responsive polypeptide by tumor cells in response to its hyperthermia-mediated phase transition," *Cancer Res*, vol. 61, pp. 7163-70, Oct 1 2001.

[32] R. E. Hileman, J. R. Fromm, J. M. Weiler, and R. J. Linhardt, "Glycosaminoglycan-protein interactions: definition of consensus sites in glycosaminoglycan binding proteins," *Bioessays*, vol. 20, pp. 156-67, Feb 1998.

CHAPTER 3: KGF-ELP ENHANCES MACROPINOCYTOSIS IN KGFR OVEREXPRESSING CELLS

3.1 Note to Reader

Part of this chapter was published in Medical Oncology: R. Iglesias and P. Koria, "Leveraging growth factor induced macropinocytosis for targeted treatment of lung cancer," Med Oncol, vol. 32, p. 259, Dec 2015. Permission is included in Appendix B

3.2 Introduction

In this chapter we show that the fusion of the keratinocyte growth factor (KGF) and elastin like polypeptide (ELP), KGF-ELP, selectively enhances macropinocytosis in keratinocyte growth factor receptor (KGFR) overexpressing cells. Furthermore, we demonstrate that this selectivity can be further used to improve the internalization of the fusion $(KLAKLAK)_2$-ELP discussed in the previous chapter. Finally, the heterogeneous nanoparticle comprising of KGF-ELP and $(KLAKLAK)_2$-ELP clearly improves the cytotoxic effect of $(KLAKLAK)_2$-ELP in KGFR overexpressing lung cancer cells.

3.3 Keratinocyte Growth Factor (KGF)

Growth factors are proteins whose functions include cell proliferation, migration, and differentiation [1]. The mode of action of these molecules is through their interaction with their receptor on the cell surface. Once this interaction occurs, intracellular signaling occurs that permits the cell to undergo several changes resulting in the functions mentioned above.

Much emphasis has been placed on growth factor receptors as target for cancer treatment.[2-4] It is well known that a common characteristic of several cancer types is the overexpression of growth factor receptors such as the epidermal growth factor receptor (EGFR) [5, 6] and the keratinocyte growth factor receptor (KGFR) [7-9]. Therefore, one method used for targeted treatment has aimed at blocking the extracellular domain of these receptors using monoclonal antibodies (mAb); so that, the ligand/receptor interaction is loss and proliferation is halted [10]. However, mAb are highly specific and a minor change in their target makes them ineffective. Another way that has been used to target receptors is the use of small molecules that block the intracellular domain of the receptors so that signaling pathways are not activated when the ligand/receptor binding occurs [11]. However, the highly mutagenic nature of cancer cells can develop an alternative pathway rendering the treatment unproductive.

Others have looked at the interaction between growth factor and its receptors as an opportunity to selectively deliver cytotoxic cargo to cells overexpressing a receptor. For instance, once the ligand/receptor interaction occurs, the process of receptor mediated endocytosis (RME) initiates [12]. In addition, another internalization process that has been recently gaining more interest is macropinocytosis [13]. This transient process can also be activated or enhanced by growth factors and offers several advantages when compared to RME. For instance, macropinocytosis allows for the uptake of several molecules on the cell periphery while RME is limited to molecules that are in the areas where the interaction occurs.

One of the most common targets in lung cancer is the EGFR. The downside of targeting EGFR is that it is ubiquitously express; thus, it is likely that targeting this receptor results in unwanted systemic toxicity due to its stimulation in normal tissue. KGFR has been identified as another receptor that is overexpressed in lung cancer [8, 14]. The advantage of using this

receptor over EGFR is that KGFR is not expressed ubiquitously; therefore, systemic toxicity may be diminished. Based on this, we opted to target KGFR. However, due to the simplicity of the system we describe in this chapter, other growth factor receptors can easily be targeted such as HGF [15] and EGF [16].

3.4 Macropinocytosis

Endocytosis is a process through which cells internalize nutrients, hormones, proteins, and lipids that are required for diverse cell functions such as their proliferation, growth and health maintenance. The vesicles formed during endocytosis fuse with endosomes for cargo sorting and then either recycle back to the cell membrane and their contents expelled out from the cell or they can fuse with lysosomes for subsequent degradation of the cargo. Endocytosis can be subdivided into clathrin-dependent and clathrin-independent endocytosis depending on whether the protein clathrin coats or not the formed vesicles, (Figure 3.1).

Clathrin-dependent endocytosis is also known as receptor mediated endocytosis (RME). It is the most studied and understood endocytotic mechanism. One major characteristic RME is that it internalizes macromolecules selectively. In addition, this process requires the interaction between a ligand and its cell membrane receptor; these receptors are found on regions called clathrin-coated pits. Upon ligand-receptor interaction, closure of these pits result in the formation of vesicles that are coated with the protein clathrin making them leak-proof; therefore, the cargo does not diffuse into the cytoplasm. As mentioned above however, these vesicles will fuse with endosomes for sorting of their contents and eventual recycle or degradation by lysosomes.

Many studies have focus on the use of RME as a targeted delivery mechanism for drugs to treat cancer. However, due to innate characteristics of this mechanism, it also provides many challenges for its use. Other works have reported endosomal entrapment of their drugs [17-19].

This occurs because of the leak proof vesicles formed during RME do not permit the diffusion of the drugs into the cytoplasm, lowering or preventing the efficacy of the treatment due its low intracellular concentration. Another limitation is the size constraint when using RME. RME vesicles have a diameter of about 100 nm, which limits the amount of therapeutics that can be internalized. Furthermore, lysosomal degradation may also prevent the treatment from being successful.

Macropinocytosis is one of the clathrin-independent endocytotic mechanisms; it is an actin-driven process. Unlike receptor-mediated endocytosis however, this process does not rely directly on cargo/receptor interaction for its activation [20]. Therefore, macropinocytosis is a non-specific internalization mechanism. It is a transient process in most cells and it can be stimulated by the interaction between growth factors, such as the keratinocytes growth factor (KGF) and epidermal growth factor (EGF), and their receptors [16, 21, 22]. This interaction leads to an increase in actin polymerization that will result in cell membrane extensions called ruffles. Falling back of these ruffles on the plasma membrane results on the formation of vesicles called macropinosomes, which are characterized for being large, uncoated and leaky vesicles [23-25].

Many of the innate characteristics of macropinocytosis make it an interesting targeted mechanism to look into for targeted therapy. As mentioned above, macropinocytosis is non-selective; therefore, it can indiscriminately internalize molecules that are bound to the cell membrane without the need for a specific cargo/receptor interaction. Consequently, the interaction between a growth factor and its receptor resulting in enhanced macropinocytosis can cause the uptake of multiple molecules bound on the cells surface [26]. In addition, the leaky

nature of macropinosomes allows for the diffusion of the uptaken molecules to the cytoplasm avoiding endosomal entrapment.

Having learned in the previous chapter that ELPs interact with heparan sulfate on the cell surface, it makes us reason that this interaction may assist in the internalization of ELP fusion molecules by allowing them to be bound to the cell surface for macropinocytosis to act on them. In addition, we reasoned that a growth factor fused to ELPs could result in enhancement of macropinocytosis. Therefore, this chapter deals with the use a heterogeneous nanoparticle consisting of $(KLAKLAK)_2$-ELP and KGF-ELP, figure 3.5. This multifunctional nanoparticle allows for the selective enhancement of macropinocytosis in cells overexpressing the keratinocyte growth factor receptor (KGFR). At the same time, due to the ELP domain, many of these nanoparticles will be bound on the cell surface of the cell; therefore, many of them could be internalized. Once inside the cell, the $(KLAKLAK)_2$-ELP fusion will cause cell death due to mitochondrial depolarization as described in the previous chapter.

3.5 KGF-ELP Fusion Selectively Enhances Macropinocytosis

3.5.1 Materials and Methods

Fetal bovine serum (FBS) and Dulbecco modified Eagle Medium (DMEM) were purchased from Life Technologies. The restriction enzymes and other enzymes used for cloning were purchased from New England Biolabs (Ipswich, MA). H292, A549, H1650, H23, and HCC827 cells were kindly donated by Dr. Haura from Moffit Cancer Center. CRCL2522, fibroblasts, were purchased from ATCC (Manassas, VA). Human Small Airway Epithelial Cells (SAEC) cells were kindly donated by Dr. Narasaiah Kolliputi from the Department of Internal Medicine at USF Health. Growth factors and apoptotic peptide genes were purchased from GenScript (Piscataway, NJ). The miniprep and gel extraction kits were purchased from

QIAGEN. The reagents for real-time polymerase chain reaction (RT-PCR) were purchased from Bio-Rad.

3.5.1.1 Synthesis of KGF-ELP

The PUC57 plasmids containing the genes **(**VPGVG)5 , (VPGVG)2VPGCG(VPGVG)2 , and KGF were purchased from Genscript (Piscataway, NJ). The V40C2 encoding gene was made using recursive direction ligation method as described previously [27]. The KGF gene was excised using PflMI and Bgll enzymes. This gene was then run on a 0.08% agarose gel and extracted using QIAquick Gel Extraction Kit. The restriction enzyme PflMI linearized the pUC19 vector containing the ELP sequence and the excised KGF gene was cloned in frame with the ELP gene. This resulted in the pUC19 vector containing the KGF-ELP fusion protein gene flanked by pfIMI and BgII sites. The sequences encoding for the fusion protein was then removed from the pUC19 vector using pflMI and BgII enzymes and recovered by gel extraction as explained above. After extraction, this gene was cloned in a modified pET25b+ expression vector through SfiI site. This vector was modified to incorporate a SfiI cloning site for the cloning of the fusion protein.

The pET25b+ vector containing the fusion protein gene was transformed into BLRD competent cells through heat shock at 42^{o}C. A starting culture of 50 ml was inoculated overnight and added to a 1 L culture the next day. The 1 L culture was then grown overnight and subsequently purified by inverse transition cycling as described previously [28]. Figure 3.2 shows a representation of the genes for KGF and ELP and the production of the fusion KGF-ELP.

3.5.1.2 Cell Culture

Cells were cultured in a humidified incubator at 37^0C and 5% CO_2. Cells were seeded on 24 or 48-well plates until they were approximately 70% confluent. CRL-2522 (non-malignant human foreskin fibroblast), A549 (human lung carcinoma), H292 (human lung carcinoma), HCC827 (human lung adenocarcinoma), H23 (human lung adenocarcinoma), and H1650 (human lung adenocarcinoma) were grown in DMEM supplemented with 10% FBS and 1% AA (Complete Medium). SAEC were cultured in airway epithelial cell basal medium (PCS-300-030) supplemented with Small Airway Epithelial Cell Growth Kit (PCS-301-040).

3.5.1.3 Internalization of KGF-ELP

Cells (HCC827) were treated for 24 Hrs. with 50 μM of KGF-ELP. After the treatment, cells were fixed with 2.5% glutaraldehyde in 100 mM phosphate buffer at pH 7. Following fixation, standard embedding protocol for resin section was followed. TEM imaging was performed at Electron Microscopy Core Lab in the Interdisciplinary Science Building at the University of South Florida. Figure 3.3 shows the internalized KGF-ELP.

3.5.1.4 Labeling of the Fusion Proteins

The cysteines present in the ELP sequence were labeled using maleimide chemistry for the particle internalization experiments. Fluorescein-5-maleimide (AnaSpec Inc cat # 81405) was mixed with the fusion proteins. The mixture was placed on an orbital shaker and incubated at room temperature for 2 hours. Unconjugated fluorescein was removed by a series of hot and cold cycles on a bench top centrifuge ran at a speed of 20000g for 10 minutes each time. The supernatant was discarded after the hot spin and an equal amount of cold sterile PBS was added. This mixture was spun at 4 ^{0}C and the supernatant was collected while the pellet was discarded.

This formed one complete cycle of inverse temperature cycling. At least 5 cycles were performed to remove of all the unconjugated Fluorescein.

3.5.1.5 Fusion Protein Internalization Assay

Cells (50,000/well) were seeded in 24-well plates and cultured as described above. They were let grow until they were about 70% confluent and were treated with the indicated treatments. For analysis, cells were washed twice with ice-cold PBS and were trypsinized using 0.25% trypsin (100 µl). Cells were pelleted and re-suspended in 300 µl of PBS containing 50 □g/ml of trypan blue to quench signal arising from the cell surface and 4',6-diamidino-2-phenylindole (DAPI) to allow exclusion of nonviable cells. The cells were analyzed using flow cytometry and either the percent of fluorescent cells or the average intensity was quantified and reported.

3.5.1.6 Dextran Assay

Twenty-four hours after the indicated treatment, dextran tetramethylrhodamine (Life Technologies cat # D1818) was added for 1 Hr. at a concentration of 100 □g/ml. Before flow cytometry analysis, cells were washed at least five times with ice-cold PBS. The steps described above for flow analysis were then followed; however, trypan blue was not added.

3.5.1.7 Gene Expression Using RT-PCR

Cells (500,000/well) were seeded on 6-well plates and let grow to about 80% confluency. RNA was isolated using the SV Total RNA isolation System (Promega cat # Z3100). cDNA synthesis was done using iScript cDNA synthesis Kit from BIO-RAD (cat # 1708890) following manufacturer's protocol. RT-PCR was performed using BIO-RAD C1000 Thermal Cycler. The following primers were used for the KGFR cDNA amplification: forward primer

CAATTATATAGGGCAGGCCAACCAG and reverse primer AAGAAGACCCCTATGCAGT-AAATGG.

3.5.1.8 Live/Dead Assay

Cells were seeded and treated with the indicated treatments for 3 days. After their respective treatments, ethidium homodimer-1 (Life Technologies cat # E1169) was added to each well to a final concentration of 4uM. Cells were then incubated for 1 hour at 37^{o}C. After the incubation time, cells were washed twice with PBS to remove floating cells. NucBlue (Life Technologies R37605) was then added for 20 minutes to stain nuclei, followed by two washes with PBS. Eight random pictures were taken per well using the EVOS fluorescence microscope (10X magnification). Pictures were taken in different channels (blue, green, red) and overlay. Live/dead cell discrimination was performed using image J. A macro was created using the functions split channel, threshold, and cell counter to count the total number of live cells (blue) in each picture. Dead cells that were not removed after the washes were stained red or magenta (blue and red); adjusting the threshold for the picture being analyzed easily isolated these cells. Therefore, the final count of cells per picture only included live cells.

3.5.1.9 Statistical Analysis

For statistical significance, the p value was calculated using ANOVA single factor. P values < 0.05 were considered significant. The reported errors indicate the ±SEM.

3.5.2 Results

3.5.2.1 KGF-ELP Enhances Internalization of $(KLAKLAK)_2$-ELP in KGFR Over-expressing Cells

Macropinocytosis is a non-specific internalization process that results from cell ruffling; furthermore, this process can be enhanced by growth factors [21]. Therefore, we reasoned that a

treatment that includes growth factors could selectively enhance macropinocytosis in growth factor receptor expressing cells. Earlier work has reported the overexpression of the keratinocyte growth factor receptor (KGFR) in lung cancer cells [8]. Consequently, we used RT-PCR to measure the expression of this receptor in several cell types including five lung cancer cell lines and two noncancerous cell lines (Figure 3.4). We selected A549 cells for subsequent experiments since they had the highest expression of this receptor. Our lab has previously synthesized the fusion comprising of KGF and ELP, KGF-ELP, this fusion is bioactive and self-assembles into nanostructures [28]. In order to test our hypothesis of selective enhancement of macropinocytosis we created heterogeneous particles comprising of KGF-ELP and $(KLAKLAK)_2$-ELP (Figure 3.5); the internalization analysis was carried out using flow cytometry. The results clearly show that the heterogeneous particles containing $(KLAKLAK)_2$-ELP improved $(KLAKLAK)_2$-ELP uptake by 21 folds compared to homogeneous particles consisting of $(KLAKLAK)_2$-ELP only (Figure 3.6). Since adding KGF-ELP to the $(KLAKLAK)_2$-ELP formulation results in an increased number of particles, we compared the uptake to homogeneous particles containing similar concentration of $(KLAKLAK)_2$-ELP as well as heterogeneous particles comprising of non-functionalized ELP and $(KLAKLAK)_2$-ELP (Figure 3.6). These data clearly suggest that inclusion of KGF-ELP in the NP formulation improved the uptake of $(KLAKLAK)_2$-ELP in KGFR overexpressing cells. To further demonstrate the role of KGF-ELP in targeted internalization, we compared the $(KLAKLAK)_2$-ELP uptake in fibroblasts, which do not express the KGFR. Indeed, the increase in $(KLAKLAK)_2$-ELP uptake induced by the inclusion of KGF-ELP was not observed in fibroblasts (Figure 3.7).

We further wanted to demonstrate the direct relation between KGF-ELP treatment and enhanced macropinocytosis. To accomplish this task, macropinosome formation was quantified

after a 24 Hr. treatment with 1μM, 10μM or 50μM of KGF-ELP on A549 cells. Fluorescent pictures were taken for visual representation (Figure 3.8). The results were quantified using flow cytometry. Our data clearly suggest a dose dependent effect on macropinosome formation in A549 cells (Figure 3.9). To show that this effect is selective, fibroblasts were also treated with 50μM of KGF-ELP as described above. The results showed no increase in macropinosome formation (Figure 3.10). Combined, the results clearly imply that KGF-ELP induces macropinocytosis selectively in KGFR expressing cells.

3.5.2.2 KGF-ELP Improves the Cytotoxic Effect of $(KLAKLAK)_2$-ELP in KGFR Overexpressing Cells

After showing that a formulation containing KGF-ELP improved the internalization of $(KLAKLAK)_2$-ELP in KGFR overexpressing cells, we tested if this higher internalization would translate to targeted cytotoxicity. While there was no effect on fibroblasts, the combination treatment resulted in about 35 % cell death in cells that had very little KGFR expression (Figure 3.11). Interestingly, the combination treatment resulted in nearly 50% to 70 % cell death in high KGFR expressing cell lines (Figure 3.11, A549, HCC827, and H1650). These data show that the combination treatment of KGF-ELP and $(KLAKLAK)_2$-ELP resulted in significantly higher cell death in high KGFR expressing cell.

3.6 Discussion and Summary

Targeted therapy is increasingly becoming popular for the treatment of lung cancer. Currently, growth factor receptor tyrosine kinase inhibitors that target highly expressed growth factor receptors in lung cancer are used for treatment [29]. Here, we describe an approach of targeting lung cancer cells by exploiting the malignant processes that are inherent to them. Specifically, we report the development of two chimeric fusion proteins namely $(KLAKLAK)_2$-

ELP and KGF-ELP that self-assemble into nanoparticles. In chapter 2 we showed that $(KLAKLAK)_2$-ELP nanoparticles are internalized by cancer cells resulting in cell death. This internalization occurs via macropinocytosis and is mediated by the interaction of the ELP domain with cell surface heparan sulfate proteoglycans (HSPG). In this chapter, we further show that KGF-ELP selectively enhances macropinocytosis in high Keratinocyte Growth Factor Receptor (KGFR) expressing cancer cells. Finally, heterogeneous NPs comprising of KGF-ELP and $(KLAKLAK)_2$-ELP selectively kill high KGFR expressing lung cancer cells with very little impact on normal cells.

Macropinocytosis is enhanced by several growth factors [30, 31]. Therefore, growth factors can be used to target high growth factor receptor expressing lung cancer cells [8, 32]. Indeed, our data demonstrate that macropinocytosis can be enhanced in KGFR over expressing cells using the KGF-ELP fusion protein. This led to an increase in $(KLAKLAK)_2$-ELP internalization by KGF-ELP only in cells overexpressing the KGFR. This uncovers the opportunity to selectively deliver therapeutics using growth factor induced macropinocytosis. While non-targeted macropinocytosis has been described for the delivery of lytic peptides or NPs using cell penetration peptides [33], no studies describe the use of the keratinocyte growth factor to achieve targeted delivery through macropinocytosis. Macropinocytosis is beneficial over the commonly described receptor mediated internalization approaches that usually involve clathrin-coated endocytosis. Firstly, macropinosomes are relatively large (>1□m) thereby allowing efficient internalization of several nanoparticles in one macropinosome [31]. Since, macropinosomes are inherently leaky, it allows rapid release of the nanoparticles in the cytosol escaping lysosomal degradation [34]. Finally, receptor mediated endocytosis results in the formation of one vesicle per ligand/receptor whereas in macropinocytosis once one nanoparticle

binds to the receptor it will result in the uptake of several nanoparticles in the vicinity of the cells due to cell surface ruffling induced by the growth factor; thereby, increasing efficiency of uptake. It is to be noted that this process involves enhancing the process of macropinocytosis through growth factor signaling as opposed to blocking it, which is in contrast to previous approaches. Therefore, care needs to be taken in using this strategy, as there might be some unwanted cancer enhancing effect due to growth factor receptor signaling.

In summary, in this chapter we have taken advantage and expanded on the findings in the previous chapter. Previously we demonstrated that $(KLAKLAK)_2$-ELP is internalized by cells through the process of macropinocytosis. Furthermore, the ELP domain also becomes critical since it facilitates the $(KLAKLAK)_2$-ELP nanoparticles to be bound to the cell surface; a step that is required for macropinocytosis. Since macropinocytosis can be stimulated by growth factors; in this chapter, we selectively enhanced macropinocytosis and the uptake of $(KLAKLAK)_2$-ELP in KGFR overexpressing lung cancer cells using the fusion KGF-ELP. While we have focused on the delivery of the mitochondriotoxic peptide $(KLAKLAK)_2$, this approach can easily be expanded to other peptides, imaging agents, or drugs thereby having broad applications in cancer as well as intracellular drug delivery.

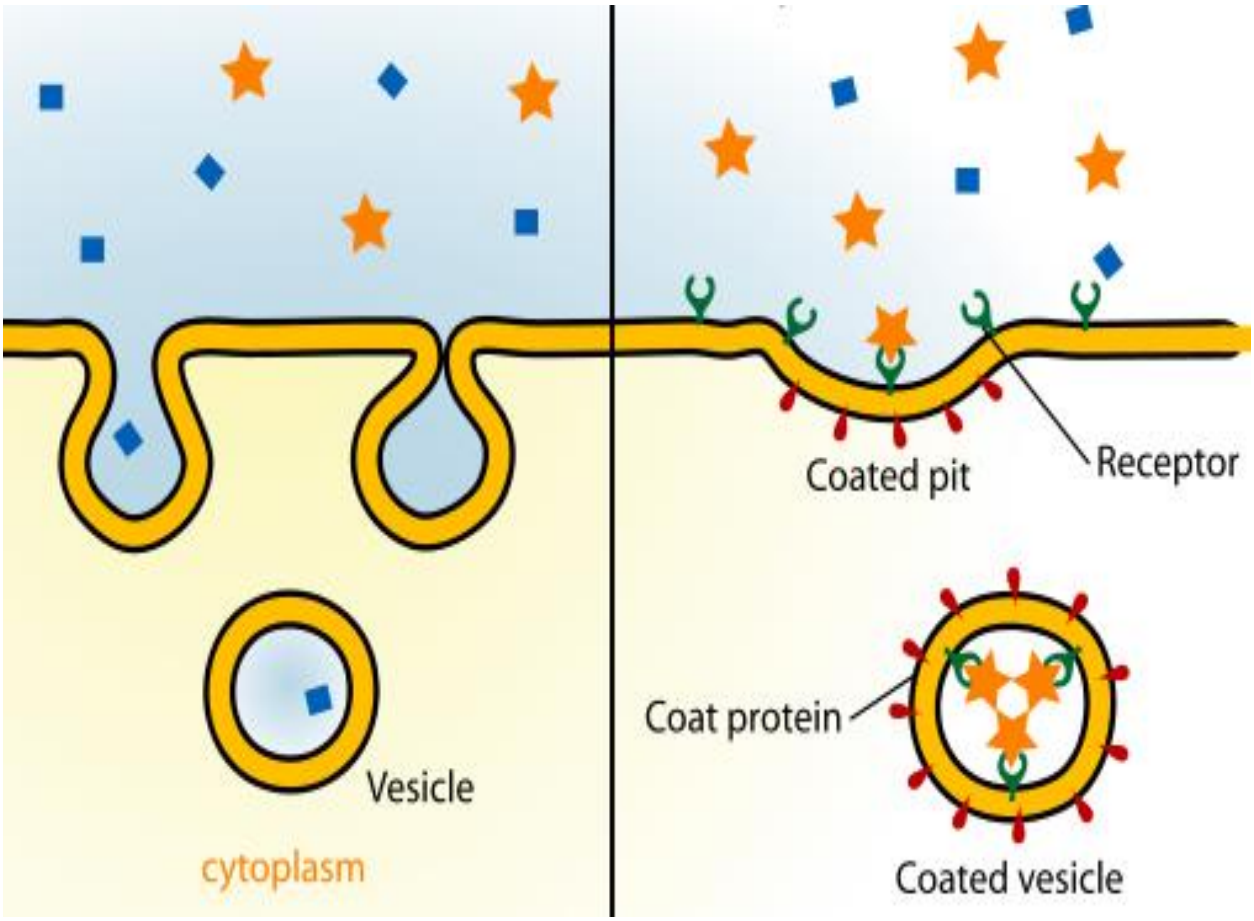

Figure 3.1 Representation of clathrin-independent and clathrin-dependent endocytosis [35]. Right figure represents clathrin-independent endocytosis while left represent clathrin-dependent endocytosis.

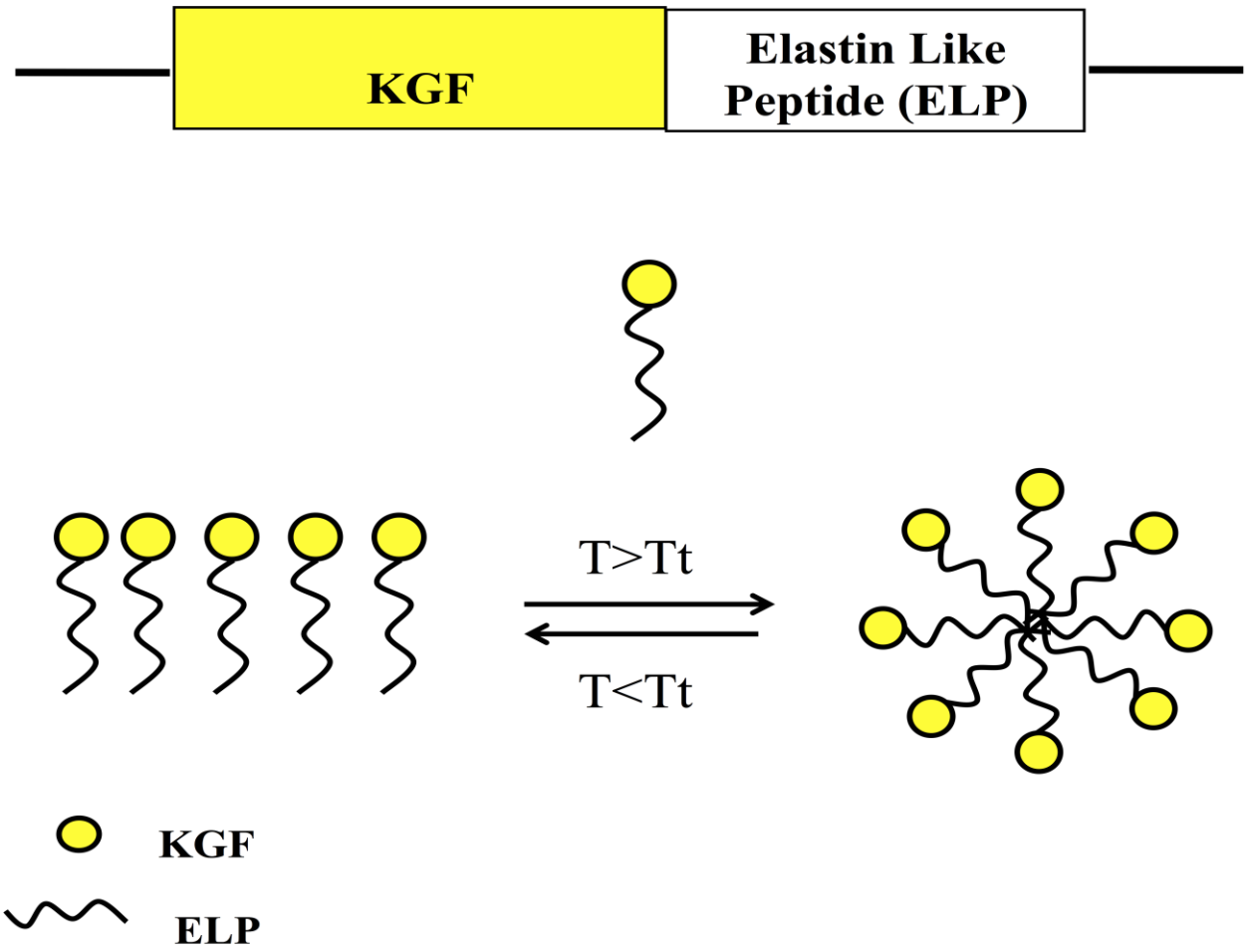

Figure 3.2 Representation of the KGF-ELP purification and self-assemble property. Top, representation of the KGF gene, ELP genes, and their translation to the fusion $(KLAKLAK)_2$-ELP. Bottom, illustration of the phase transition property of the fusion above and below its transition temperature (T_t).

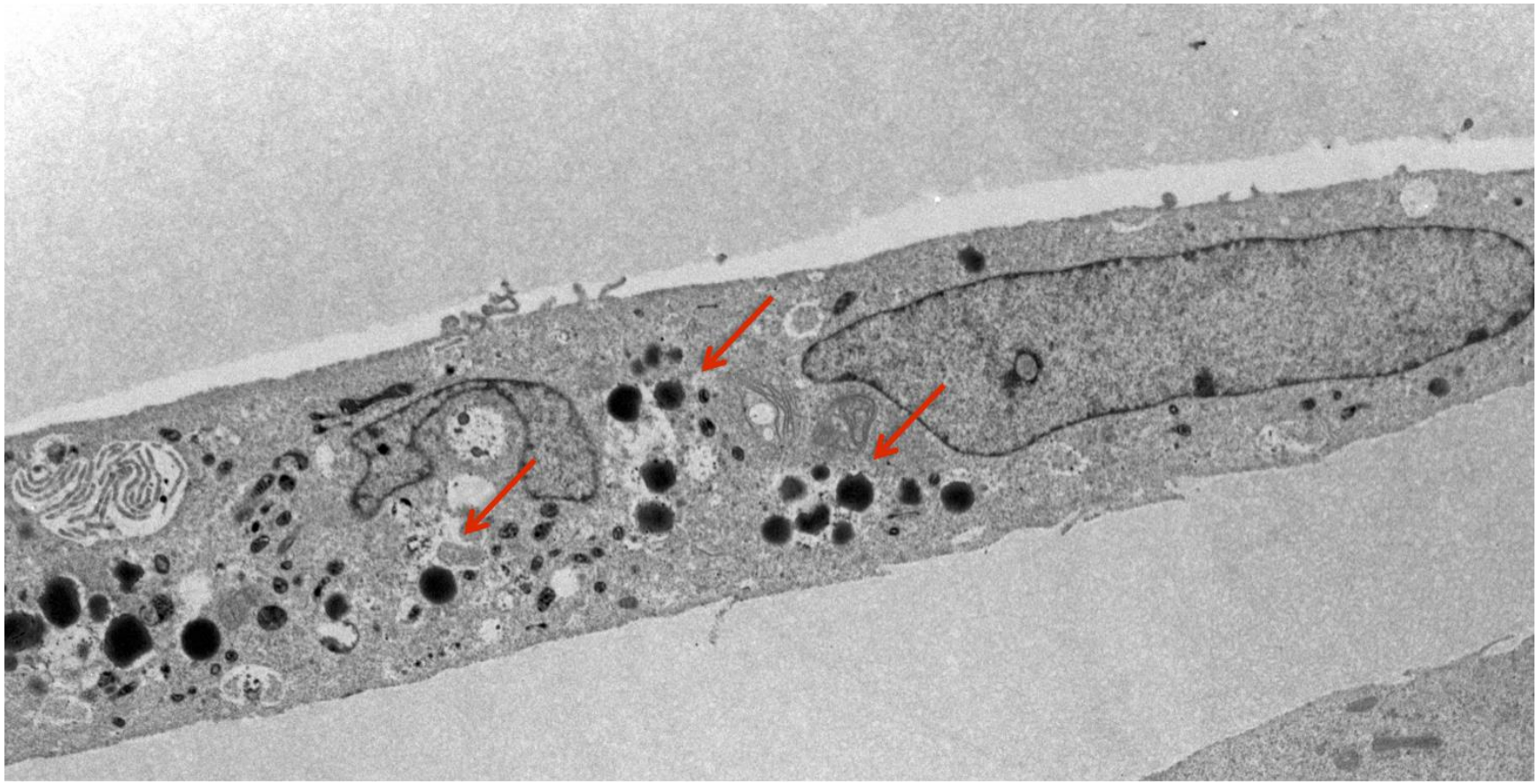

Figure 3.3 Internalization of KGF-ELP as seen by TEM. HCC827 cells were treated for 24 Hrs. with 50 μM of KGF-ELP; they were then prepared and analyzed as described in the materials and methods section. The red arrows show the location of the KGF-ELP nanoparticle.

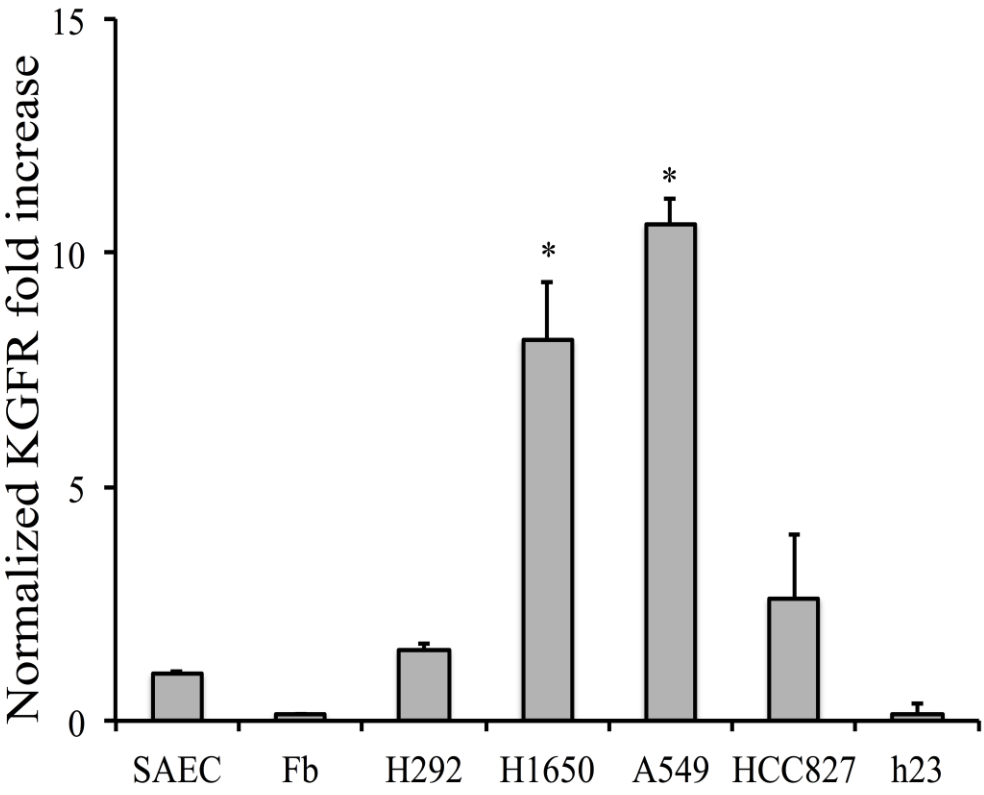

Figure 3.4 KGFR expression in lung cancer and normal cells. RT-PCR was used to determine the Keratinocyte growth factor receptor (KGFR) expression in different cell lines. Normal lung cells (SAEC), cancerous lung cells (H292, H1650, A549, HCC827, H23), and normal skin cells (fibroblast) were tested for KGFR expression level. Cells were cultured in 6 well plates; once they were about 90% confluent, their total RNA was extracted and cDNA was produced as described in the material section. The results were normalized to Primary Small Airway Epithelial cells (SAEC).

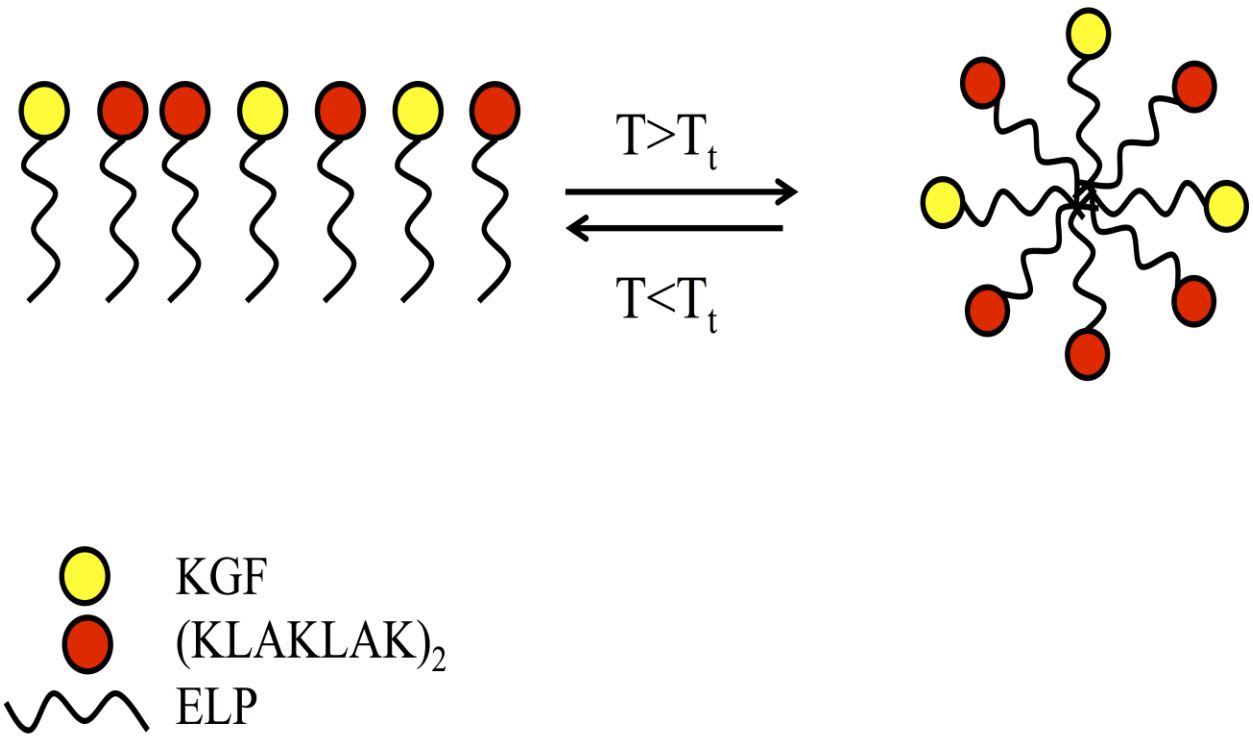

Figure 3.5 Representation of the heterogeneous nanoparticle comprising of KGF-ELP and $(KLAKLAK)_2$-ELP.

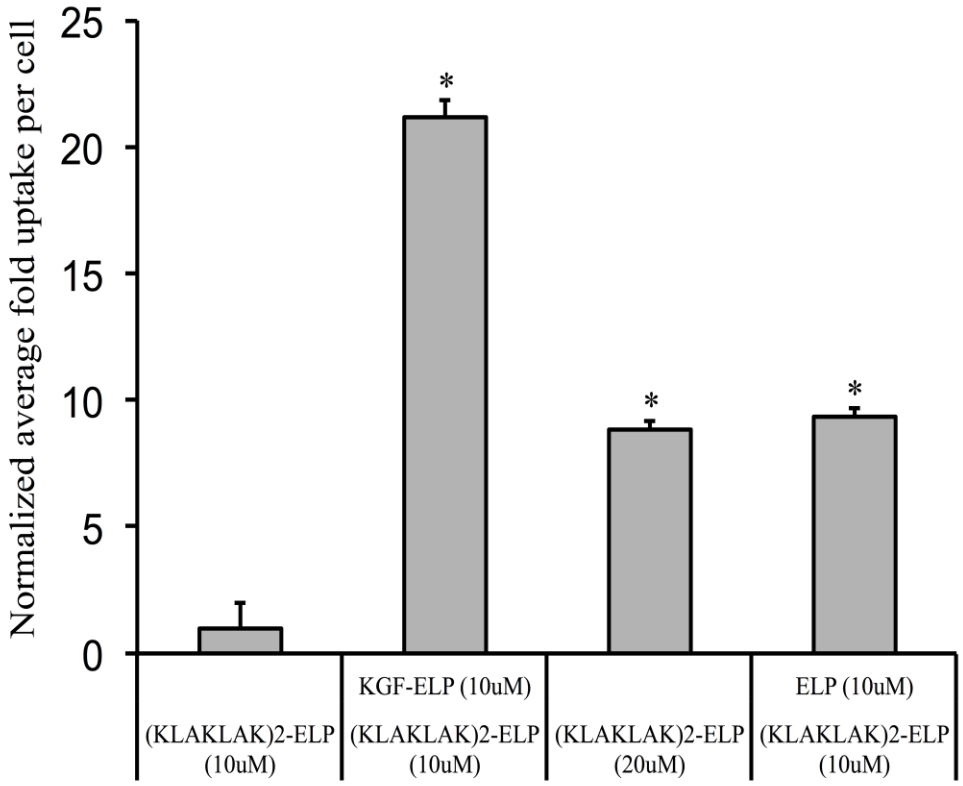

Figure 3.6 Enhanced internalization of $(KLAKLAK)_2$-ELP assisted by KGF-ELP in KGFR overexpressing cells. A549 cells were treated for 24 Hrs. with four different formulations to test for improved internalization due to KGF-ELP. Since nanoparticle formation, which also improves internalization, is dependent on concentration, equimolar treatments in the absence of KGF-ELP were also included. Labeled $(KLAKLAK)_2$-ELP (10 μM) was used in all treatments. The analysis was carried out using flow cytometry. Trypan blue was used in the sample suspensions before analysis to prevent the inclusion of particles bound on the cell surface in the analysis. These experiments were repeated two times with triplicates. * indicates $p < 0.05$ when compared to $(KLAKLAK)_2$-ELP (10μ).

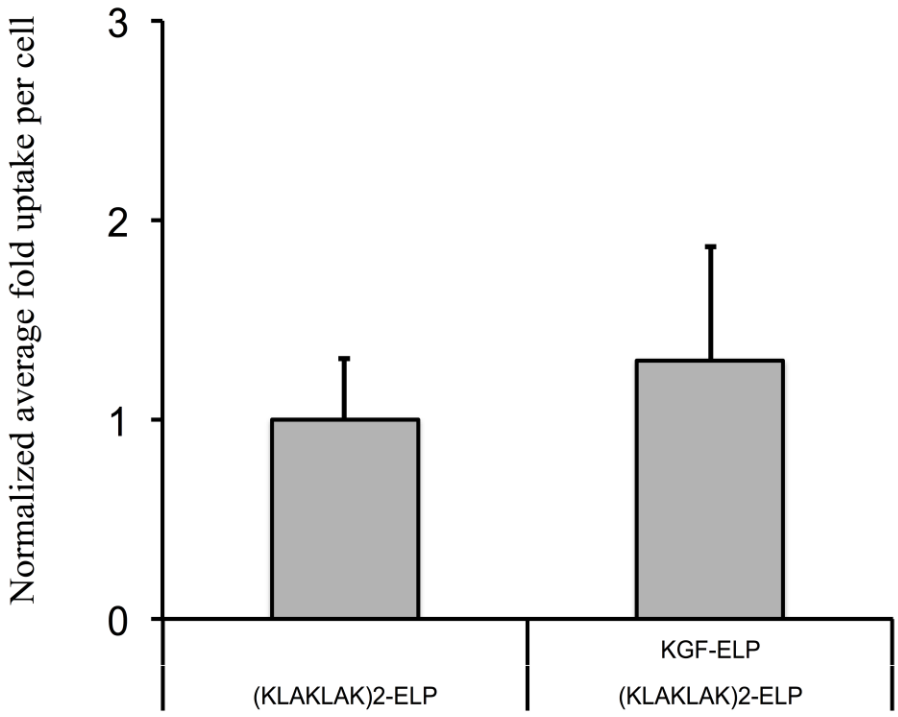

Figure 3.7 KGF-ELP does not improve internalization of $(KLAKLAK)_2$-ELP in low KGFR expressing cells. Fibroblasts were treated with either labeled $(KLAKLAK)_2$-ELP (10μ) or a combination of labeled $(KLAKLAK)_2$-ELP (10μ) and KGF-ELP (10μ) as described above. The analysis was carried out as described above. These experiments were repeated two times with triplicates. * indicates $p < 0.05$ when compared to $(KLAKLAK)_2$-ELP (10μ).

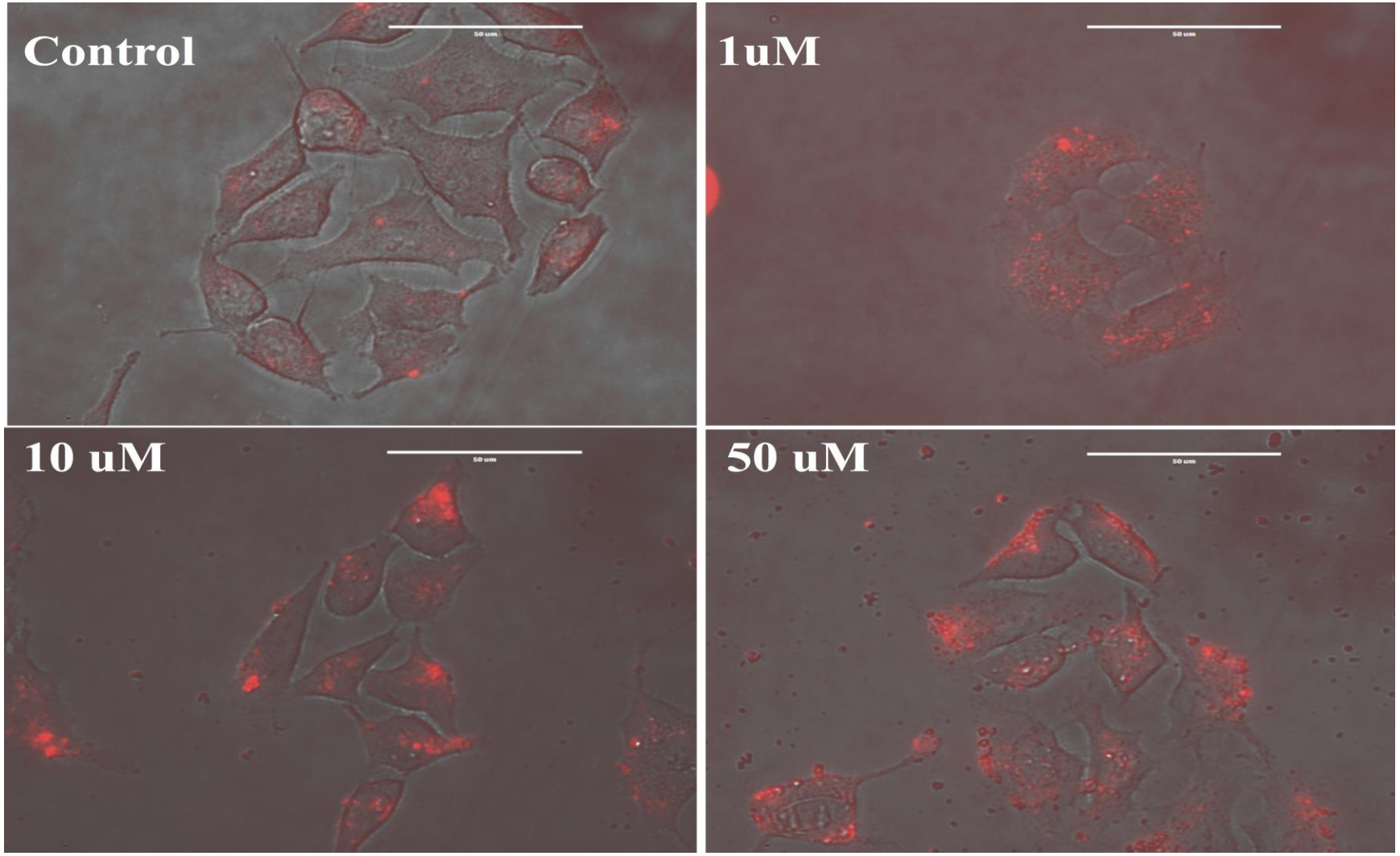

Figure 3.8 Dose-dependent enhancement of macropinosome formation in KGFR overexpressing cells. A549 cells were treated with varying concentrations of KGF-ELP (1 μM, 10 μM, and 50 μM). After 24 Hrs., dextran tetramethylrhodamine was added for 1 Hr. before analysis. Fluorescent picture were taken at 10x magnification.

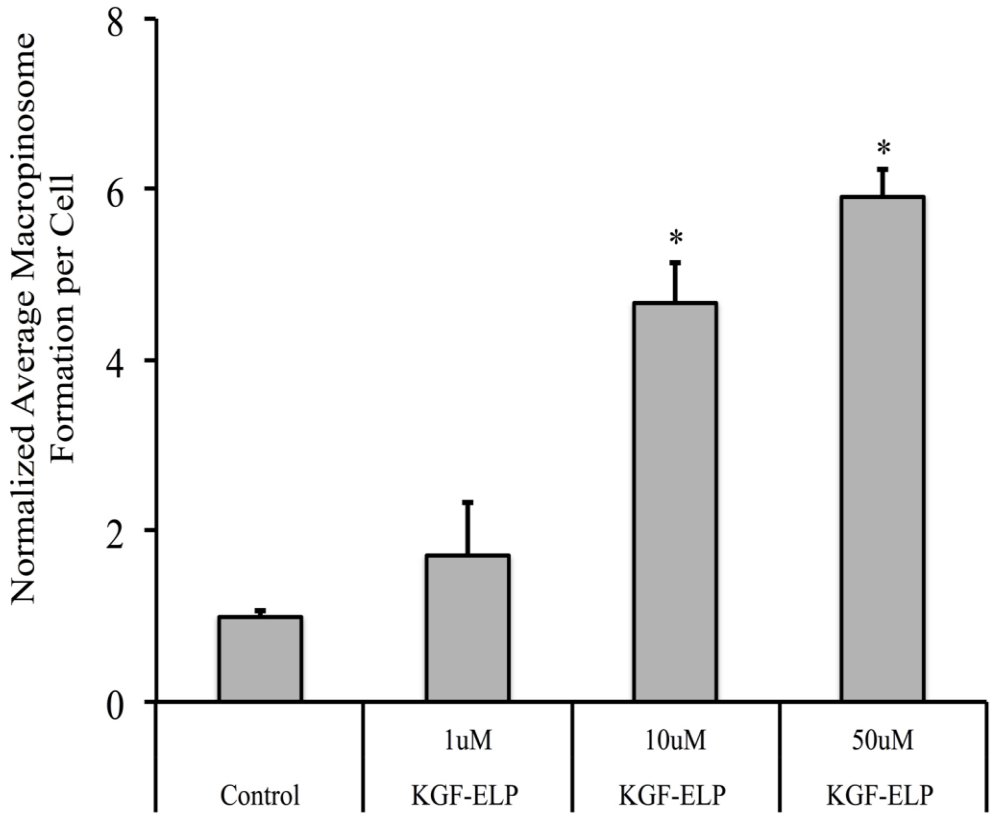

Figure 3.9 Quantification of macropinosome formation in A549 cells after KGF-ELP treatment. A549 cells were serum starved for 24 Hrs. and then treated for 24 Hrs. with different concentration of KGF-ELP (1μM, 10μM or 50μM). After treatment, rhodamine-labeled dextran was added for 1 Hr. and cells were washed at least 5 times with ice cold PBS before analysis using flow cytometry. Treatments were normalized to the control (no treatment). These experiments were repeated two times with triplicates. * indicates $p < 0.05$ when compared to control (no treatment).

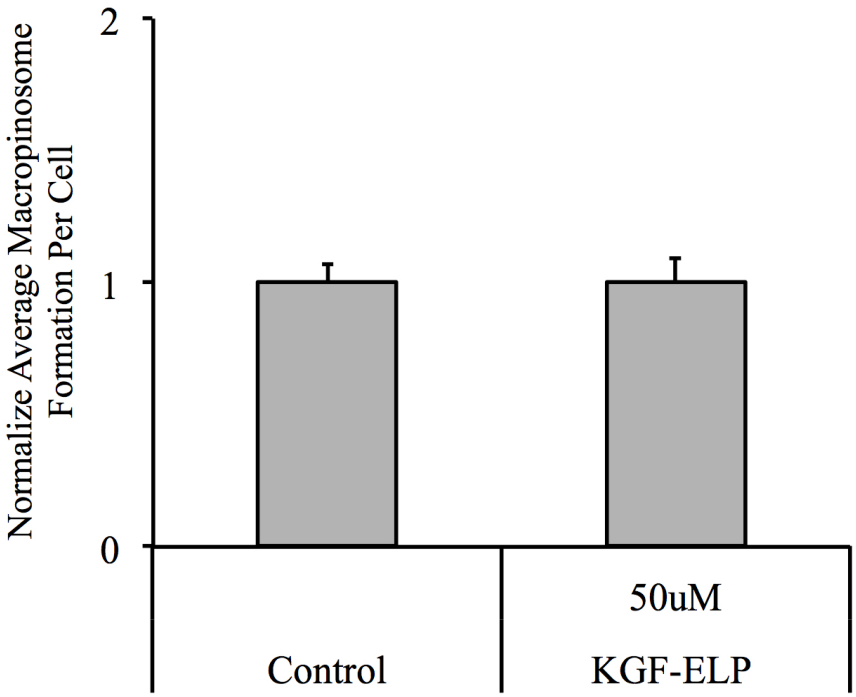

Figure 3.10 Quantification of macropinosome formation in fibroblast cells after KGF-ELP treatment. Fibroblasts were treated with 50μM of KGF-ELP following the steps described in figure 3.9; they were then analyzed by flow cytometry also following the aforementioned steps. These experiments were repeated two times with triplicates. * indicates $p < 0.05$ when compared to control (no treatment).

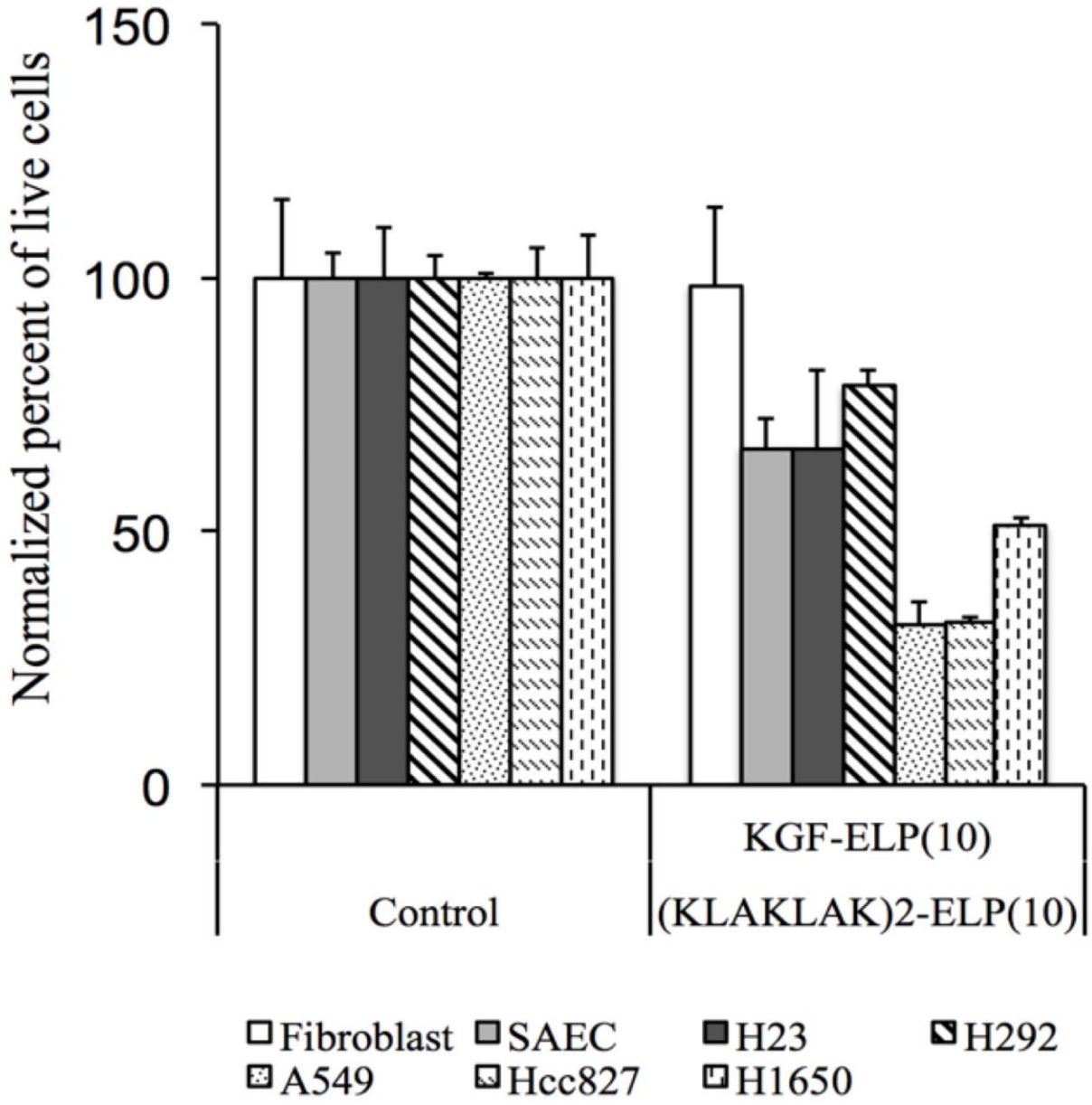

Figure 3.11 Cytotoxic effect of $(KLAKLAK)_2$-ELP is higher in KGFR overexpressing cells when KGF-ELP is present. Fibroblasts, SAEC, H23, H292, A549, H1650 and HCC827 cells were serum starved for 24 Hrs. and then treated for 36 Hrs. with $(KLAKLAK)_2$-ELP (10μM) combined with KGF-ELP (10μM). After treatment, cells were analyzed with a life/dead assay and quantified using image J. The treatments were normalized to their respective control (no treatment). These experiments were repeated two times with triplicates. * indicates $p < 0.05$ when compared to control (no treatment).

3.7 References

[1] Q. M. Nunes, Y. Li, C. Sun, T. K. Kinnunen, and D. G. Fernig, "Fibroblast growth factors as tissue repair and regeneration therapeutics," *PeerJ*, vol. 4, p. e1535, 2016.

[2] K. Koole, P. M. van Kempen, J. E. Swartz, T. Peeters, P. J. van Diest, R. Koole, *et al.*, "Fibroblast growth factor receptor 3 protein is overexpressed in oral and oropharyngeal squamous cell carcinoma," *Cancer Med*, Dec 28 2015.

[3] N. Xu, W. Fang, L. Mu, Y. Tang, L. Gao, S. Ren, *et al.*, "Overexpression of wildtype EGFR is tumorigenic and denotes a therapeutic target in non-small cell lung cancer," *Oncotarget*, Dec 4 2015.

[4] V. Syed, "TGF-beta Signaling in Cancer," *J Cell Biochem*, Jan 16 2016.

[5] G. A. Milano, "Targeted therapy in non-small cell lung cancer: a focus on epidermal growth factor receptor mutations," *Chin Clin Oncol*, vol. 4, p. 47, Dec 2015.

[6] J. Xu, T. Chu, B. Jin, X. Dong, Y. Lou, X. Zhang, *et al.*, "Epidermal Growth Factor Receptor Tyrosine Kinase Inhibitors in Advanced Squamous Cell Lung Cancer," *Clin Lung Cancer*, Dec 1 2015.

[7] J. M. Otte, F. Schmitz, T. Banasiewicz, M. Drews, U. R. Folsch, and K. H. Herzig, "Expression of keratinocyte growth factor and its receptor in colorectal cancer," *Eur J Clin Invest*, vol. 30, pp. 222-9, Mar 2000.

[8] T. Yamayoshi, T. Nagayasu, K. Matsumoto, T. Abo, Y. Hishikawa, and T. Koji, "Expression of keratinocyte growth factor/fibroblast growth factor-7 and its receptor in human lung cancer: correlation with tumour proliferative activity and patient prognosis," *J Pathol*, vol. 204, pp. 110-8, Sep 2004.

[9] M. Yoshino, T. Ishiwata, M. Watanabe, T. Matsunobu, O. Komine, Y. Ono, *et al.*, "Expression and roles of keratinocyte growth factor and its receptor in esophageal cancer cells," *Int J Oncol*, vol. 31, pp. 721-8, Oct 2007.

[10] M. Lee, M. Draoui, F. Zia, A. Gazdar, H. Oie, G. Bepler, *et al.*, "Epidermal growth factor receptor monoclonal antibodies inhibit the growth of lung cancer cell lines," *J Natl Cancer Inst Monogr*, pp. 117-23, 1992.

[11] A. Rossi, P. Maione, G. Colantuoni, C. Ferrara, E. Rossi, C. Guerriero, *et al.*, "Recent developments of targeted therapies in the treatment of non-small cell lung cancer," *Curr Drug Discov Technol,* vol. 6, pp. 91-102, Jun 2009.

[12] D. H. M. D. Hyojin Lee, Ji Won Ha, Jun Yue, and Teri W. Odom, "Enhanced Human Epidermal Growth Factor Receptor 2 Degradation in Breast Cancer Cells by Lysosome-Targeting Gold Nanoconstructs," *ACS NANO,* vol. 9, 2010.

[13] M. C. Kerr and R. D. Teasdale, "Defining macropinocytosis," *Traffic*, vol. 10, pp. 364-71, Apr 2009.

[14] Z. Timsah, J. Berrout, M. Suraokar, C. Behrens, J. Song, J. J. Lee, *et al.*, "Expression pattern of FGFR2, Grb2 and Plcgamma1 acts as a novel prognostic marker of recurrence recurrence-free survival in lung adenocarcinoma," *Am J Cancer Res,* vol. 5, pp. 3135-48, 2015.

[15] P. Dowrick, P. Kenworthy, B. McCann, and R. Warn, "Circular ruffle formation and closure lead to macropinocytosis in hepatocyte growth factor/scatter factor-treated cells," *Eur J Cell Biol,* vol. 61, pp. 44-53, Jun 1993.

[16] I. Nakase, Kobayashi, N. B., Takatani-Nakase, T., Yoshida, T., "Active macropinocytosis induction by stimulation of epidermal growth factor receptor and oncogenic Ras expression potentiates cellular uptake efficacy of exosomes," *Sci Rep,* vol. 5, p. 10300, 2015.

[17] A. Fu, R. Tang, J. Hardie, M. E. Farkas, and V. M. Rotello, "Promises and pitfalls of intracellular delivery of proteins," *Bioconjug Chem,* vol. 25, pp. 1602-8, Sep 17 2014.

[18] S. Dokka, D. Toledo-Velasquez, X. Shi, L. Wang, and Y. Rojanasakul, "Cellular delivery of oligonucleotides by synthetic import peptide carrier," *Pharm Res,* vol. 14, pp. 1759-64, Dec 1997.

[19] P. E. Nielsen, "Addressing the challenges of cellular delivery and bioavailability of peptide nucleic acids (PNA)," *Q Rev Biophys,* vol. 38, pp. 345-50, Nov 2005.

[20] J. M. A. Helenius, "Virus entry by macropinocytosis," *Nat Cell Biol*, vol. 11, pp. 510-520, 2009.

[21] J. P. Lim and P. A. Gleeson, "Macropinocytosis: an endocytic pathway for internalising large gulps," *Immunol Cell Biol*, vol. 89, pp. 836-43, Nov 2011.

[22] N. B. K. Ikuhiko Nakase, Tomoka Takatani-Nakase & Tetsuhiko Yoshida, "Active macropinocytosis induction by stimulation of epidermal growth factor receptor and oncogenic Ras expression potentiates cellular uptake efficacy of exosomes," *Sci Rep*, vol. 5, 2015.

[23] J. Mercer and A. Helenius, "Gulping rather than sipping: macropinocytosis as a way of virus entry," *Curr Opin Microbiol*, vol. 15, pp. 490-9, Aug 2012.

[24] X. X. Zhang, P. G. Allen, and M. Grinstaff, "Macropinocytosis is the major pathway responsible for DNA transfection in CHO cells by a charge-reversal amphiphile," *Mol Pharm*, vol. 8, pp. 758-66, Jun 6 2011.

[25] C. W. Joel A. Swanson, "Macropinocytosis," *Trends in Cell Biology*, vol. 5, pp. 424-428, 1995.

[26] J. A. Swanson, "Shaping cups into phagosomes and macropinosomes," *Nat Rev Mol Cell Biol*, vol. 9, pp. 639-49, Aug 2008.

[27] D. E. Meyer and A. Chilkoti, "Genetically encoded synthesis of protein-based polymers with precisely specified molecular weight and sequence by recursive directional ligation: examples from the elastin-like polypeptide system," *Biomacromolecules*, vol. 3, pp. 357-67, Mar-Apr 2002.

[28] P. Koria, H. Yagi, Y. Kitagawa, Z. Megeed, Y. Nahmias, R. Sheridan, *et al.*, "Self-assembling elastin-like peptides growth factor chimeric nanoparticles for the treatment of chronic wounds," *Proc Natl Acad Sci U S A*, vol. 108, pp. 1034-9, Jan 18 2011.

[29] J. E. Larsen, T. Cascone, D. E. Gerber, J. V. Heymach, and J. D. Minna, "Targeted therapies for lung cancer: clinical experience and novel agents," *Cancer J*, vol. 17, pp. 512-27, Nov 2011.

[30] D. M. Bryant, M. C. Kerr, L. A. Hammond, S. R. Joseph, K. E. Mostov, R. D. Teasdale, *et al.*, "EGF induces macropinocytosis and SNX1-modulated recycling of E-cadherin," *J Cell Sci*, vol. 120, pp. 1818-28, May 15 2007.

[31] S. D. Conner and S. L. Schmid, "Regulated portals of entry into the cell," *Nature*, vol. 422, pp. 37-44, Mar 6 2003.

[32] J. R. Goffin and K. Zbuk, "Epidermal growth factor receptor: pathway, therapies, and pipeline," *Clin Ther*, vol. 35, pp. 1282-303, Sep 2013.

[33] S. Nishimura, S. Takahashi, H. Kamikatahira, Y. Kuroki, D. E. Jaalouk, S. O'Brien, *et al.*, "Combinatorial targeting of the macropinocytotic pathway in leukemia and lymphoma cells," *J Biol Chem*, vol. 283, pp. 11752-62, Apr 25 2008.

[34] I. A. Khalil, K. Kogure, H. Akita, and H. Harashima, "Uptake pathways and subsequent intracellular trafficking in nonviral gene delivery," *Pharmacol Rev*, vol. 58, pp. 32-45, Mar 2006.

[35] M. Ruiz. (2007). *Different Types of Endocytosis*. Available: https://commons.wikimedia.org/wiki/File:Endocytosis_types_sv.svg

CHAPTER 4: INHIBITION OF GLYCOLYSIS AS A POSSIBLE CANCER THERAPY

4.1 Introduction

The enzyme phosphoglycerate mutase (PGM) has recently received much attention because it is the point at which glycolysis and anabolic biosynthesis are coordinated; this is done through the conversion of 3-phosphoglycerate (3PG) to 2-phosphoglycerate (2PG). PGM is activated by the phosphorylation of the histidine 11 (H11). In this chapter we show the synthesis of a fusion comprising of a peptide, KLVLIRHGESAW, derived from PGM and elastin like polypeptides (ELPs), PGM-ELP. The PGM domain in PGM-ELP comprises the H11 and a few more peptides from PGM; therefore, it acts as a competitive inhibitor for the phosphorylation of the PGM enzyme; the ELP domain will provide stability. Furthermore, we explore the cytotoxic effect of having multiple copies of the PGM peptide fused to ELP, (PGM)4-ELP, where the number indicates the number of PGM peptide copies in the fusion.

4.2 Glycolysis and the Phosphoglycerate Mutase (PGM) Enzyme

One of the hallmarks of cancer is the uncontrolled proliferation and growth of cells. The formation of one cell is a very complex process that requires energy as well as the synthesis of macromolecules such as phospholipids, amino acids, and nucleic acids [1]. Energy in the form of ATP can be produced in two different areas of the cells and in the presence (aerobic) or not (anaerobic) of oxygen. ATP can be produced in the cytosol via glycolysis; this is very inefficient ATP producing pathway since it happens in the absence of oxygen; during glycolysis a net of 2 ATP molecules are synthesized. ATP can also be synthesized within the mitochondria; this

process occurs in the presence of oxygen via oxidative phosphorylation; this process is called cell respiration. In the mitochondria, a net of 36 ATP molecules are obtained from a single molecule of glucose [2]. One could conclude that cancer cells, because of the high-energy requirements needed for proliferation, would favor aerobic respiration. However, several studies have consistently shown that the glycolytic rate in cancer cells is higher that in normal cells [3, 4]; therefore, targeting glycolysis is an attractive alternative [5-7].

Several studies have argued that higher ATP production is not likely the reason for high glycolytic rate; instead, they claimed that glycolysis provides the building blocks required for the synthesis of macromolecules (DNA, RNA, lipids, and proteins) needed for giving rise to new cells [8, 9]. Others maintained that glycolysis is responsible for faster ATP production needed for proliferating cells. Regardless of the conclusion of either of the arguments, it is clear that the inhibition of glycolysis can prove fruitful in the development of a targeted cancer therapy.

Glycolysis is a catabolic pathway through which a molecule of glucose is converted to two molecules of pyruvate through ten enzyme-catalyzed steps (Figure 4.1). Pyruvate is then taken into the mitochondria for energy production. During the different glycolytic steps, molecules that are the building block for macromolecules are synthetized. After glucose is internalized, it is phosphorylated forming glucose-6-phosphate (G6P). G6P participates in the pentose phosphate pathway that gives rise to nucleic acid synthesis. Glyceraldehyde-3-phosphate (G3P), an intermediate of glycolysis, participates in the synthesis of lipids. Also, the glycolytic intermediate 3-phosphoglycerate (3PG) contributes to the synthesis of amino acids.

Due to the involvement of glycolysis in biosynthesis, there are several possible targets in the glycolytic pathway that could result in proliferation and growth being halted [10-12]. Some of them are already being explored. For example, the compound 2-Deoxyglucose (2-DG) is a

glucose analog that reduces the phosphorylation of glucose by the enzyme hexokinase (HK) . HK does not distinguish between 2-DG and glucose; therefore, the phosphorylation of the analog by HK reduces the amount of phosphorylated glucose available for glycolysis [6, 13]. This blocks the pentose phosphate pathway resulting in the synthesis of ribose, precursor of nucleic acids, being halted. Furthermore, because 2-DG acts in the early steps of glycolysis, it also disrupt other anabolic reactions occurring downstream from the pentose phosphate pathway such as lipid and protein synthesis. Several studies have reported the positive results associate with 2-DG when used alone [14] and in combination with other therapeutic agents [15, 16]; however, development of resistance has also being reported [17, 18]. Moreover, other studies have argued that the mechanism by which 2-DG inhibits cell growth need to be further studied since its mechanism of action is not fully understood [19].

Other groups have focus on the enzyme phosphoglycerate mutase (PGM) as a possible target to block glycolysis [20]. This enzyme is considered a useful target for cancer treatment because it is located at the branching point between glycolysis and anabolic biosynthesis [21-23], both required for cell growth and proliferation. In addition, PGM has been found to be overexpress in some cancers [24, 25]. This enzyme catalyzes the conversion of 3-phosphoglycerate (3PG) to 2-phosphoglycerate (2PG). Inhibition of PGM will result in increase 3PG and decrease 2PG, both of which have detrimental consequences for the cell. Accumulation of 3PG results in inhibition of the enzyme 6-phosphogluconate dehydrogenase (6PGD) [22]; this enzyme is part of the pentose phosphate pathway, which is responsible for the synthesis of nucleotide precursors. The reduction of 2PG reduces the activity of the enzyme phosphoglycerate dehydrogenase enzyme (PHGDH), preventing the synthesis of serine from 3PG and further increasing the amount of 3PG. Furthermore, decrease in 2PG results in

reduction of phosphoenolpyruvate (PEP) and its conversion to pyruvate carried out by the enzyme pyruvate kinase (PK) isoform 2 (PKM2) which is stimulated by serine. In short, inhibiting this enzyme will have a dual effect; it will result in the reduction of ATP due to decrease in pyruvate synthesis (catabolic reaction) and inhibition of anabolic biosynthesis.

Previous work used a synthetic peptide (Leu-Ile-Arg-His-Gly-Glu or LIRHGE) derived from the PGM domain that included a histidine amino acid that is phosphorylated when PGM is in its active form [21]. This sequence was functionalized by the addition of a cell penetrating peptide (CPP) to increase its internalization. The results show a decrease in cell growth; however, the effect of the peptide dissipated after approximately three days and cancer cells continued proliferating. The study suggested that this could be due to degradation of the peptide.

4.3 Fusion PGM-ELP

4.3.1 Materials and Methods

Fetal bovine serum (FBS) and Dulbecco modified Eagle Medium (DMEM) were purchased from Life Technologies. The restriction enzymes and other enzymes used for cloning were purchased from New England Biolabs (Ipswich, MA). H292, A549, H1650, H23, and HCC827 cells were kindly donated by Dr. Haura from Moffit Cancer Center. CRCL2522, fibroblasts, were purchased from ATCC (Manassas, VA). Human Small Airway Epithelial Cells (SAEC) cells were kindly donated by Dr. Narasaiah Kolliputi from the Department of Internal Medicine at USF Health. The PGM gene was purchased from GenScript (Piscataway, NJ). The miniprep and gel extraction kits were purchased from QIAGEN. The reagents for RT-PCR were purchased from Bio-Rad.

4.3.1.1 Synthesis of PGM-ELP and (PGM)4-ELP

The PUC57 plasmids containing the genes **(**VPGVG)5 , (VPGVG)2VPGCG(VPGVG)2 , and KLVLIRHGESAW (PGM sequence) were purchased from Genscript (Piscataway, NJ). The V40C2 encoding gene was made using recursive direction ligation method as described previously [26]. The PGM gene was excised using PflMI and Bgll enzymes. This gene was then run on a 0.08% agarose gel and extracted using QIAquick Gel Extraction Kit. The restriction enzyme PflMI linearized the pUC19 vector containing the ELP sequence and the excised PGM gene was cloned in frame with the ELP gene. This resulted in the pUC19 vector containing the PGM-ELP fusion protein gene flanked by pfIMI and BgII sites. The sequences encoding for the fusion protein was then removed from the pUC19 vector using pflMI and BgII enzymes and recovered by gel extraction as explained above. After extraction, this gene was cloned in a modified pET25b+ expression vector through SfiI site. This vector was modified to incorporate a SfiI cloning site for the cloning of the fusion protein.

The pET25b+ vector containing the fusion protein gene was transformed into BLRD competent cells through heat shock at 42^{o}C. A starting culture of 50 ml was inoculated overnight and added to a 1 L culture the next day. The 1 L culture was then grown overnight and subsequently purified by inverse transition cycling as described previously [27]. Figure 4.2 shows a representation of the genes for PGM and ELP and the production of the fusion PGM-ELP. The fusion (PGM)4-ELP was synthesized as described above, but four copies of the PGM gene were cloned in frame with the ELP gene resulting in the fusion (PGM)4-ELP.

4.3.1.2 Cell Culture

Cells were cultured in a humidified incubator at 37^{0}C and 5% CO_2. Cells were seeded on 24 or 48-well plates until they were approximately 70% confluent. CRL-2522 (non-malignant

human foreskin fibroblast), A549 (human lung carcinoma), H292 (human lung carcinoma), HCC827 (human lung adenocarcinoma), H23 (human lung adenocarcinoma), and H1650 (human lung adenocarcinoma) were grown in DMEM supplemented with 10% FBS and 1% AA (Complete Medium). SAEC were cultured in airway epithelial cell basal medium (PCS-300-030) supplemented with Small Airway Epithelial Cell Growth Kit (PCS-301-040).

4.3.1.3 Live/Dead Assay

Cells were seeded and treated only once for 1,2 ,or 6 days as indicated. The media was changed every two to three days but the treatment was not repeated. After their respective treatments, ethidium homodimer-1 (Life Technologies cat # E1169) was added to each well to a final concentration of 4uM. Cells were then incubated for 1 hour at 37^{o}C. After the incubation time, cells were washed twice with PBS to remove floating cells. NucBlue (Life Technologies R37605) was then added for 20 minutes to stain nuclei, followed by two washes with PBS. Eight random pictures were taken per well using the EVOS fluorescence microscope (10X magnification). Pictures were taken in different channels (blue, green, red) and overlay. Live/dead cell discrimination was performed using image J. A macro was created using the functions split channel, threshold, and cell counter to count the total number of live cells (blue) in each picture. Dead cells that were not removed after the washes were stained red or magenta (blue and red); adjusting the threshold for the picture being analyzed easily isolated these cells. Therefore, the final count of cells per picture only included live cells.

4.3.1.4 2-Phosphoglycerate (2PG) Assay

Cells (H292) were seeded in six-well plates (500,000/well). After 24 Hrs. they were treated for 48 Hrs. with either 10 μM or 100 μM of PGM-ELP. After treatment they were lysed following the assay protocol. The 2-phosphoglycerate colorimetric assay kit (BioVision cat #

k778-100) was used to measure the concentration of 2PG and the protocol was followed as described in the kit.

4.3.1.5 Labeling of the Fusion Proteins

The cysteines present in the ELP sequence were labeled using maleimide chemistry for the particle internalization experiments. Fluorescein-5-maleimide (AnaSpec Inc cat # 81405) was mixed with the fusion proteins. The mixture was placed on an orbital shaker and incubated at room temperature for 2 hours. Unconjugated fluorescein was removed by a series of hot and cold cycles on a bench top centrifuge ran at a speed of 20000g for 10 minutes each time. The supernatant was discarded after the hot spin and an equal amount of cold sterile PBS was added. This mixture was spun at 4 ^{0}C and the supernatant was collected while the pellet was discarded. This formed one complete cycle of inverse temperature cycling. At least 5 cycles were performed to get rid of all the unconjugated Fluorescein.

4.3.1.6 Fusion Protein Internalization Assay

Cells (50,000/well) were seeded in 24-well plates and cultured as described above. They were let grow until they were about 70% confluent and were treated with the indicated treatments. For analysis, cells were washed twice with ice-cold PBS and were trypsinized using 0.25% trypsin (100 µl). Cells were pelleted and re-suspended in 300 µl of PBS containing 50 □g/ml of trypan blue to quench signal arising from the cell surface and 4',6-diamidino-2-phenylindole (DAPI) to allow exclusion of nonviable cells. The cells were analyzed using flow cytometry and either the percent of fluorescent cells or the average intensity was quantified and reported.

4.3.1.7 Statistical Analysis

For statistical significance, the p value was calculated using ANOVA single factor. P values < 0.05 were considered significant. The reported errors indicate the ±SEM.

4.3.2 Results

4.3.2.1 The Fusion PGM-ELP Interferes with the Phosphoglycerate Mutase Enzyme

The glycolytic enzyme phosphoglycerate mutase (PGM) controls both the glycolytic pathway and the synthesis of macromolecules needed for cell growth and proliferation. Previous works showed that a using a peptide derived from the PGM domain could act as a competitive inhibitor for this enzyme and inhibit cell proliferation. However, this inhibition was transient and lasted for about 3 days; the study concluded this occurred because of the peptide degradation [21]. We reasoned that ELPs could increase stability of the peptide since previous works have shown that ELPs are resistant to degradation [28]. Therefore, we purified the fusion PGM-ELP and first tested for its bioactivity. Our results clearly show that the fusion PGM-ELP is bioactive and causes cell death at high concentration after 24 and 48 Hrs. (Figures 4.3, 4.4 and 4.5). Furthermore, since PGM-ELP competes with the phosphorylation of PGM (Figure 4.6), a decreased in PGM phosphorylation would result in the 2PG concentration decrease. Indeed, we found that treatments with PGM-ELP decreased the amount of 2PG (Figure 4.7) after 48 hours. Combined, these results suggest that PGM-ELP is bioactive and causes cell death by competing with an enzyme (PGM) in the glycolytic pathway.

We wanted to test the cytotoxicity of PGM-ELP in different cells lines. Therefore, lung cancer cells (A549, H23, HCC827, H292), connective tissue cells (Fibroblasts, Fb), and normal lung cells (Small airway epithelial cells, SAEC) were tested for PGM-ELP cytotoxicity. Cells were treated as describe in the material and methods section with 50 μM of PGM-ELP. After 6

days, PGM-ELP displays cytotoxic effects in all cell lines; however, its effect is noticeable higher in the lung cancer cells (Figure 4.8). Furthermore, to test if the ELP domain assisted in improving the killing effect of the PGM domain, cells were also treated with the PGM peptide (50 μM) and the results were compared to the PGM-ELP 50 μM treatment (Figure 4.9). The results clearly show that the fusion PGM-ELP is much more cytotoxic than the PGM peptide.

4.3.2.2 The Internalization of PGM-ELP is Improved by KGF-ELP

We reasoned that the internalization and therefore cytotoxic effect of PGM-ELP could be enhanced if the endocytotic mechanism of macropinocytosis is stimulated. As described in chapter 3, the fusion KGF-ELP induces macropinocytosis in keratinocyte growth factor receptor (KGFR) overexpressing cells (A549); therefore, an heterogeneous nanoparticle comprising of PGM-ELP and KGF-ELP (Figure 4.10) could improve the internalization of PGM-ELP in A549 cells. Indeed, our results clearly show that including KGF-ELP in the treatment resulted in an approximately 20 fold increase when compared to the PGM-ELP 10 μM treatment (Figure 4.11). However, since adding 5 μM of KGF-ELP changes the molarity of the treatment, we also included and 15 μM PGM-ELP treatment; this still shows more than a 2-fold increase when KGF-ELP is part of the treatment (Figure 4.11). In addition, the treatment consisting of unfunctionalized ELP and PGM-ELP shows no increased in PGM-ELP internalization when compared to the 15 μM PGM-ELP (Figure 4.11). Altogether, the data implies that KGF-ELP improves internalization of PGM-ELP.

4.3.2.3 KGF-ELP Enhances the Cytotoxic Effect of PGM-ELP in KGFR Overexpressing Cells

Having found that KGF-ELP increases PGM-ELP internalization in A549 cells, we tested if this would translate to higher cytotoxicity in these cells. Cells were treated as described in the

material and methods section and a concentration of PGM-ELP that did not cause cytotoxicity after 3 days was used (50 μM). The results show clearly that after 6 days PGM-ELP is cytotoxic and about 55% of cells have died (Figure 4.12). Interestingly, the treatment that included the fusion KGF-ELP caused almost 95% of cell death (Figure 4.12). These results further confirmed that the inclusion of KGF-ELP improves internalization and cytotoxicity of PGM-ELP.

Cells with different levels of KGFR expression (chapter 3) were treated with the formulations PGM-ELP (50 μM) or PGM-ELP (50 μM) and KGF-ELP (20 μM). All cells, except A549, show no improvement by the inclusion of KGF-ELP in the treatment (Figure 4.13). A549, having the highest KGFR expression, shows a definite increase in cells death. Altogether, the results propose that the presence of KGF-ELP adds selectivity to the treatment.

4.3.2.4 The Addition of Multiple PGM Domains to ELP Enhances Cytotoxicity

Having observed that PGM-ELP is cytotoxic, we reasoned that this effect could be boosted if multiple PGM domains are fused to ELP. To this end, we added four PGM domains to ELP, (PGM)4-ELP. We treated HCC827 cells, as described above, with varying concentrations of (PGM)4-ELP (10 μM, 50 μM, and 100 μM) for 3 days. Interestingly, all concentrations induced cell death (Figure 4.14) after this short period of time. Furthermore, Figure 4.15 clearly shows that the same treatment (50 μM) of (PGM)4-ELP and PGM-ELP induced approximately the same amount of cells death but (PGM)4-ELP only took 3 days compared to the 6 days needed for PGM-ELP.

4.4 Discussion and Summary

The tumor microenvironment is very complex; a single tumor has cells with different genotypes; therefore, a single therapeutic might not be enough to prevent the tumor from growing. Many have looked into targeting glycolysis since higher than normal glycolytic rate has

been observed in cancer cells regardless of their genotype. Herein, we report the synthesis of the fusion protein PGM-ELP that inhibits glycolysis resulting in cell death. Furthermore, we show that the heterogeneous nanoparticle comprising of PGM-ELP and KGF-ELP enhances internalization and cytotoxic effect of PGM-ELP in KGFR overexpressing cells. Finally, a fusion consisting of multiple copies of the PGM domain fuse to ELP, (PGM)4-ELP, improves the fusion cytotoxic effect.

Previous works have demonstrated that using an amino acid sequence from the phosphoglycerate mutase enzyme (PGM) that encompasses the histidine 11 (H11) prevents cell proliferation. However, the promising observations are only temporary; the study suggested the degradation of the peptide as the cause. We synthesized the fusion PGM-ELP; the PGM domain in this fusion is derived from the PGM enzyme and encompasses H11. The ELP would provide stability by preventing degradation. Our results clearly show this fusion to be bioactive and causing cell death after three days but only at high concentrations (100 μM). Furthermore, the cytotoxic effect is also observed in various cell lines after 6 days, even at low concentrations (50 μM). We believe this observation is because of the number of H11 sites available. The lower concentration offers less number of H11 sites; therefore, glycolytic inhibition takes longer. This could explain why a 50 μM treatment does not cause cell death after 3 days, but it does after 6 days. In addition, since the cells were treated only once during the 6-day period, it is reasonable to conclude that the PGM-ELP was still present within the cells. Therefore, the ELP domain provided stability to the fusion. Moreover, the treatment with the PGM peptide was much less cytotoxic than the fusion PGM-ELP. We reasoned that this could be attributed to the stability imparted by the ELP domain as well as the interaction between the ELP domain and the cell surface. This interaction permits the PGM-ELP fusion to be bound to the cell surface; therefore,

allowing cells to have more access to the molecules compared to the unbound PGM peptide. Our data also demonstrates that the fusion PGM-ELP acts by affecting glycolysis; this can be concluded from the approximately 60% reduction in the concentration of 2PG in the treated cells. 2PG is the product of the PGM enzyme; therefore, a drastic reduction in its concentration can safely be attributed to an inhibited PGM enzyme.

Additionally, our data shows that not all cells responded equally to the PGM-ELP treatment. The most obvious difference is observed in groups, cancer cell group versus normal cell group. One reason why cancer cells responded better to the treatment can be attributed to their inherently more active nature; cancer cells exhibit higher levels of macropinocytosis compared to normal cells. Another plausible explanation is that cancer cells are highly dependent on glycolysis; therefore, inhibiting this pathway may have more impact in cancer than in normal cells.

Our results show that the addition of the KGF-ELP fusion to the treatment resulted in higher PGM-ELP uptake in KGFR overexpressing cells. Some of the internalization can be attributed to the higher concentration of the treatment that included KGF-ELP. However, when the same concentration treatments are compared, there still exist an increase in PGM-ELP uptake when KGF-ELP is part of the formulation. This can be associated to the enhancement of macropinocytosis due to the interaction between KGF-ELP and the KGFR as demonstrated in chapter 3. Furthermore, the increase in internalization also resulted in improved cytotoxicity in cells overexpressing the KGFR. Our data clearly shows that KGFR overexpressing cells decreased by approximately 80% when compared to the formulation containing only PGM-ELP.

Previously, we hypothesized that the number H11 sites available may be the reason for the lower concentration treatment (50 μM) to take effect after 6 days; therefore, we synthesized a

fusion containing four H1 sites, (PGM)4-ELP. The results clearly display a dose dependent cytotoxic effect. Interestingly, the killing effect was observed after only 3 days. Comparing the HCC827 data for the 50 μM PGM-ELP treatment (6 days) and 50 μM (PGM)4-ELP treatment (3 days) , it becomes very apparent the improvement in efficiency and cytotoxicity due to the higher number of H11 sites. The HCC827 6-day treatment resulted in an approximately 60% cell death while the 3-day treatment resulted in about 70% cell death. Therefore, our data validates the idea that increasing the number of H11 sites improves toxicity by PGM-ELP.

In summary, we have demonstrated that the fusion PGM-ELP induces cell death by inhibiting glycolysis. Furthermore, this fusion seems to have a higher effect in cancer cells, which could be related to their high dependence in glycolysis and/or their intrinsic more active nature. We also showed that the heterogeneous nanoparticle comprising of KGF-ELP and PGM-ELP enhances the internalization and cytotoxic effect of PGM-ELP in KGFR overexpressing cells. Lastly, our data suggests a correlation between the number of H11 sites and the efficacy of the PGM-ELP; that is, (PGM)4-ELP is more efficient than PGM-ELP in terms of killing time and percent of killing.

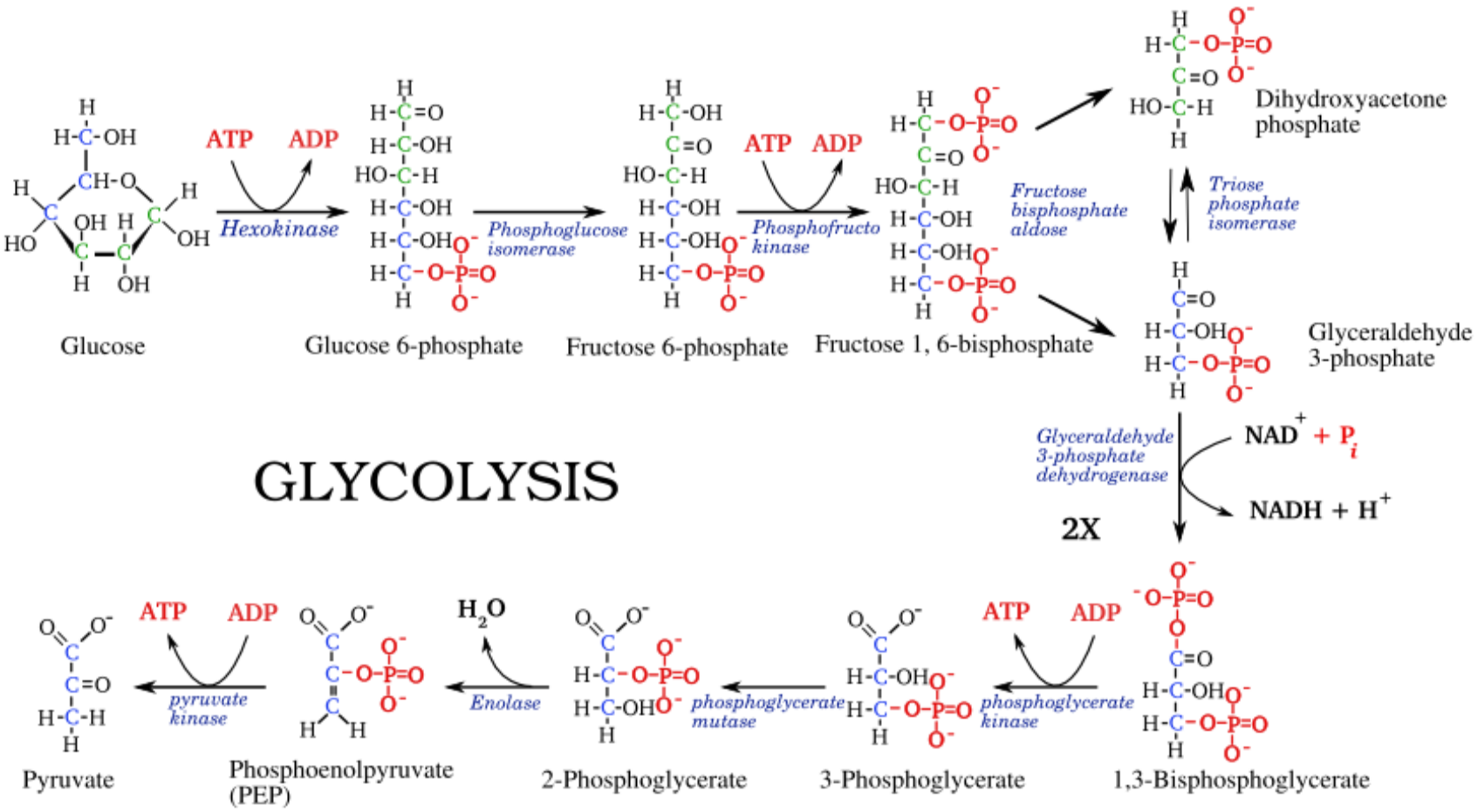

Figure 4.1 Representation of the glycolytic pathway [29].

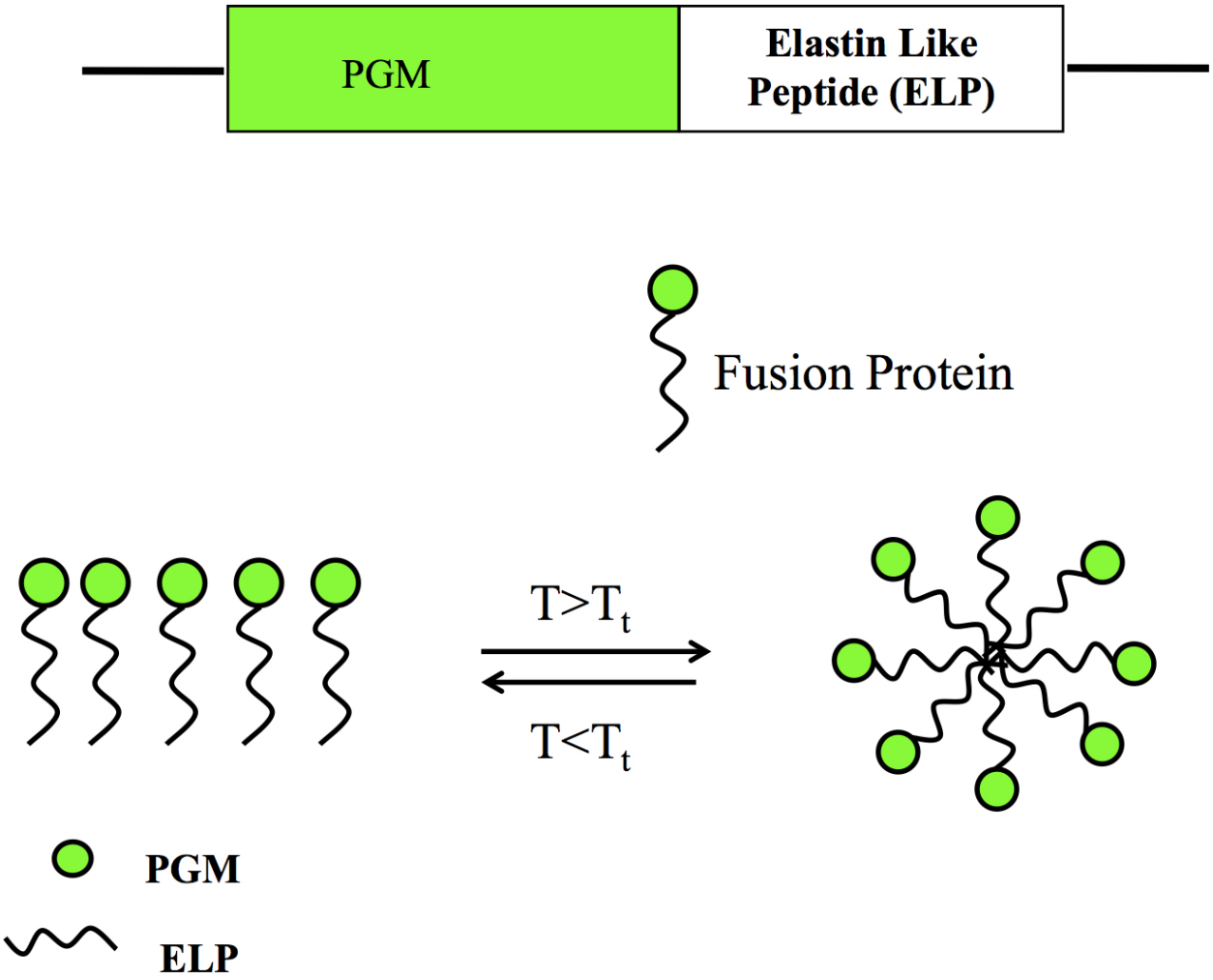

Figure 4.2 Graphical representation of PGM-ELP synthesis and its self-assemble property. Top, representation of the PGM gene, ELP genes, and their translation to the fusion PGM-ELP. Bottom, illustration of the phase transition property of the fusion above and below its transition temperature (T_t). The fusion is soluble below its T_t and aggregates above its T_t.

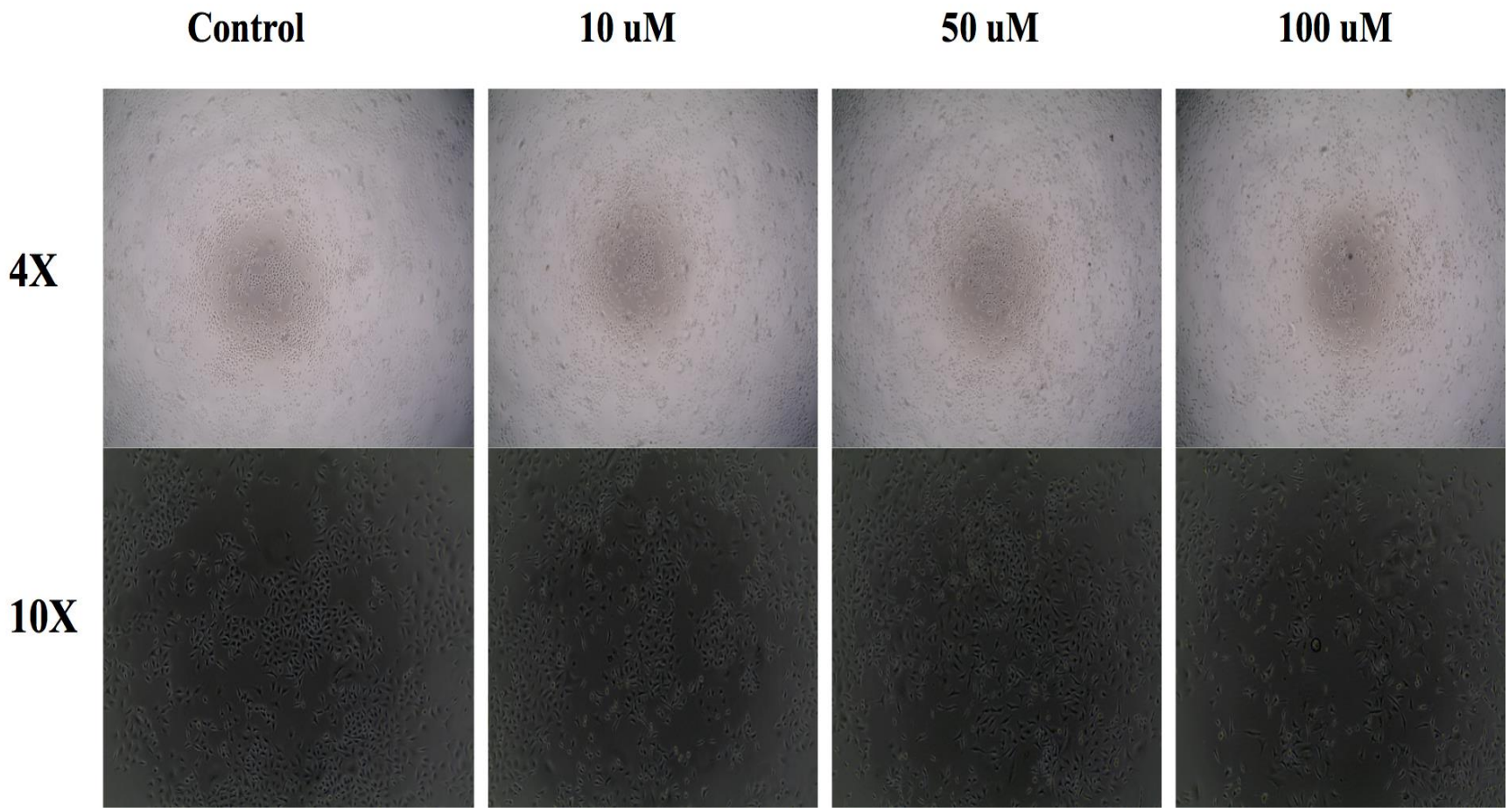

Figure 4.3 Phase contrast picture of the PGM-ELP treatment. A549 cells were treated for 3 days; after which, phase contrast microscope pictures were taken. Top row show 4X magnification and bottom row 10X magnification, the columns show the different concentrations used (10 μM, 50 μM, and 100 μM). The control received no treatment.

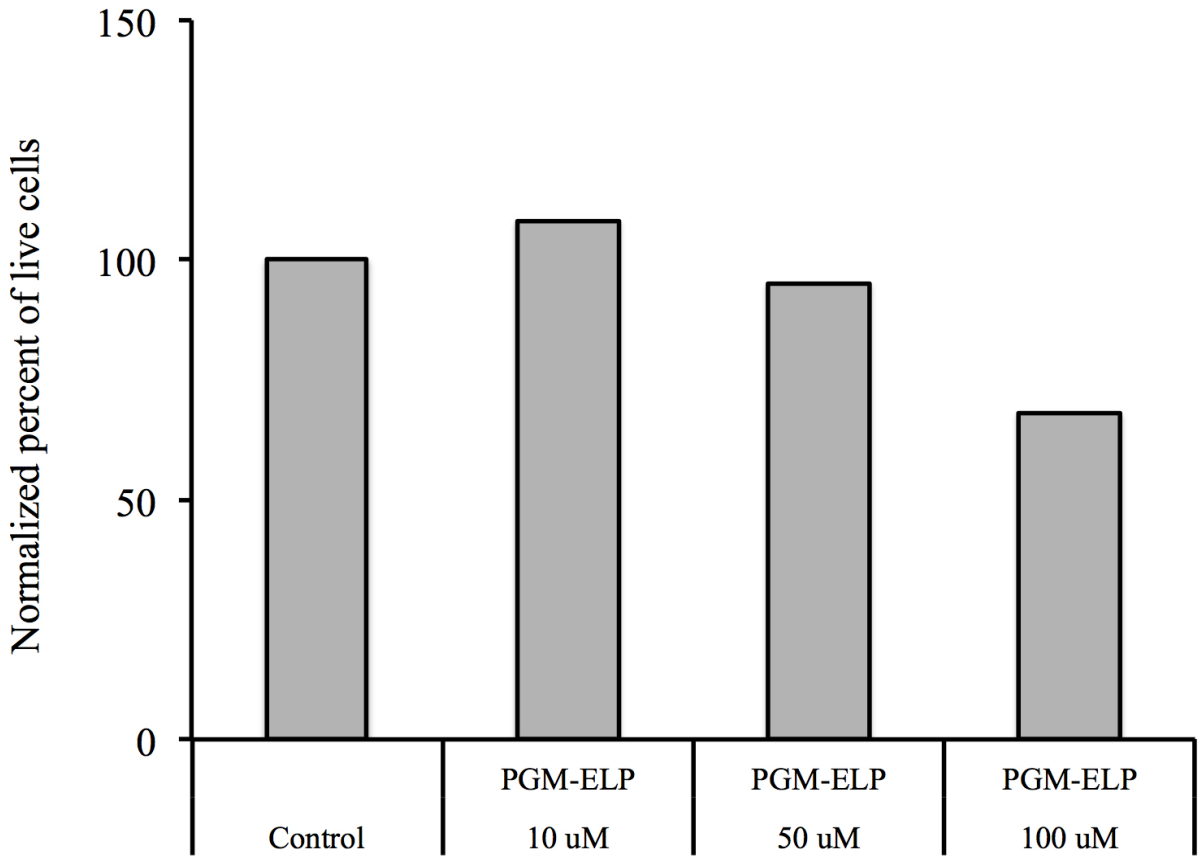

Figure 4.4 Quantification of live cells after a 24 Hr. treatment with PGM-ELP. A549 were seeded and quantified as described in M&M. All the treatments have been normalized to the control.

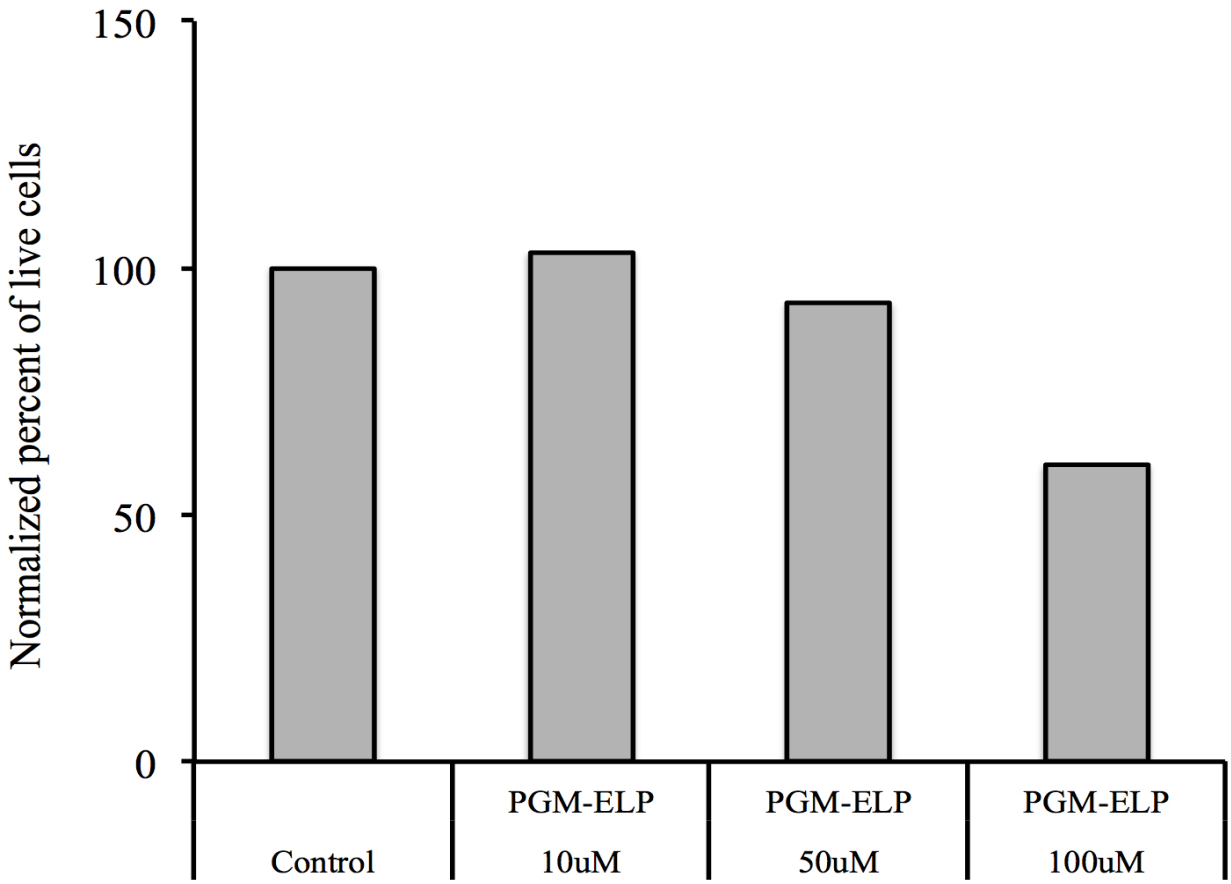

Figure 4.5 Quantification of live cells after a 48 Hr. treatment with PGM-ELP. A549 were seeded and quantified as described in M&M. All the treatments have been normalized to the control.

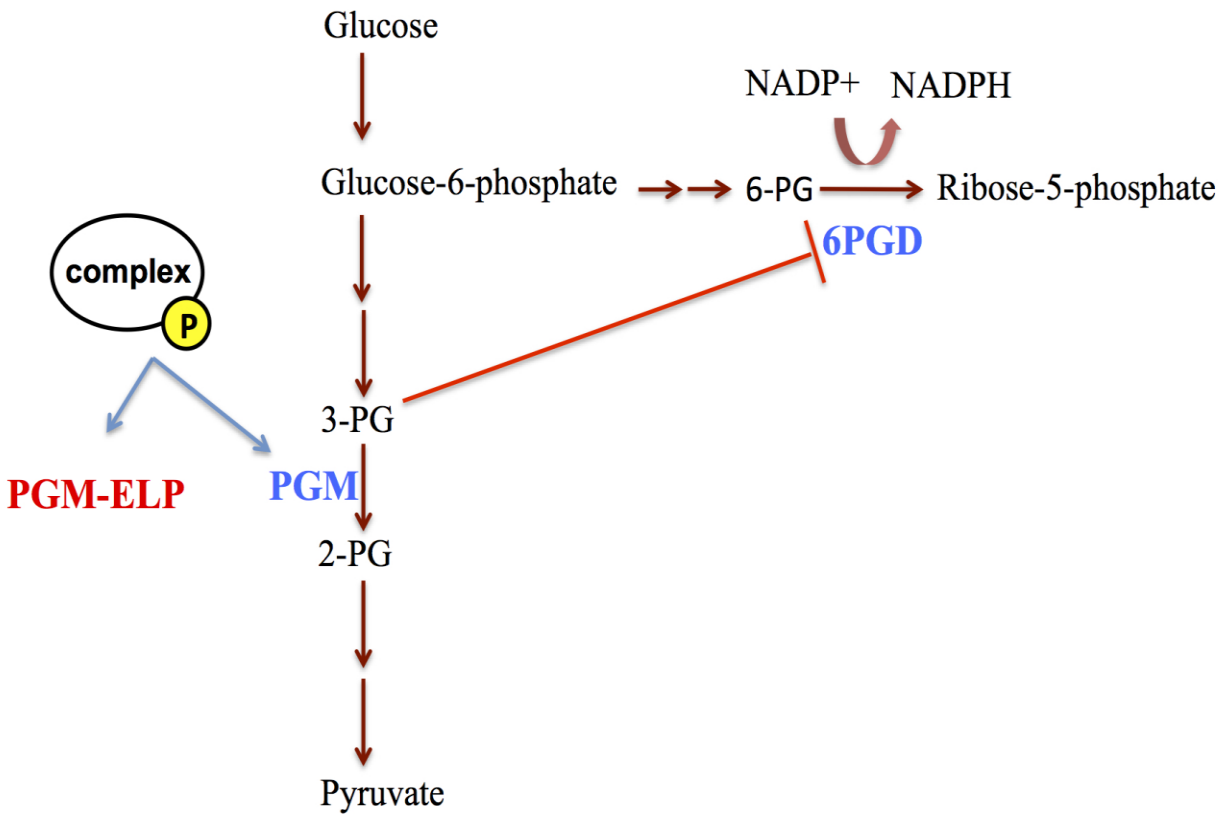

Figure 4.6 Graphical representation of the intracellular effect of PGM-ELP on the glycolytic pathway. Briefly, the phosphorylating complex that activates the PGM enzyme will also phosphorylate the PGM-ELP fusion. This reduces the availability of activated PGM, which results in increase 3-PG and decrease 2-PG. Higher 3-PG concentration blocks 6PGD; therefore, glycolysis and macromolecule synthesis (Ribose-5-phosphate) are inhibited.

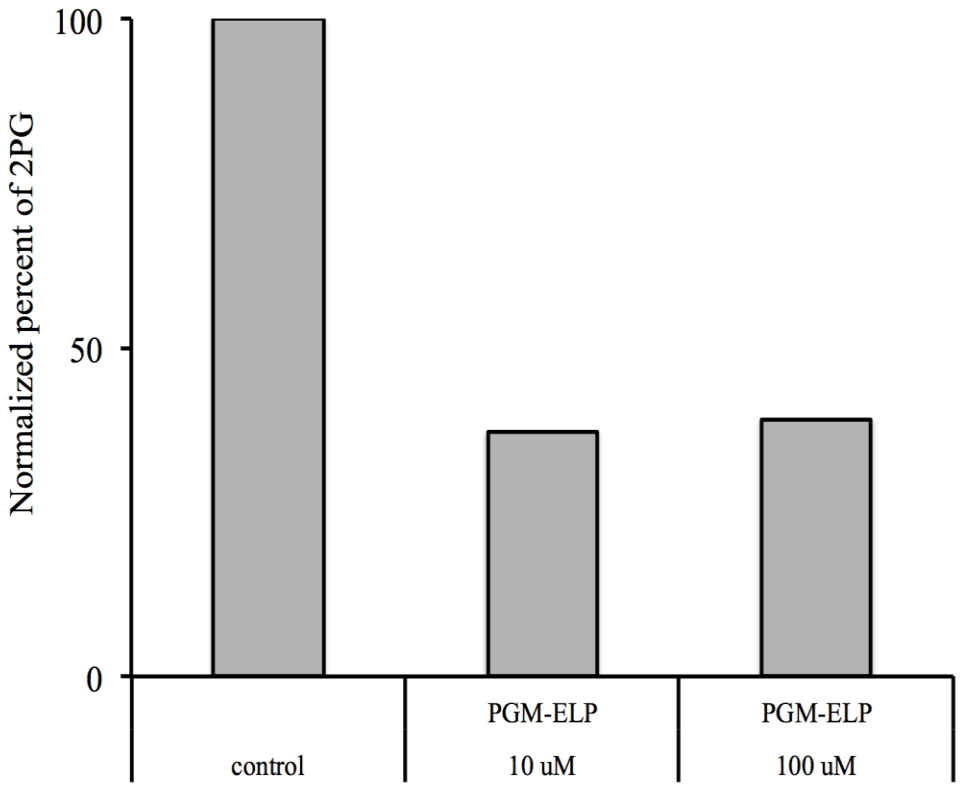

Figure 4.7 2PG intracellular concentration in H292 cells after PGM-ELP treatment. A 2PG colorimetric assay was used to show inhibition of the PGM enzyme. H292 cells were treated with PGM-ELP (10 μM and 100 μM) for 48 Hrs. After the treatment the concentration of 2PG was measured and normalized to the control (no treatment).

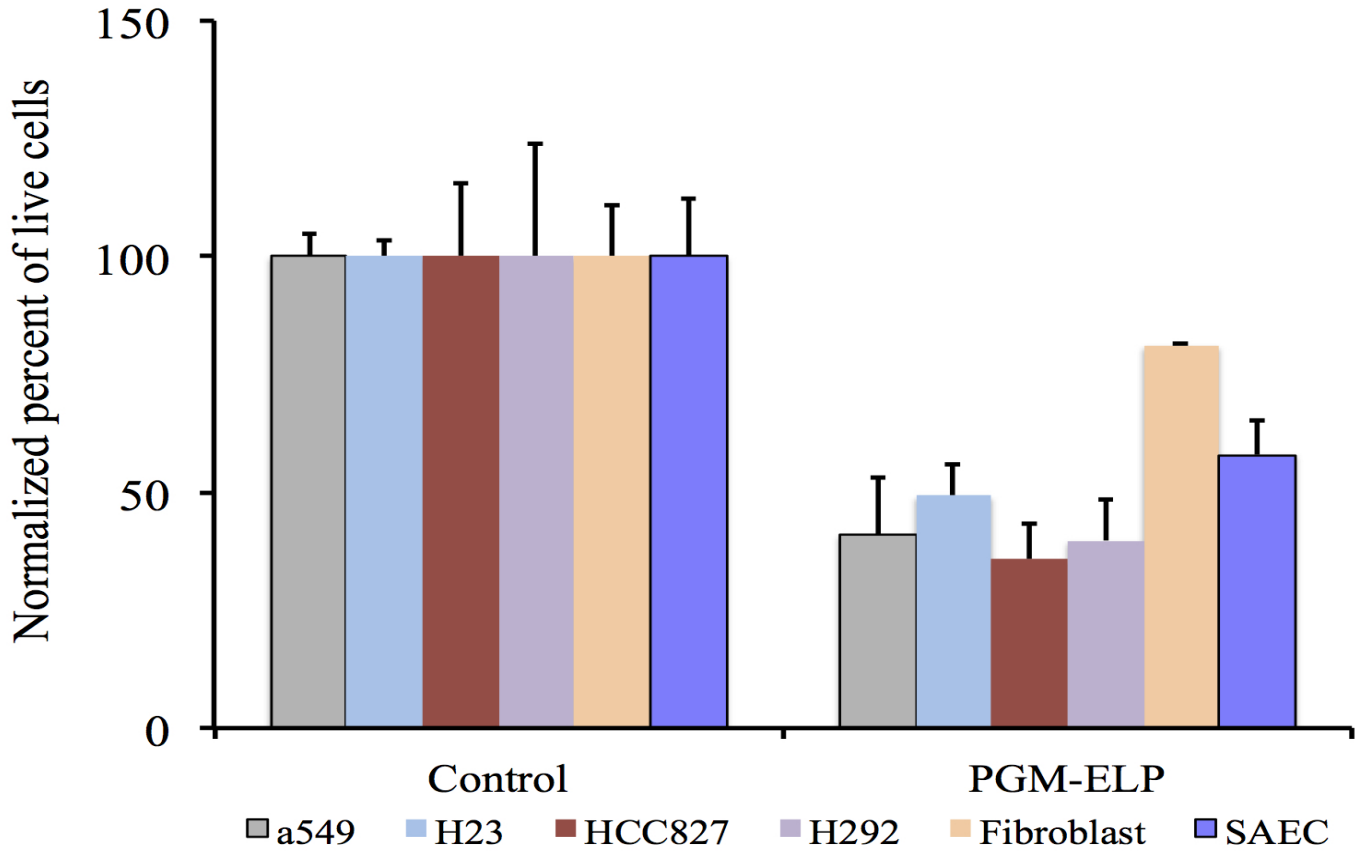

Figure 4.8 Quantification of live cells in various cell types after PGM-ELP treatment. Various cell lines (cancerous and non cancerous) were treated with 50 μM of PGM-ELP. The media was changed every two days after treatment and the cells were not retreated. Six days after treatment, the quantification was done as described in the M&M section.

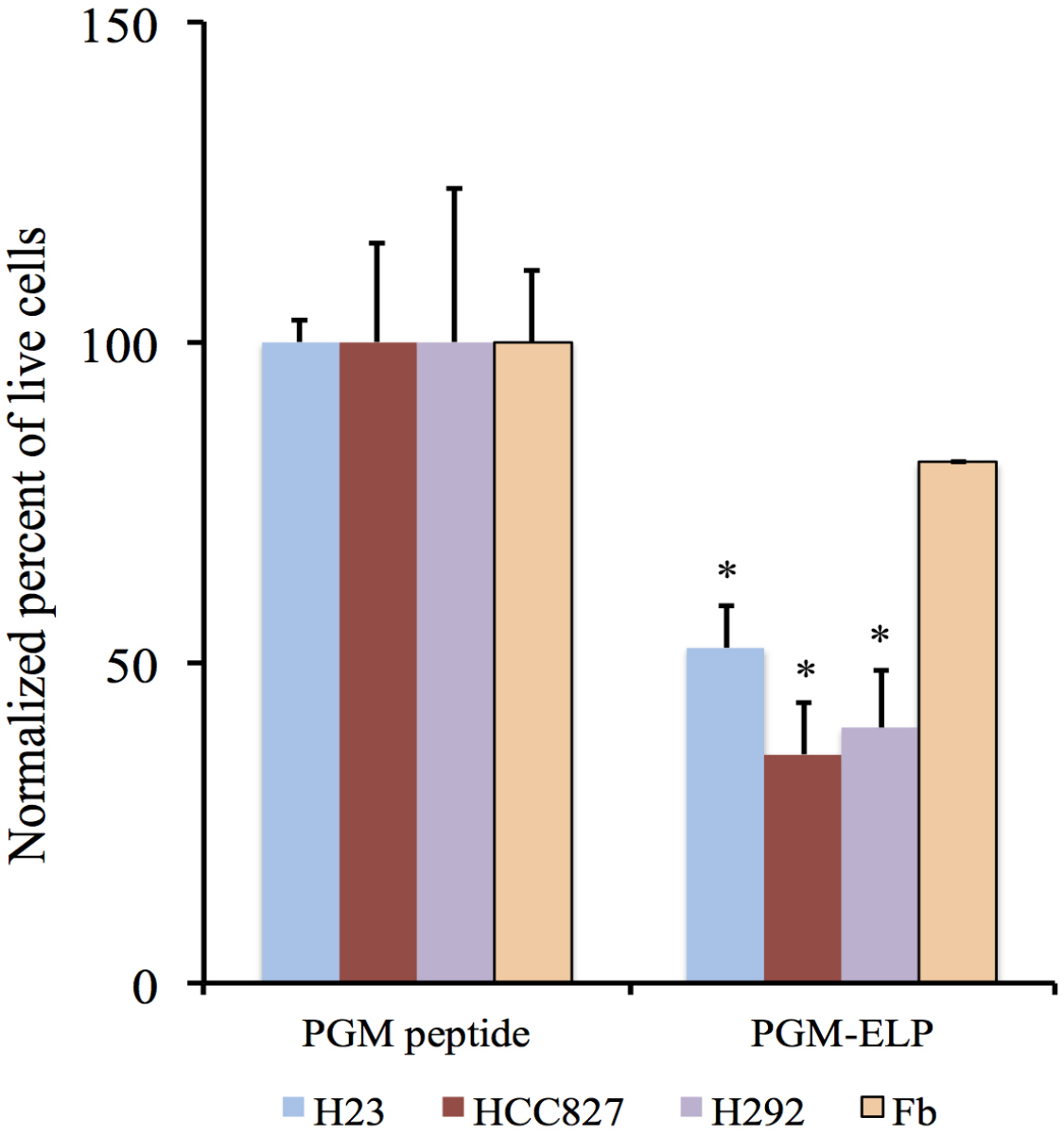

Figure 4.9 PGM peptide and PGM-ELP treatments. Cells were treated with 50 μM of either PGM peptide or PGM-ELP for 6 days. The media was changed every two days, but the treatments were not repeated. Clearly, the data shows that PGM-ELP is more cytotoxic than the PGM peptide. Treatments were normalized to their respective PGM peptide treatment.

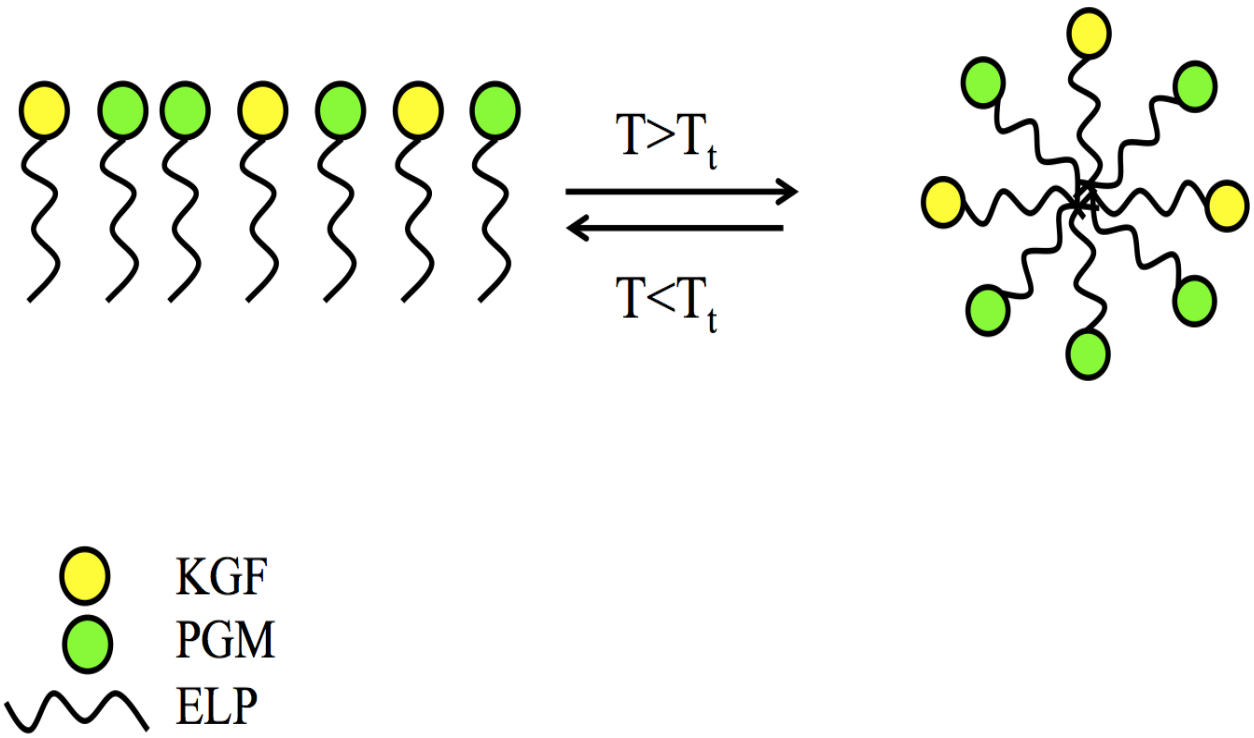

Figure 4.10 Graphical representation of the heterogeneous nanoparticle comprising of KGF-ELP and PGM-ELP.

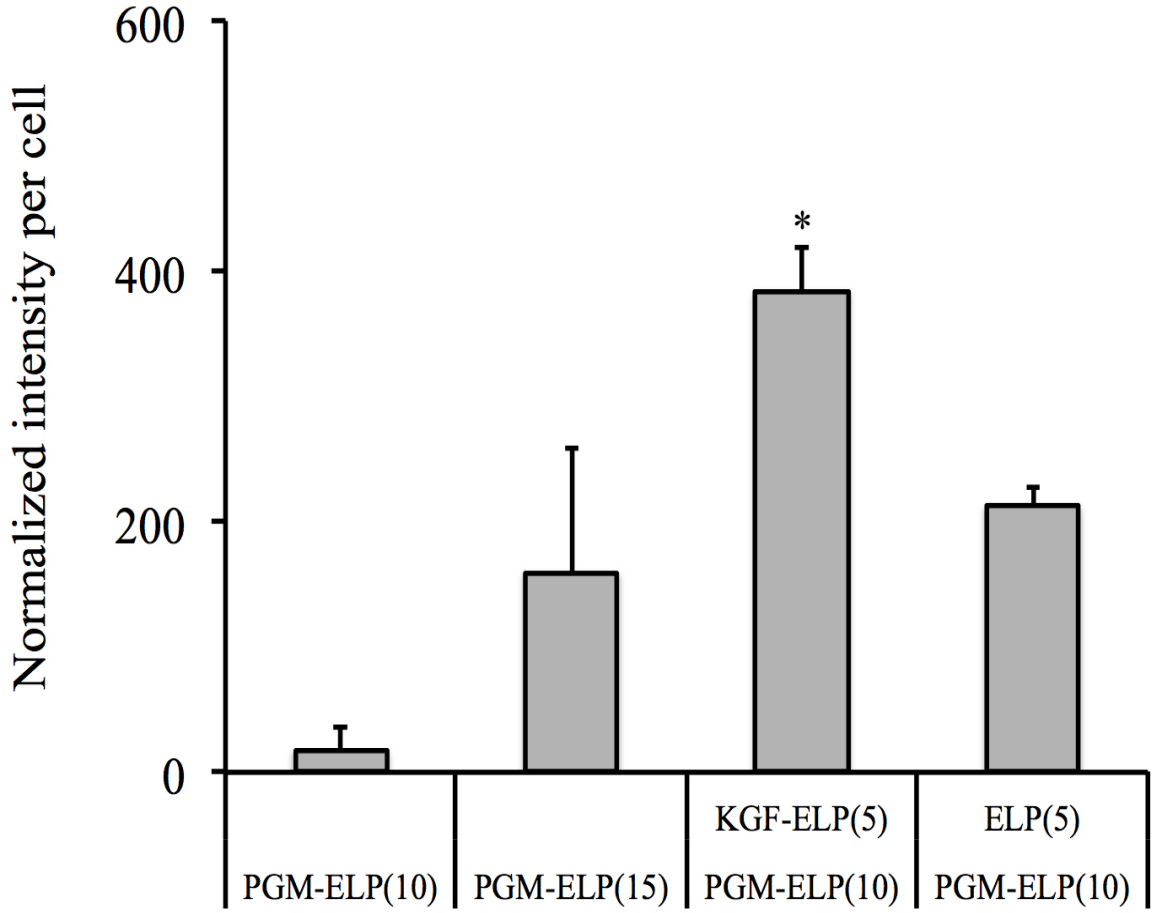

Figure 4.11 Normalized internalization of PGM-ELP in the presence and absence of KGF-ELP. A549 cells were treated with the described formulations for 24 Hrs. All formulations consist of 10 μM labeled PGM-ELP. The intensity relates to the amount of labeled PGM-ELP internalized per cell. The quantification was carried out by flow cytometry. * = $p < 0.05$. Number in parenthesis represent the concentration in μM.

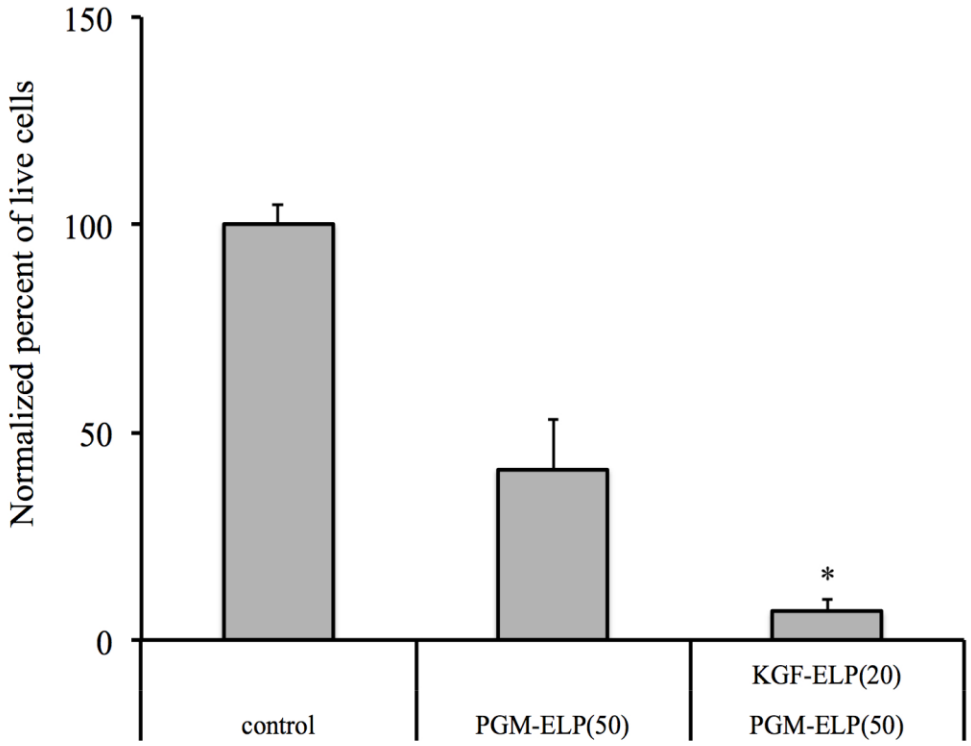

Figure 4.12 KGF-ELP enhances the PGM-ELP cytotoxic effect in KGFR overexpressing cells. A549 were treated once and the media was changed every two days. Six days after treatment, the quantification was done as described in the M&M section; the results were normalized to the control (no treatment). * = $p < 0.05$.Number in parenthesis represent the concentration in μM.

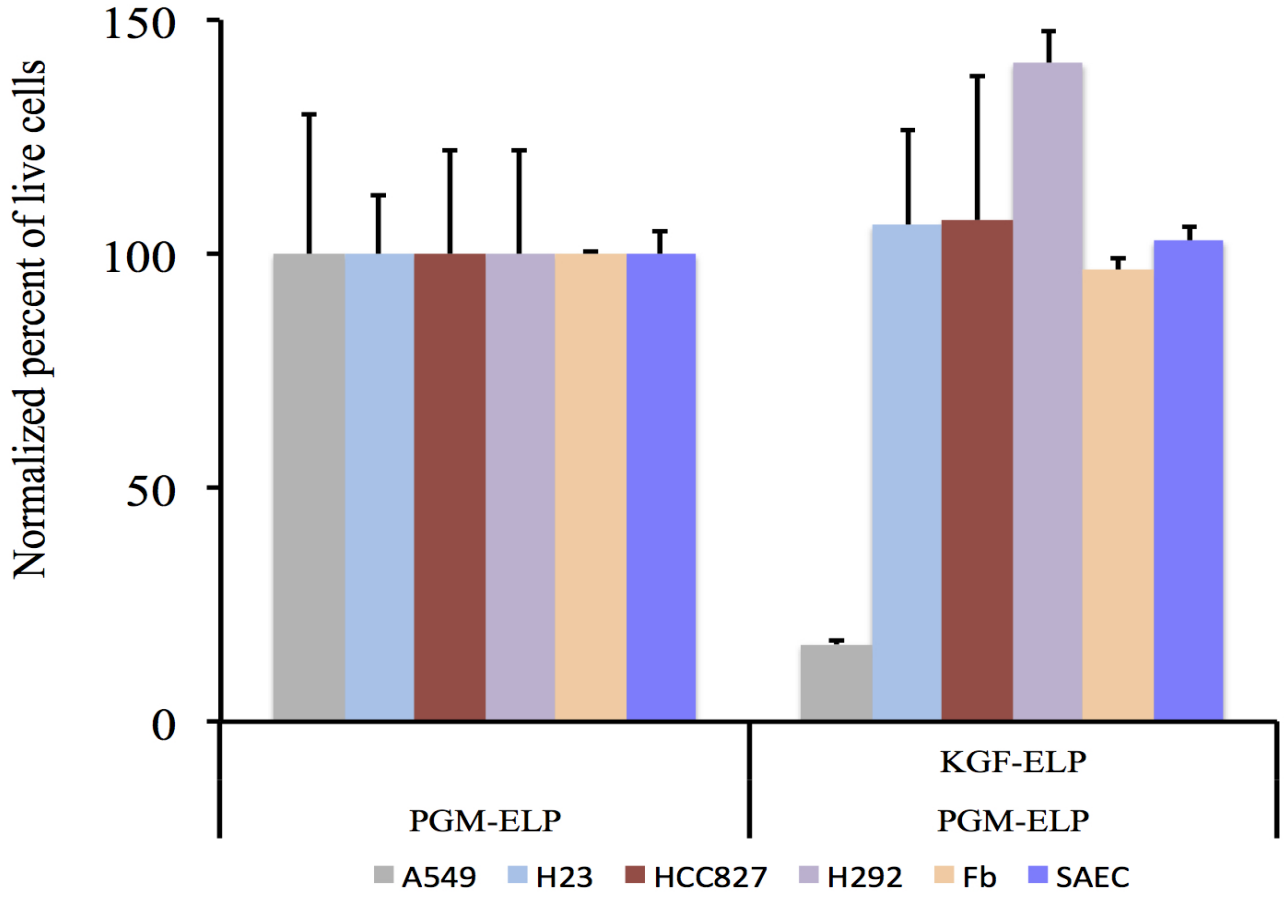

Figure 4.13 KGF-ELP enhances PGM-ELP cytotoxicity only in KGFR overexpressing cells. Various cell lines (cancerous and non cancerous) were treated with 50 μM of PGM-ELP and 20 μM of KGF-ELP. The media was changed every two days after treatment and the cells were not retreated. Six days after treatment, the quantification was done as described in the M&M section. Results were normalized to the PGM-ELP treatment.

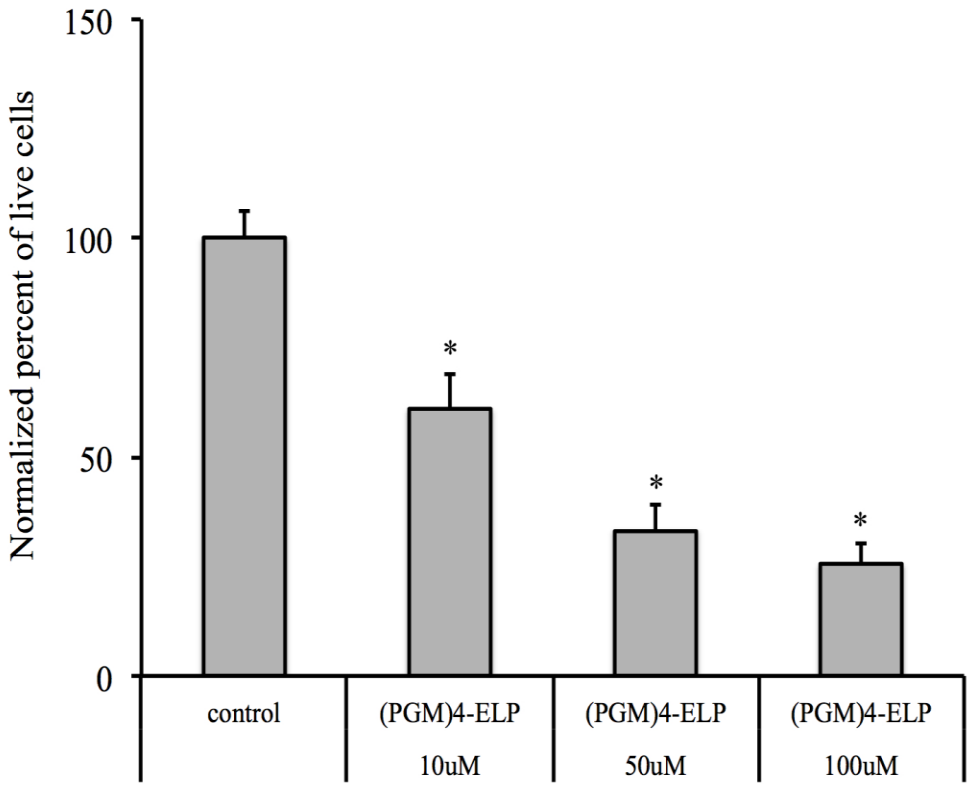

Figure 4.14 (PGM)4-ELP induces killing in a dose dependent manner. HCC827 cells were treated for 3 days with the (PGM)4-ELP fusion with the shown concentrations. The results were normalized to the control (no treatment). * = $p < 0.05$.

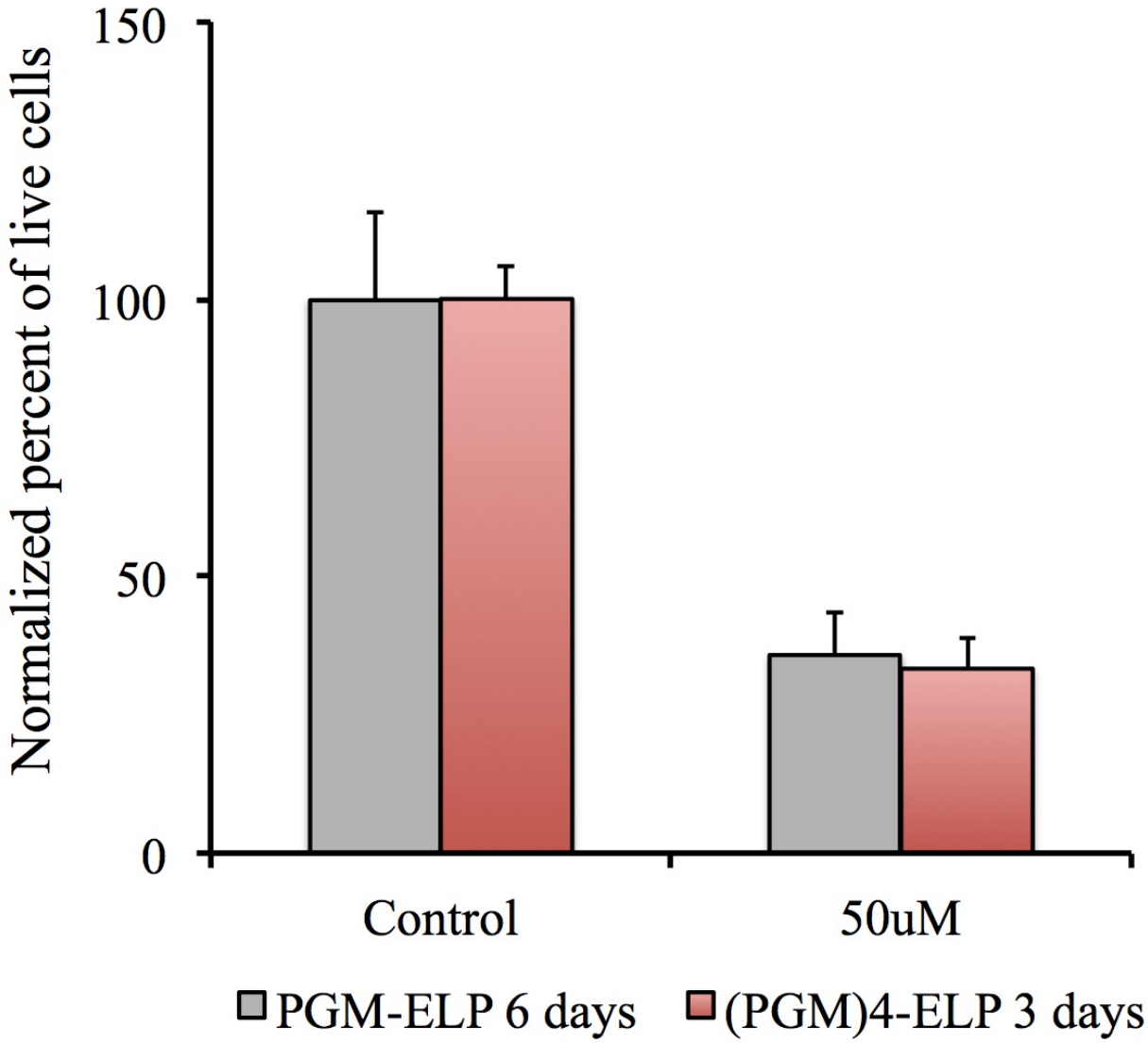

Figure 4.15 (PGM)4-ELP is more cytotoxic than PGM-ELP. HCC827 cells were treated with the same concentrations of (PGM)4-ELP and PGM-ELP for 3 and 6 days, respectively. The graph clearly shows approximately the same percent of live cells after treatment when each is compared to its respective control (no treatment).

4.5 References

[1] N. N. Pavlova and C. B. Thompson, "The Emerging Hallmarks of Cancer Metabolism," *Cell Metab*, vol. 23, pp. 27-47, Jan 12 2016.

[2] J. L. T. Jeremy M Berg, and Lubert Stryer, *Biochemistry*. New York: W H Freeman, 2002.

[3] S. J. Bensinger and H. R. Christofk, "New aspects of the Warburg effect in cancer cell biology," *Semin Cell Dev Biol*, vol. 23, pp. 352-61, Jun 2012.

[4] T. M. Maher, "Aerobic Glycolysis and the Warburg Effect. An Unexplored Realm in the Search for Fibrosis Therapies?," *Am J Respir Crit Care Med*, vol. 192, pp. 1407-9, Dec 15 2015.

[5] J.-F. H. G. Shanmugasundaram Ganapathy-Kanniappan, "Tumor glycolysis as a target for cancer therapy: progress and prospects," *Molecular Cancer*, vol. 12, 2013.

[6] H. Pelicano, D. S. Martin, R. H. Xu, and P. Huang, "Glycolysis inhibition for anticancer treatment," *Oncogene*, vol. 25, pp. 4633-46, Aug 7 2006.

[7] F. Bost, A. G. Decoux-Poullot, J. F. Tanti, and S. Clavel, "Energy disruptors: rising stars in anticancer therapy?," *Oncogenesis*, vol. 5, p. e188, 2016.

[8] S. Y. Lunt and M. G. Vander Heiden, "Aerobic glycolysis: meeting the metabolic requirements of cell proliferation," *Annu Rev Cell Dev Biol*, vol. 27, pp. 441-64, 2011.

[9] X. L. Zu and M. Guppy, "Cancer metabolism: facts, fantasy, and fiction," *Biochem Biophys Res Commun*, vol. 313, pp. 459-65, Jan 16 2004.

[10] P. E. Porporato, S. Dhup, R. K. Dadhich, T. Copetti, and P. Sonveaux, "Anticancer targets in the glycolytic metabolism of tumors: a comprehensive review," *Front Pharmacol*, vol. 2, p. 49, 2011.

[11] Z. Leni, G. Parakkal, and A. Arcaro, "Emerging metabolic targets in the therapy of hematological malignancies," *Biomed Res Int*, vol. 2013, p. 946206, 2013.

[12] S. Daniele, C. Giacomelli, E. Zappelli, C. Granchi, M. L. Trincavelli, F. Minutolo, *et al.*, "Lactate dehydrogenase-A inhibition induces human glioblastoma multiforme stem cell differentiation and death," *Sci Rep,* vol. 5, p. 15556, 2015.

[13] L. Arzoine, N. Zilberberg, R. Ben-Romano, and V. Shoshan-Barmatz, "Voltage-dependent anion channel 1-based peptides interact with hexokinase to prevent its anti-apoptotic activity," *J Biol Chem,* vol. 284, pp. 3946-55, Feb 6 2009.

[14] D. Zhang, J. Li, F. Wang, J. Hu, S. Wang, and Y. Sun, "2-Deoxy-D-glucose targeting of glucose metabolism in cancer cells as a potential therapy," *Cancer Lett,* vol. 355, pp. 176-83, Dec 28 2014.

[15] G. Maschek, N. Savaraj, W. Priebe, P. Braunschweiger, K. Hamilton, G. F. Tidmarsh, *et al.*, "2-deoxy-D-glucose increases the efficacy of adriamycin and paclitaxel in human osteosarcoma and non-small cell lung cancers in vivo," *Cancer Res,* vol. 64, pp. 31-4, Jan 1 2004.

[16] D. Zhong, X. Liu, K. Schafer-Hales, A. I. Marcus, F. R. Khuri, S. Y. Sun, *et al.*, "2-Deoxyglucose induces Akt phosphorylation via a mechanism independent of LKB1/AMP-activated protein kinase signaling activation or glycolysis inhibition," *Mol Cancer Ther,* vol. 7, pp. 809-17, Apr 2008.

[17] D. Zhong, L. Xiong, T. Liu, X. Liu, X. Liu, J. Chen, *et al.*, "The glycolytic inhibitor 2-deoxyglucose activates multiple prosurvival pathways through IGF1R," *J Biol Chem,* vol. 284, pp. 23225-33, Aug 28 2009.

[18] E. D. Xiao Dong Zhang, Marie VilledieuI, Laurent Poulant, Marilyne Duval, Pascal Gauduchon, Laurent Schwarts and Philippe Icard, "Effect of 2-Deoxy-D-glucose on Various Malignant Cell Lines In Vitro," *Anti Cancer Research,* vol. 26, pp. 3561-3566, 2006.

[19] M. M. W. Markus Ralsera, Eduard A. Struysb, Christian Joppicha, Sylvia Krobitscha, Cornelis Jakobsb, and Hans Lehracha, "A catabolic block does not sufficiently explain how 2-deoxy-D-glucose inhibits cell growth," *PNAS,* vol. 105, pp. 17807-17811, 2008.

[20] M. G. Vander Heiden, J. W. Locasale, K. D. Swanson, H. Sharfi, G. J. Heffron, D. Amador-Noguez, *et al.*, "Evidence for an alternative glycolytic pathway in rapidly proliferating cells," *Science,* vol. 329, pp. 1492-9, Sep 17 2010.

[21] M. Engel, S. Mazurek, E. Eigenbrodt, and C. Welter, "Phosphoglycerate mutase-derived polypeptide inhibits glycolytic flux and induces cell growth arrest in tumor cell lines," *J Biol Chem,* vol. 279, pp. 35803-12, Aug 20 2004.

[22] T. Hitosugi, L. Zhou, S. Elf, J. Fan, H. B. Kang, J. H. Seo, *et al.*, "Phosphoglycerate mutase 1 coordinates glycolysis and biosynthesis to promote tumor growth," *Cancer Cell,* vol. 22, pp. 585-600, Nov 13 2012.

[23] T. Hitosugi, L. Zhou, J. Fan, S. Elf, L. Zhang, J. Xie, *et al.*, "Tyr26 phosphorylation of PGAM1 provides a metabolic advantage to tumours by stabilizing the active conformation," *Nat Commun,* vol. 4, p. 1790, 2013.

[24] J. J. N Durany, E Campo, R Molina and J Carreras, "Phosphoglycerate mutase, 2,3-bisphosphoglycerate phosphatase and enolase activity and isoenzymes in lung, colon and liver carcinomas," *British Journal of Cancer,* vol. 75, pp. 969-977, 1997.

[25] R. I. Buhrens, Amelung, J. T.,Reymond, M. A.,Beshay, M., "Protein expression in human non-small cell lung cancer: a systematic database," *Pathobiology,* vol. 76, pp. 277-85, 2009.

[26] D. E. Meyer and A. Chilkoti, "Genetically encoded synthesis of protein-based polymers with precisely specified molecular weight and sequence by recursive directional ligation: examples from the elastin-like polypeptide system," *Biomacromolecules,* vol. 3, pp. 357-67, Mar-Apr 2002.

[27] P. Koria, H. Yagi, Y. Kitagawa, Z. Megeed, Y. Nahmias, R. Sheridan, *et al.*, "Self-assembling elastin-like peptides growth factor chimeric nanoparticles for the treatment of chronic wounds," *Proc Natl Acad Sci U S A,* vol. 108, pp. 1034-9, Jan 18 2011.

[28] M. Shah, P. Y. Hsueh, G. Sun, H. Y. Chang, S. M. Janib, and J. A. MacKay, "Biodegradation of elastin-like polypeptide nanoparticles," *Protein Sci,* vol. 21, pp. 743-50, Jun 2012.

[29] R. Chan. (2007). *Glycolysis*. Available: https://commons.wikimedia.org/wiki/File:GlycolysiscompleteLabelled.png

CHAPTER 5: SUMMARY, CONCLUSIONS AND FUTURE WORK

5.1 Summary and Conclusions

In this doctoral research, we have shown the selective enhancement of macropinocytosis for the treatment of lung cancer. This is a novel approach that takes advantage of an endocytotic mechanism that is inherently present in cancer cells, macropinocytosis. Macropinocytosis is transient and can be stimulated by the interaction between growth factors and their receptors on the cell surface. Herein, we used the keratinocyte growth factor receptor (KGFR) as the target for our treatment; this receptor has been reported to be overexpressed in lung cancer. We used the fusion comprising of the keratinocyte growth factor (KGF) and elastin like polypeptides (ELPs), KGF-ELP, previously synthesized in our lab to enhance macropinocytosis in KGFR overexpressing cells. After this selective enhancement, a mitochondriotoxic fusion peptide comprising of $(KLAKLAK)_2$ and ELP, $(KLAKLAK)_2$–ELP, was delivered causing mitochondrial depolarization and subsequent cell death. Finally, we used a glycolytic inhibitory peptide and fuse it to ELPs, PGM-ELP. This peptide was also delivered selectively to KGFR overexpressing cells using the KGF-ELP fusion; this also resulted in selective killing.

In chapter 2, we found that the fusion $(KLAKLAK)_2$-ELP is mitochondriotoxic without the need to be functionalized; the nanoparticle conformation provided by the ELP backbone was enough to cause the internalization and cytotoxicity of the fusion. Furthermore, cell death occurs via mitochondrial depolarization and swelling. We found that the mechanism of internalization of $(KLAKLAK)_2$-ELP is macropinocytosis; we believe the interaction between the ELP domain

of the fusion and heparan sulfate on the cell membrane allows for the proximity required for macropinocytosis to act on the $(KLAKLAK)_2$-ELP nanoparticles.

In chapter 3, we have taken advantage and expanded on the findings in the previous chapter. Previously we demonstrated that $(KLAKLAK)_2$-ELP is internalized by cells through the process of macropinocytosis. Furthermore, the ELP domain also becomes critical since it facilitates the $(KLAKLAK)_2$-ELP nanoparticles to be bound to the cell surface; a step that is required for macropinocytosis. Since macropinocytosis can be stimulated by growth factors; in this chapter, we selectively enhanced macropinocytosis and the uptake of $(KLAKLAK)_2$-ELP in KGFR overexpressing lung cancer cells using the fusion KGF-ELP. While we have focused on the delivery of the mitochondriotoxic peptide $(KLAKLAK)_2$, this approach can easily be expanded to other peptides, imaging agents, or drugs thereby having broad applications in cancer as well as intracellular drug delivery.

In chapter 4, we have demonstrated that the fusion PGM-ELP induces cell death by inhibiting glycolysis. Furthermore, this fusion seems to have a higher effect in cancer cells, which could be related to their high dependence in glycolysis and/or their intrinsic more active nature. We also showed that the heterogeneous nanoparticle comprising of KGF-ELP and PGM-ELP enhances the internalization and cytotoxic effect of PGM-ELP in KGFR overexpressing cells. Lastly, our data suggests a correlation between the number of H11 sites and the efficacy of the PGM-ELP; that is, (PGM)4-ELP is more efficient than PGM-ELP in terms of killing time and percent of killing.

5.2 Future Work

The work we presented in this dissertation shows an innovative approach for targeted therapy; therefore, we believe it lays the groundwork for its advancement. Furthermore, due to

the adaptability of this system, it can easily be expanded to treat other types of cancers that may overexpress different growth factor receptors than the one we targeted such as the epidermal growth factor receptor as it occurs in breast and pancreatic cancers.

In addition, we focused on the selective delivery of cytotoxic peptides that aimed at either the mitochondria or glycolysis. However, due to the simplicity of our system, it is possible the formation of multivalent nanoparticles that could selectively aim at multiple targets. For instance, instead of targeting either the mitochondria or glycolysis, a multivalent nanoparticle could disrupt the mitochondria while blocking glycolysis; this could have synergistic effects on the treatment of cancer. Moreover, this targeted system is not limited to the delivery of cytotoxic peptides. Due to the cysteine amino acid that forms part of our ELP construct, using simple maleimide chemistry allows the conjugation of cancer therapeutics that can be selectively delivered by macropinocytosis. This could result in improved intracellular concentration of the therapeutics, prevention of endosomal entrapment and lysosomal degradation.

Finally, the application of selectively stimulating macropinocytosis is not limited to the treatment of cancer. We believe that it can be further exploited in other fields such as in gene therapy. In this field, the targeted delivery of a gene is critical since unwanted gene insertion or inactivation may have severe consequences on the patient. Therefore, a selective delivery of the gene by macropinocytosis can ensure the therapy reaches its target and minimizes side effects.

Overall, we envision that further study of our work can result in improving current targeted treatments for cancer. Additionally, we see the possibility of expanding this research to other fields for which selective delivery is paramount.

APPENDICES

Appendix A: List of Abbreviations

$(KLAKLAK)_2$ .....KLAKLAKKLAKLAK

2-DG 2-Deoxyglucose

2PG 2-Phosphoglycerate

3PG 3-Phosphoglycerate

6PGD.....6-phosphogluconate dehydrogenase

A.....Alanine

A549.....Adenocarcinoma cells, non-small cell lung cancer

ATP .....Adenosine triphosphate

CCCP .....Carbonylcyanide m- chlorophenylhydrazone

CO_2.....Carbon dioxide

Cyt c .....Cytochrome c

DAPI .....4',6-diamidino-2-phenylindole

DLS .....Dynamic light scattering

DNA .....Dioxyribose nucleic acid

E .....Glutamate

EGF .....Epidermal growth factor

EGFR .....Epidermal growth factor receptor

ELP .....Elastin like polypeptide

ETC .....Electron transport chain

Fb .....Fibroblast

FBS .....Fetal bovine serum

FITC .....Fluorescein isothiocyanate

G3P Glyceraldehyde-3-phosphate

G6P Glucose-6-phosphate

Gly.....Glycine

H.....Histidine

H11.....Histadine at location 11

H1650.....Adenocarcinoma cells, non-small cell lung cancer

H23.....Adenocarcinoma cells, non-small cell lung cancer

H292.....Adenocarcinoma cells, non-small cell lung cancer

HCC827 .....Adenocarcinoma cells, non-small cell lung cancer

HGF.....Hepatocyte growth factor

HK.....Hexokinase

HSPG .....Heparan sulfate proteoglycan

I .....Isoleucine

ITC .....Inverse temperature cycling

K.....Lysine

KGF.....Keratinocyte growth factor

KGFR .....Keratinocyte growth factor receptor

L .....Leucine

LCST.....Lower critical solution temperature

M&M .....Materials and methods

mAb.....Monoclonal antibodies

MET .....MET proto-oncogene

NSCLC.....Non-Small Cell Lung Cancer

O_2 .....Oxygen

PBS .....Phosphate buffered-saline

PEP.....phosphoenolpyruvate

PGM.....Phosphoglycerate mutase

PHGDH.....phosphoglycerate dehydrogenase enzyme

PK .....Pyruvate kinase

PKM2.....Pyruvate kinase isoform 2

Pro.....Proline

R.....Arginine

RME.....Receptor mediated endocytosis

RNA .....Ribonucleic acid

RT-PCR.....Real-time polymerase chain reaction

S .....Serine

SAEC .....Small airway epithelial cells

SEM .....Square error of the mean

TEM .....Transmission electron microscopy

TKI.....Tyrosine kinase inhibitor

T_t .....Transition temperature

Val.....Valine

W.....Tryptophan

X.....Guest amino acid residue

µM.....Micromolar

Appendix B: Copyright Permission

The permission below is for material in Chapters 2 and 3.